Detection and Resource Allocation Algorithms for Cooperative MIMO Relay Systems

Thomas John Hesketh

Ph.D.

University of York

Electronics

February 2014

Abstract

Cooperative communications and multiple-input multiple-output (MIMO) communication systems are important topics in current research that will play key roles in the future of wireless networks and standards. In this thesis, the various challenges in accurately detecting and estimating data signals and allocating resources in the cooperative systems are investigated.

Firstly, we propose a cross-layer design strategy that consists of a cooperative maximum likelihood (ML) detector operating in conjunction with link selection for a cooperative MIMO network. Two new link selection schemes are proposed, along with an iterative detection and decoding (IDD) scheme that utilises channel coding techniques. Simulation results show the performance and potential gains of the proposed schemes.

Secondly, a successive interference cancellation (SIC) detector is proposed for a MIMO system that has dynamic ordering based on a reliability ordering (RO), and an alternative multiple feedback (MF) candidate cancellation method. The complexity of these schemes is analysed and a hard decision feedback IDD system is also proposed. Results show that the proposed detector can give gains over existing schemes for a minimal amount of extra complexity.

Lastly, a detector is proposed that is based upon the method of widely linear (WL) filtering and a multiple branch (MB) SIC, for an overloaded, multi-user cooperative MIMO system. The use of WL methods is explained, and a new method of choosing cancellation branches for an MB detector is proposed with an analysis of the complexity required. A list-based IDD system is developed, and simulation results show that the proposed detector can operate in an overloaded system and provide improved performance gains.

Contents

List of Figures

List of Tables

Acknowledgements

My utmost gratitude goes to my supervisors, Dr. Rodrigo C. de Lamare and Stephen Wales for their support, guidance and patience during my research, which made the completion of this work possible.

I am forever grateful to my family, whose unwavering encouragement and moral support throughout my education has enabled me to achieve so much.

Finally, I thank all my friends and colleagues in York and beyond, whose advice, friendship and goodwill has helped me immensely.

The research presented in this thesis has been jointly funded by Roke Manor Research Ltd. and the University of York.

Declaration

All work presented in this thesis is original to the best knowledge of the author. References and acknowledgements to work by other researchers have been given as appropriate.

Some of the research presented in this thesis has resulted in some publications. These publications are listed below.

Journal Papers

1. T. Hesketh, R. C. de Lamare and S. Wales, ”Joint Maximum Likelihood Detection and Link Selection for Cooperative MIMO Relay Systems”, *IET Communications*, 2013 (Accepted for publication).

2. T. Hesketh, R. C. de Lamare and S. Wales, ”Widely-Linear Interference Cancellation with Parallel Branch Ordering for Overloaded Cooperative MIMO Systems”, (under preparation)

Chapter 1

Introduction

1.1 Overview

In recent years, advances in wireless communications technology for the business and consumer sectors have led to the exponential growth of data consumption via wireless communications, which results in increasing demand for the rate of data transmission and large numbers of users attempting to transmit and receive data simultaneously, while still maintaining signal coverage and accurately receiving data.

One solution to increasing the rate of data transmission and reception is multiple-input multiple-output (MIMO) systems, where each device transmits several streams of data simultaneously, but this presents new challenges for wireless system engineers that have to devise efficient techniques for power allocation, parameter estimation and data reception and detection. Thus, different considerations for this expanded system have to be made as compared with a simpler single data stream system, and the design of algorithms to exploit the full potential of MIMO systems is a rich and extensive field of research.

However, focus on communications research has also turned to the problem of reliably transmitting signals in cluttered or obstructed environments, such as built-up urban areas [1–3]. In such situations, line of sight (LOS) transmissions are heavily attenuated or otherwise impossible to receive without a significant amount of errors in the detection

and decoding of the signal. To address this problem, cooperative communication systems have been proposed, where the original transmission is received by relay devices, which then retransmit the received signal to the destination device. As the signal does not need to be transmitted directly to the destination device, use of relay(s) can provide alternative paths for the signal to the destination, thus increasing the likelihood that the signal is received correctly. But this also presents challenges for both the detection of the data at the destination, and for resource allocation and management of the relays.

In this thesis, a number of detection and resource allocation algorithms are proposed for cooperative MIMO systems, with the aim of decreasing the bit error rate (BER) of the received data at the destination as compared with previously proposed methods. Firstly, a cross-layer design which introduces a cooperative maximum likelihood (ML) detector with power adjustment and relay selection is proposed for a multiple-relay MIMO system utilising amplify-and-forward (AF) relays, with consideration given for the data available in the system. The system has a global power constraint, and the channels are modelled with path loss fading and log normal shadowing (LNS) large scale fading, which attempts to describe the effects of distance-based signal attenuation and slow signal fading due to random objects partially obstructing the signal transmission. Two relay link selection techniques based upon the idea of relay channel sets are proposed with complexity analysis, and are shown to provide a superior BER performance as compared with previously proposed methods. Iterative detection and decoding (IDD) methods are also considered and implemented using a list based maximum *a posteriori* detector and convolutional channel encoding.

Secondly, an interference cancellation detector is proposed which considers the use of multiple-feedback (MF) techniques and reliability-ordering (RO) methods to produce a successive interference cancellation (SIC) detector, with the algorithm developed in such a manner as to reduce the computational complexity of the proposed detector. IDD techniques based on convolutional codes are applied to the system with the proposed detector. The results show that the proposed detection strategy can obtain significant gains over standard SIC algorithms.

Lastly, an overloaded multiple user system is considered, where there are more transmitters than receive antennas in the system, with a small number of relays in a cooperative

scenario. Using widely linear (WL) filtering and multiple-branch (MB) detection, a detector is proposed to improve the BER at the destination, demonstrating the ability to successfully detect a greater number of transmitting devices than previous methods, with only a small number of relays available. Also proposed is a method of dynamically choosing the branch permutations to use, reducing the average computational complexity for the system, whilst maintaining performance. An IDD implementation is also presented, along with a study of different detection techniques in an overloaded system.

1.2 Contributions

- The extension of a cooperative ML detector from the single relay case to the multiple relay case, with the substitution of an approximation for the second transmission phase received signal and a summated channel, in order to accommodate the system information available to the destination device. The cooperative detector is derived by expanding the ML detection rule for the first and second transmission phases, and then collapsing the expansion into an equivalent single cooperative ML rule, using a matrix square root.

- Two relay link selection techniques are proposed, based upon the powers of the channels associated with each relay, but by also considering the powers of the combined channels in the second phase, expanding the possible selection set space beyond the individual relay links. This is to avoid the possibility of destructive interference cancellation for the second transmission phase within the set of relay links selected. This principle is applied to the maximum minimum criterion for relay link selection, and also the maximum harmonic mean selection method.

- A cross-layer design strategy is also proposed that integrates the cooperative ML detection and the relay link selection techniques to produce a method that also considers a global power constraint.

- The development of a SIC detection algorithm for MIMO systems, incorporating the concepts of log likelihood ratio (LLR) based cancellation reliability ordering for dynamic cancellation orders, which is derived using a Gaussian probability distribution function (PDF) approximation for the output of a linear filter, and alternative

cancellation candidate MF techniques, which rely on the concept of an unreliable shadow area in the modulation scheme's constellation diagram, defined by a shadowing parameter and Voronoi regions. These methods are integrated into a single algorithm, with improvements and optimisations discussed for the reduction of the computational complexity.

- A new SIC detector is proposed for heavily overloaded multiple-user cooperative relay MIMO systems with non-circular symbol modulation schemes, using WL filtering techniques for interference cancellation. The proposed SIC detector is an extension to traditional linear schemes, and takes advantage of the covariance and pseudo-covariance matrix of the received signal. Furthermore, MB alternative cancellation orders are introduced, which follows several parallel detection orders to obtain a list of detection candidates, with decisions on the final detected symbols made using an Euclidean distance rule. The proposed list-based WL SIC algorithm is shown to perform very close the optimum ML detector.

- Discussion and investigation on the methods of obtaining the ordering branches used, involving predetermined patterns and cancellation order shuffling are considered. A proposed dynamic branching based upon the constellation shadowing area utilised in MF techniques is developed, and a study of the trade-off between the number of branches used, computational complexity and BER performance is carried out.

1.3 Thesis Outline

The structure of the thesis is as follows:

- Chapter 2 presents an overview of the theory relevant to this thesis and introduces the system models that are used to present the work in this thesis. The topics of MIMO systems, cooperative networks, relay link selection, ML detection, SIC detection and WL filtering are covered, with an outline of previous work in these fields.

- Chapter 3 presents the cooperative ML detector for a multiple-relay cooperative two-phase MIMO system, with relay link selection strategies proposed and studied for several scenarios of interest. IDD techniques are also utilised, alongside a complexity analysis of the relay link selection strategies used.

- Chapter 4 presents a novel interference cancellation detector, based upon the methods of MF and RO, with the development of the algorithm organised around reducing the computational complexity required. The effects of altering the parameter values of the algorithm are investigated, which include IDD results.

- Chapter 5 presents the application of WL techniques to a multiple-user multiple-relay system, with the added technique of MB processing. Methods of determining the WL branch orders are presented, including a permutation based selection, and a dynamic branching algorithm, alongside the application of IDD.

- Chapter 6 presents the conclusions of this thesis, and suggests directions in which further research could be carried out.

1.4 Notation

Throughout this thesis, lowercase non-bold letters represent scalar values, whilst bold lowercase and uppercase letters represent vectors and matrices, respectively. The superscripts $(\cdot)^*$,$(\cdot)^{-*}$, $(\cdot)^T$ and $(\cdot)^H$ denote the complex conjugate, the inverse complex conjugate, the standard transpose and the Hermitian transpose, respectively. The absolute value of a scalar is denoted by $|\cdot|$, the Euclidean norm of a vector or matrix is given by $\|\cdot\|$, the Frobenius norm of a vector or matrix is given by $\|\cdot\|_F$, whilst the expectation of a vector is given by $\mathbf{E}[\cdot]$. The factorial of a scalar is shown by $\cdot!$, and for a cooperative system, the first and second subscripts denote the source and destination of the transmission, *i.e.* from a relay to the destination is denoted by $\cdot_{rd}$. Identity matrices of size N are denoted by the representation $\mathbf{I}_N$.

Chapter 2

Literature Review

Contents

2.1 Introduction

This section presents an introduction to the fields of research in wireless communication systems, and the principles and techniques from which the contents of this thesis are based upon. Firstly, an overview of the system setups and models on which the work presented is based upon is provided, namely MIMO systems, two-phase cooperative systems, modulation schemes, channel modelling and channel coding. Secondly, estimation techniques for the determination of system parameters and algorithms that can be applied to resource allocation within the system are reviewed. Finally, detection techniques for the recovery of the transmitted data symbol at the receiver will be presented, covering the topics of linear filtering, WL filtering, SIC techniques, ML detection and iterative decoding techniques.

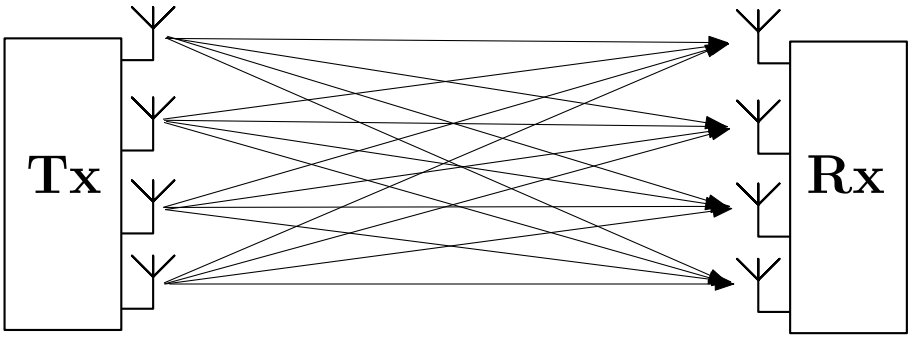

Figure 2.1: 4x4 antenna MIMO model

2.2 System Setup and Modelling

The system in which an algorithm or technique is presented within is an important part of the design of communication techniques, and may influence the derivation and design of the techniques through the conditions and challenges present in the scenario. In this section, MIMO and cooperative system setups are highlighted, the modelling of channel and noise effects is discussed and a brief introduction into channel coding is given.

2.2.1 MIMO Systems

MIMO systems use multiple antennas at both the transmitter and receiver in a communications system, which enables multiple data streams to be transmitted per time slot, as shown by Figure 2.1 [4], [5], [6], [7]. The antennas provide transmit diversity in space, *i.e.* different paths for the signal to travel from the source to the destination, which is known as spatial diversity. This can potentially increase the rate of data successfully transmitted in a system due to the additional data streams [8]. The MIMO system in Figure 2.1 can be represented by the following equation:

$$\mathbf{y} = \mathbf{H}\mathbf{x} + \mathbf{n}, \tag{2.1}$$

where $\mathbf{y}$ is a vector of length N_r, which represents the received signal at the receiver, $\mathbf{x}$ is a vector of length N_t, which represents the transmitted data symbols from the transmitter, $\mathbf{H}$ is an $N_r \times N_t$ matrix which represents the fading channel that the data is transmitted through, and $\mathbf{n}$ is a vector of length N_r, which represents the noise at the receiver. N_r is

the number of antennas at the receiver and N_t is the number of antennas at the transmitter.

A downside to MIMO transmission is that the simultaneously transmitted signals from each antenna will potentially interfere with each other, which can make the detection and decoding process at the destination more difficult, and increase the error rate. However, by transmitting multiple data streams via the multiple antennas available in the system, the channel capacity (*i.e.* the upper bound on the amount of information that can be reliably transmitted through the channel) is increased by $\min(N_t, N_r)$, as compared with a single antenna system, assuming that there is uncorrelated fading between the different transmission paths [9]. This increase in channel capacity due to the MIMO system setup can be referred as the multiplexing or diversity gain [10] of the system.

2.2.2 Cooperative Systems

A cooperative system is an extension of the point-to-point system described in the previous section, where the transmission of data signals from the source to destination is aided by relays [11], [12], [13], [14], [15]. The relays receive the signal from the source device in the same time instant that the destination receives the data signal, and then the relays forward the received signal onwards to the destination. The destination therefore receives two different copies of the signal transmitted by the source, as the fading channels associated with the relays will be different than the direct transmission channel, so the relays can give an extra form of spatial diversity, known as cooperative diversity.

Figure 2.2 illustrates a two-phase cooperative MIMO system with a single relay where the transmission takes place over two time instances, the first phase consisting of the source transmission, followed by the transmission by the relay in the second phase.

How the relay forwards the received signal data from the source depends on the forwarding scheme being used, the primary two being Amplify and Forward (AF) [16], [17], [18] and Decode and Forward (DF) [19], [20]. In AF, the relay simply amplifies the received signal from the source by a scalar factor, and retransmits the result to the destination. In DF, the relay uses a detector to decode the signal into estimated data bits, then re-encodes the estimated bits into a signal and transmits this to the destination. AF has

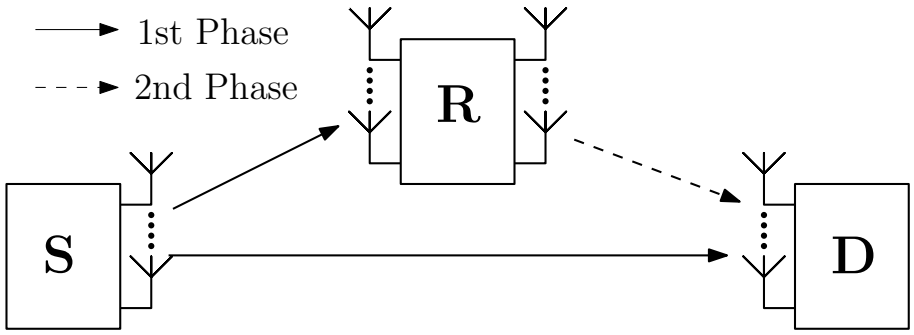

Figure 2.2: MIMO two-phase single relay system model

an advantage in that the processing at the relay is simple, as only the amplification factor and the multiplication of the received signal are required, whereas for DF the relay needs to detect and decode the received signal, which can introduce estimation errors, and is generally more complex to calculate than AF at the relay. DF can also be much more complex to calculate analytically than AF due to the possibility of errors being introduced in the decoding stage at the relay, and an analytical function would be needed for the detection algorithm used. However, for DF the destination does not require the knowledge of the channel between the source and relay to decode the data transmitted by the relay, whereas for AF the destination does require the source to relay channel knowledge as this channel affects the received signal at the destination directly, which means there must be a method in place for the destination to acquire this information.

The first phase of transmission in a cooperative system can be described as follows:

$$\mathbf{y}_{sr} = \mathbf{H}_{sr}\mathbf{x} + \mathbf{n}_r, \tag{2.2}$$

$$\mathbf{y}_{sd} = \mathbf{H}_{sd}\mathbf{x} + \mathbf{n}_d^{(1)}. \tag{2.3}$$

The subscripts on $\mathbf{y}$ and $\mathbf{H}$ denote the devices associated with the values, with the first subscript denoting the originating device, and the second subscript denoting the endpoint device. *e.g.* $\mathbf{H}_{sr}$ is the MIMO channel between the source and relay. In the case of just one subscript, *e.g.* for noise $\mathbf{n}$, the subscript denotes the device which the value is associated with. The superscript $^{(1)}$ or $^{(2)}$ shows which phase of transmission the receive antenna noise is associated with, where it may need to be differentiated.

Depending on the relay forwarding scheme being used, the second phase transmission

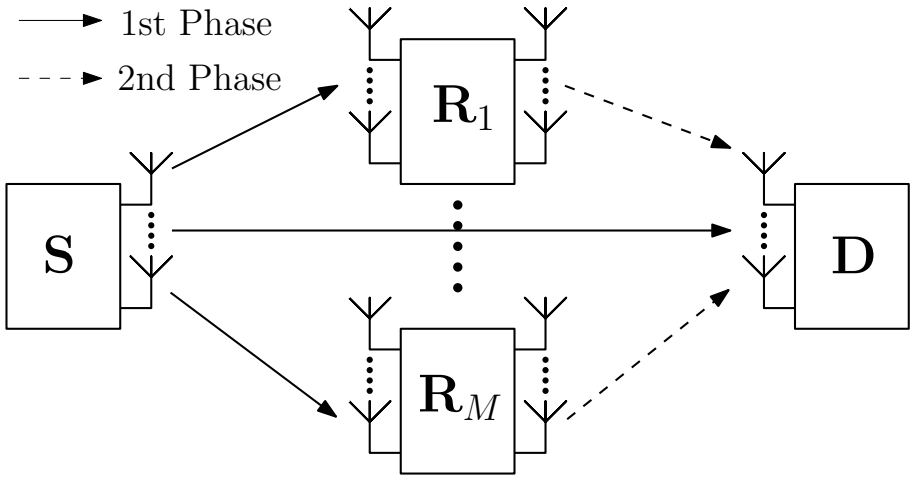

Figure 2.3: MIMO two-phase multiple relay system model

from the relay changes. For AF, the second phase transmission is described as:

$$\mathbf{y}_{rd} = \mathbf{H}_{rd}\gamma_r\mathbf{y}_{sr} + \mathbf{n}_d^{(2)} \tag{2.4}$$

where the scalar γ_r is the AF amplification factor calculated at the relay. There are a number of ways of calculating the amplification factor in literature, but the commonly used method designed to normalise the average power output of the relay to unity power is as follows:

$$\gamma_r = \sqrt{\frac{1}{\|\mathbf{H}_{sr}\|_F^2 + {\sigma_n}^2}}, \tag{2.5}$$

where σ_n^2 is the variance of the random noise, which is often modelled as complex Gaussian random variables with zero mean.

For DF systems, the amplification factor and the received signal are replaced by an estimate of the data symbols transmitted from the source, estimated by the detection and decoding algorithm used at the relay which is described by:

$$\mathbf{y}_{rd} = \mathbf{H}_{rd}\tilde{\mathbf{x}}_r + \mathbf{n}_d^{(2)}, \tag{2.6}$$

where $\tilde{\mathbf{x}}_r$ is the vector of the estimated data symbols at the relay. An extension of the single relay system is the multiple relay system, where there are M relays receiving the signal transmitted from the source device in the first phase, which all transmit the forwarded signal simultaneously to the destination in the second phase, as shown in Figure 2.3.

This system's transmission phases can be described similarly to the single relay system, but now most symbols with the r subscript have an extended subscript to take into account the extra relays, by means of a relay number m that the symbol is associated with. In effect, the individual receive vectors, channel matrices and noise vectors for each relay can be stacked or summed to produce the same form of equations as for a single vector.

$$\begin{bmatrix} \mathbf{y}_{sr_1} \\ \vdots \\ \mathbf{y}_{sr_M} \end{bmatrix} = \begin{bmatrix} \mathbf{H}_{sr_1} \\ \vdots \\ \mathbf{H}_{sr_M} \end{bmatrix} \mathbf{x} + \begin{bmatrix} \mathbf{n}_{r_1} \\ \vdots \\ \mathbf{n}_{r_M} \end{bmatrix} \tag{2.7}$$

$$\mathbf{y}_{rd} = \sum_{m=1}^{M} \mathbf{H}_{rd_m} \gamma_{r_m} \mathbf{y}_{sr_m} + \mathbf{n}_d^{(2)} \tag{2.8}$$

Eq. (2.7) and Eq. (2.8) describe the form of the signal vectors for the first and second phases of transmission involving the relays for an AF system. The direct transmission from the source to the destination remains the same.

2.2.3 Channel and Noise Modelling

In previous sections, the quantities $\mathbf{H}$ and $\mathbf{n}$ have been used to represent the channel (*i.e.* the medium in which the signal travels through) and the noise at the receive antennas respectively. These values, or the parameters that dictate these values, are important to model in a relatively realistic way, as these quantities can affect the performance of the whole system to a great degree. The values that make up the channel and noise quantities at each time instant are usually randomly generated, but the parameters governing the generation of these values can vary.

Channel values are defined by statistical probability distributions, which have parameters such as mean and variance that will affect the properties and form of the probability functions. The channel values are represented by a complex number within the system model, as are most other values such as the transmitted and received signals and the noise values, and typically distribution of the magnitude of the complex values, and the distribution of the separate real and imaginary components are dictated by statistical

probability distributions. The most common channel distribution for the magnitude of the channel coefficients is the Rayleigh distribution [21] and occurs when the real and imaginary components have Gaussian distributions. Rayleigh fading is considered for systems in which the line-of-sight (LOS) propagation between the source and destination is not significant. Alternative probability distributions that can be considered include the Rician [22], Weibull [23], Nakagami [26] and log-normal distributions [27].

A Rician channel distribution can be used to model a scenario where a particular path of transmission in a multiple path channel has much more power than the other channel paths, typically the LOS path. A Weibull probability distribution can be used in modelling dispersion of signals in a channel due to significant amounts of clutter in the transmission area, and can approximate the Normal distribution for certain parameter definitions. A Weibull distribution has also been shown to provide good fits to empirically measured channel measurements in some scenarios [24], [25]. The Nakagami distribution is related to a gamma distribution in mathematics, and has been used to approximate environments with multiple signal propagation effects. The Log-normal distribution is useful in that any quantity that has a normal distribution on a linear scale will have a log-normal distribution in a logarithmic scale.

However, choosing a distribution only defines the characteristics of a single overall effect on the channel. Other factors may affect the overall channel value, such as distance-based fading and shadowing. Distance based fading (or path loss) is a representation of how a signal is attenuated the further it travels in the medium the system operates within, and can be heavily affected by the signal environment [28], [25]. An exponential based path loss model can be described by:

$$\alpha = \frac{\sqrt{L}}{\sqrt{d^{\rho}}}, \tag{2.9}$$

where α is the distance based path loss, L is the known path loss at a base distance D, d is the distance of interest relative to D and ρ is the path loss exponent, which can be varied to account for the environment. ρ is typically set between 2 and 5, with a lower value representing a clear and uncluttered environment which has a slow attenuation and a higher value describing a cluttered and highly attenuating environment [29].

Shadow fading describes the phenomenon where objects can obstruct the propagation of the signal, and thus attenuate the signal further. Shadowing can also be described as a random variable with a probability distribution, and for the case of large scale fading (where the random variables change slowly over time), a common function used is the log-normal probability distribution given by:

$$\beta = 10^{\left(\frac{\sigma_s \mathcal{N}(0,1)}{10}\right)} \tag{2.10}$$

where β is the shadowing variable, $\mathcal{N}(0,1)$ represents a Gaussian distribution with mean zero and unit variance and σ_s is the shadowing spread in dB. The shadowing spread represents the severity of the attenuation of the shadow fading, and is typically given between 0-9dB. A channel model which has Rayleigh fading, with path-loss and shadowing can thus be described as:

$$\mathbf{H} = \alpha\beta\mathbf{H}_o, \tag{2.11}$$

where $\mathbf{H}_o$ is the base Rayleigh distributed channel.

Noise in communication systems is normally modelled as additive white Gaussian noise (AWGN) in both the real and imaginary parts of a signal, which represents the random noise that the receiving device receives in addition to the signal that has been modified by the channel. AWGN is modelled as a complex Gaussian process with a mean of zero and a variance of σ_n^2, with the variance defining the power of the noise, as below:

$$\mathbf{n} = \left(\frac{\sigma_n}{\sqrt{2}}\right)\mathcal{CN}(0,1), \tag{2.12}$$

where $\mathcal{CN}(0,1)$ represents a complex normal or Gaussian distribution with mean zero and unit variance, and σ_n is given by:

$$\sigma_n = \sqrt{\frac{1}{SNR}} \tag{2.13}$$

Typically, a system's performance is measured over a range of signal-to-noise ratio (SNR), with the signal's power remaining the same, and the variance (and thus power) of the noise values being varied to determine the performance of the system in different SNR conditions. Other noise models that can be considered are brown noise and pink noise, so called 'coloured' noise models [30], [31], [32].

2.2.4 Channel Coding

Channel coding is a process operating at the transmitter and the receiver, manipulating the raw bit data to be transmitted at the transmitter before conversion to symbols, and attempting to undo that manipulation at the receiver after demodulation to reconstruct the original data bits [33], [34]. Channel coding is designed to add redundancy in the form of extra parity bits to a transmission, thus reducing the efficiency of the transmission, but with the objective of reducing the BER at the receiver. There are two types of functions associated with channel coding, automatic repeat-request (ARQ) and forward error correction (FEC). ARQ is designed to just detect errors, and if errors are detected the receiver sends a message back to the transmitter requesting that the last transmission is repeated, in an effort to correct the transmitted data a second time. FEC techniques actually try and correct errors with the received data transmission, requiring less retransmission of data, but they generally need a greater complexity in design and processing than ARQ.

For error correction codes (ECC), a common type of codes are convolutional codes [35], [36] which are constructed such that the output of b bits are dependent on the previous a bits, where a is the memory length of the code (as well as the order of the generator polynomial that defines the code) and where $b \geq a$, giving the rate of the code as $\frac{a}{b}$. Convolutional codes encode the input data as a stream, and a convolutional code has a length of c input bits that are used for encoding at every a bit instance(s). Associated with convolutional codes is the generator polynomial, which determines how the c input bits are added together with modulo-2 addition, and is typically defined as b row vectors of length c.

The decoding of convolutional codes is implemented through the use of trellis style decoders, based upon Markov modelling and state based transitions, the most common of which that implement maximum likelihood decoding is the Viterbi algorithm [37], [38], but other decoders are available, such as the BCJR algorithm [39], which operates using the maximum a posteriori (MAP) criterion.

Iterative detection and decoding (IDD) methods are techniques which refine the estimates of the transmitted bits several times per time instance by iteratively passing information between the detector and decoder at the receiver, improving the accuracy of

the estimates with each iteration. Two high-performance classes of FEC codes are turbo codes [40, 41], and low-density parity check (LDPC) codes [42], which are implemented in current commercial wireless communication systems [43, 44].

2.3 Parameter Estimation

During the operation of a communications system, some algorithms and processes that are used in the system will require knowledge of quantities or values within the system which may not be available to the device computing the algorithms. Examples of these values include the channel state information (CSI), noise variance, shadowing parameters and relay locations, or for other parameters that may not be known a priori such as the receive filters at the destination device, which may be required for the operation of the system.

Channel estimation techniques are designed to determine accurately the current values of the channel that the system is transmitting through, and can be crucial to the successful operation of a communication system setup, as a large amount of detection techniques for the recovery of transmitted data require accurate knowledge of the channel to perform well. It is unlikely that the system will have any prior knowledge of the channel values in a real system, and also the likelihood is that the channel will randomly change between or during the transmission of signals.

A common set of methods of determining the channel values are data-aided methods, where the transmitter and receiver have prior knowledge of a set of data called pilot data [45]. Pilot data are perfectly known to both devices, and as such the receiver can use the received signal to determine how the data have been altered by the channel, and thus the channel values. Pilot data can be transmitted immediately before the information data is transmitted as to provide the most accurate representation of the channel values at that time, assuming the channel does not change significantly during the transmission of the information data.

For cooperative systems, it is generally required that the channels for each transmission link in the system (source to destination, source to relays and relays to destination) are

known, and so when channel estimation techniques are applied, each channel needs to be estimated [46], [47]. For a DF system, the destination only requires the source to destination and relays to destination channel knowledge for the purposes of detection algorithms, with the relays requiring the source to relays channel knowledge, but for AF, the destination requires knowledge of all the channels in the system for detection methods.

Firstly, the simplest method of channel estimation is the least squares (LS) channel estimation technique [48], [49], [50], but the mean square error (MSE) performance of this method is typically not adequate in low SNR regions. The LS channel estimation method in a MIMO system is derived as follows from an initial cost function:

$$\begin{aligned}
\mathcal{E} &= E[\|\mathbf{Y} - \hat{\mathbf{H}}\mathbf{G}\|^2], \\
&= E[(\mathbf{Y} - \hat{\mathbf{H}}\mathbf{G})(\mathbf{Y} - \hat{\mathbf{H}}\mathbf{G})^H] \\
&= E[\mathbf{Y}\mathbf{Y}^H] - E[\hat{\mathbf{H}}\mathbf{G}\mathbf{Y}^H] - E[\mathbf{Y}\mathbf{G}^H\hat{\mathbf{H}}^H] + E[\hat{\mathbf{H}}\mathbf{G}\mathbf{G}^H\hat{\mathbf{H}}^H], \\
\frac{\partial \mathcal{E}}{\partial \hat{\mathbf{H}}^H} &= -E[\mathbf{Y}\mathbf{G}^H] + E[\hat{\mathbf{H}}\mathbf{G}\mathbf{G}^H] = 0, \\
\hat{\mathbf{H}} &= \mathbf{Y}\mathbf{G}^\dagger.
\end{aligned} \tag{2.14}$$

where † represents the MoorePenrose pseudoinverse, $\mathbf{G}$ is the pilot data transmitted that forms the received signal matrix $\mathbf{Y}$ and $\hat{\mathbf{H}}$ is the estimated channel matrix of the MIMO system that $\mathbf{G}$ has been transmitted through.

A refinement of the LS method is the minimum mean square error (MMSE) channel estimation method [51], [52], [53] which takes into account the noise at the receive antennas, improving performance over the LS method at low SNR regions and is derived as follows by substituting $\hat{\mathbf{H}}$ with a filter matrix $\mathbf{W}_{CE}$ multiplied by the received matrix $\mathbf{Y}$:

$$
\begin{aligned}
\mathcal{E} &= E[\|\mathbf{H} - \hat{\mathbf{H}}\|^2], \\
&= E[\|\mathbf{H} - \mathbf{W}_{CE}\mathbf{Y}\|^2], \\
&= E[(\mathbf{H} - \mathbf{W}_{CE}\mathbf{Y})(\mathbf{H} - \mathbf{W}_{CE}\mathbf{Y})^H], \\
&= E[\mathbf{H}\mathbf{H}^H] - E[\mathbf{W}_{CE}\mathbf{Y}\mathbf{H}^H] - E[\mathbf{H}\mathbf{Y}^H\mathbf{W}_{CE}^H] + E[\mathbf{W}_{CE}\mathbf{Y}\mathbf{Y}^H\mathbf{W}_{CE}^H], \\
\frac{\partial \mathcal{E}}{\partial \mathbf{W}_{CE}^H} &= -E[\mathbf{H}\mathbf{Y}^H] + E[\mathbf{W}_{CE}\mathbf{Y}\mathbf{Y}^H] = 0, \\
E[\mathbf{H}\mathbf{Y}^H] &= E[\mathbf{W}_{CE}\mathbf{Y}\mathbf{Y}^H], \\
\mathbf{R}_{HH}\mathbf{G}^H &= \mathbf{W}_{CE}(\mathbf{G}\mathbf{R}_{HH}\mathbf{G}^H + \mathbf{I}\sigma_n^2), \\
\mathbf{W}_{CE} &= \mathbf{R}_{HH}\mathbf{G}^H(\mathbf{G}\mathbf{R}_{HH}\mathbf{G}^H + \mathbf{I}\sigma_n^2)^{-1}, \\
\hat{\mathbf{H}} &= \mathbf{W}_{CE}\mathbf{Y},
\end{aligned}
\tag{2.15}
$$

where $\mathbf{R}_{HH}$ is the auto-correlation matrix of $\mathbf{H}$, also defined as:

$$
\mathbf{R}_{HH} = E[\mathbf{H}\mathbf{H}^H] \tag{2.16}
$$

Although the MMSE channel estimation method can offer gains over the LS method, $\mathbf{R}_{HH}$ and σ_n need to also be estimated, but it is possible to estimate these during the pilot data transmission. Figure 2.4 shows a plot of the MSE performance of the LS and MMSE channel estimators for a QPSK 4x4 MIMO system, and it can be seen that the MMSE channel estimator has a lower MSE than the LS method, especially in the low SNR region.

2.4 Resource Allocation

In a MIMO system there are a number of resources available which the communication system can use or exploit, but in a given environment there are many ways in which the resources can be distributed, and this distribution could be optimised in order to maximise and minimise particular metrics such as BER, capacity, throughput etc. Examples of resources that can be allocated in a cooperative system include the transmission power allocated to each antenna on a device, and between the relays in the system considering any transmission power constraints imposed, the partitioning of bandwidth between de-

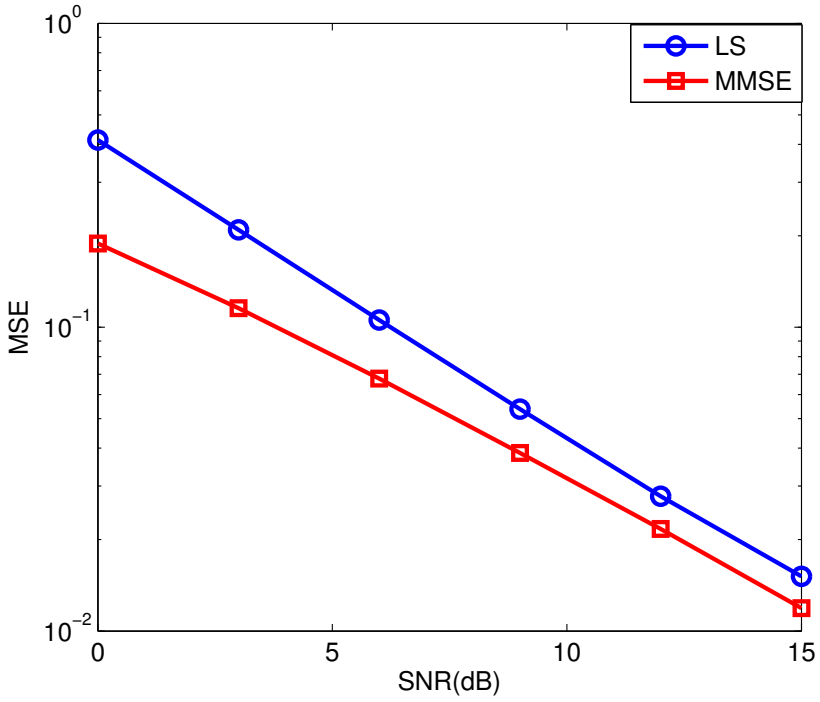

Figure 2.4: Comparison of MSE performance of LS and MMSE channel estimators in a 4x4 QPSK point-to-point MIMO system

vices or users in the system, the selection of relays within the system to cooperate with from a prospective pool of relay devices etc [54–56].

The transmission power of a device is defined as the total power that the device uses to transmit in a time instant, but for a fair comparison with MIMO systems with different numbers of antennas, or with single antenna systems, it can be necessary to set the power of each antenna on a MIMO system to a fraction of the overall power to ensure the transmission power remains constant over the different scenarios. A simple way of distributing power is to share the power equally across the antennas, but BER gains can be obtained by altering the individual transmit power of each antenna based upon the scenario the system is operating in. For a cooperative system, the transmission power can be defined differently, as the total power that is transmitted in the system, or as the transmission power per device in the system, with it being possible that the source and relay devices have different transmission power limitations. If any of the devices in the cooperative system have multiple antennas, then the transmission power per antenna may vary between the different devices also.

Similar to channel estimation techniques, it is possible to use pilot data to create a data aided method of determining a better power distribution across antennas. One such method is the least mean squares (LMS) method, which is a stochastic gradient (SG) descent technique [57]. If we assume a MIMO system as below, considering the power allocation vector $\mathbf{a}$, where each value of the vector corresponds to a different antenna and it's transmission power:

$$\mathbf{y} = \mathbf{H}\mathbf{X}_d\mathbf{a} + \mathbf{n}, \tag{2.17}$$

where $\mathbf{X}_d$ represents diag$(\mathbf{x})$ which consists of pilot data, we can define a cost function to minimise the error between the received signal and the transmitted data through the channel:

$$\begin{aligned} \hat{\mathbf{a}} &= \arg \min_{\mathbf{a} \in \mathcal{C}^{N_t \times 1}} \|\mathbf{y} - \mathbf{H}\mathbf{X}_d\mathbf{a}\|^2, \\ \mathcal{E} &= (\mathbf{y} - \mathbf{H}\mathbf{X}_d\mathbf{a})^H(\mathbf{y} - \mathbf{H}\mathbf{X}_d\mathbf{a}), \\ \frac{\partial \mathcal{E}}{\partial \mathbf{a}^H} &= -\mathbf{X}_d^H\mathbf{H}^H\mathbf{y} + \mathbf{X}_d^H\mathbf{H}^H\mathbf{H}\mathbf{X}_d\mathbf{a}, \\ &= \mathbf{X}_d^H\mathbf{H}^H\mathbf{e}, \end{aligned} \tag{2.18}$$

where $\mathcal{E}$ is the mean squared error, and $\mathbf{e}$ is the estimation error vector, calculated as:

$$\mathbf{e} = \mathbf{y} - \mathbf{H}\mathbf{X}_d\mathbf{a}. \tag{2.19}$$

With a minimised error expression defined, it is possible to use this as a correction factor with a small step size μ, in order to update the estimate $\hat{\mathbf{a}}$ at every time instance i, forming the SG method that is designed to converge on a local optimum, thus giving:

$$\hat{\mathbf{a}}[i+1] = \hat{\mathbf{a}}[i] + \mu\mathbf{X}_d^H\mathbf{H}^H\mathbf{e}. \tag{2.20}$$

However, in the case of $\hat{\mathbf{a}}$ is restricted to a maximum transmit power, the returned value from the SG method must be normalised to a maximum transmit power P as follows:

$$\hat{\mathbf{a}}_n = \frac{\hat{\mathbf{a}}\sqrt{P}}{\sqrt{\mathrm{tr}(\hat{\mathbf{a}}\hat{\mathbf{a}}^H)}}, \tag{2.21}$$

where $\hat{\mathbf{a}}_n$ is the normalised power allocation vector. For a cooperative system, the power across different relay can be distributed in a similar fashion, if $\mathbf{a}$ is the result of stacking each relay's power vector with the source antenna power vector, and $\mathbf{y}$ is the stacked received signal at the destination from both the source and relay's in the two phases of

transmission.

Relay selection or link selection can be interpreted as a form of power allocation, but in this case the relay can be assigned no power, and so effectively is not present in the system in that scenario. This allows the system to be designed to select relays in cooperative system according to an algorithm with which to cooperate. This can be crucial to a system's performance, as this allows the system to discard relays which may be in a disadvantageous position, which can cause performance loss if included, and also to free up relays for other potential users in the system for which the relay may be useful [90–94].

2.5 Detection Techniques

Detection techniques are the methods by which a device can attempt to recover or reconstruct the transmitted data from a received signal, through the use of filtering, searches and algorithmic processes. The main detection techniques areas that will be highlighted here are the linear techniques that rely on a filter [58], [59], [60], the extension of linear techniques for certain types of signals known as Widely Linear (WL) techniques [61], [62], [63], [64], Successive Interference Cancellation (SIC) detection which is based upon the cancellation of multiple data streams as interference [65], [66], and the concept of ML detection [67], [68].

2.5.1 Linear Detection

Linear detection techniques are derived from cost functions designed to reduce the difference between two values. The two commonly used linear detection techniques are the zero forcing (ZF) [58], [59] and MMSE detectors [60], [69], [70]. The ZF method is derived from the cost function:

$$\mathcal{E} = E[\|\mathbf{y} - \mathbf{H}\hat{\mathbf{x}}\|^2], \tag{2.22}$$

where $\mathcal{E}$ is the cost function error and $\hat{\mathbf{x}}$ is the estimated transmitted symbols. From this cost function, the ZF solution can be derived as a filter $\mathbf{W}_{ZF}$:

$$\begin{aligned}
\mathcal{E} &= E[\|\mathbf{y} - \mathbf{H}\hat{\mathbf{x}}\|^2], \\
&= E[(\mathbf{y} - \hat{\mathbf{H}}\hat{\mathbf{x}})^H(\mathbf{y} - \hat{\mathbf{H}}\hat{\mathbf{x}})] \\
&= E[\mathbf{y}^H\mathbf{y}] - E[\mathbf{y}^H\hat{\mathbf{H}}\hat{\mathbf{x}}] - E[\hat{\mathbf{x}}^H\hat{\mathbf{H}}^H\mathbf{y}] + E[\hat{\mathbf{x}}^H\hat{\mathbf{H}}^H\hat{\mathbf{H}}\hat{\mathbf{x}}], \\
\frac{\partial\mathcal{E}}{\partial\hat{\mathbf{x}}^H} &= -E[\mathbf{H}^H\mathbf{y}] + E[\hat{\mathbf{H}}^H\hat{\mathbf{H}}\hat{\mathbf{x}}] = 0, \\
\hat{\mathbf{x}} &= (\mathbf{H}^H\mathbf{H})^{-1}\mathbf{H}^H\mathbf{y} = \mathbf{H}^\dagger\mathbf{y} = \mathbf{W}_{ZF}\mathbf{y}.
\end{aligned} \tag{2.23}$$

The ZF solution is simple to calculate and only requires the knowledge of the channel, but the accuracy of $\hat{\mathbf{x}}$ suffers as compared to other detectors, especially at lower SNR values, as there is no attempt to compensate for the noise at the receiver.

The MMSE filter detector is also derived from a cost function, but instead focuses on the optimisation of a filter matrix $\mathbf{W}_M$, which is applied to the received signal to produce $\hat{\mathbf{x}}$, as follows:

$$\begin{aligned}
\mathcal{E} &= E[\|\mathbf{x} - \hat{\mathbf{x}}\|^2], \\
&= E[\|\mathbf{x} - \mathbf{W}_M^H\mathbf{y}\|^2], \\
&= E[(\mathbf{x} - \mathbf{W}_M^H\mathbf{y})(\mathbf{x} - \mathbf{W}_M^H\mathbf{y})^H], \\
&= E[\mathbf{x}\mathbf{x}^H] - E[\mathbf{W}_M^H\mathbf{y}\mathbf{x}^H] - E[\mathbf{x}\mathbf{y}^H\mathbf{W}_M] + E[\mathbf{W}_M^H\mathbf{y}\mathbf{y}^H\mathbf{W}_M], \\
\frac{\partial\mathcal{E}}{\partial\mathbf{W}_M^H} &= -E[\mathbf{y}\mathbf{x}^H] + E[\mathbf{y}\mathbf{y}^H]\mathbf{W}_M = 0, \\
E[\mathbf{y}\mathbf{x}^H] &= E[\mathbf{y}\mathbf{y}^H]\mathbf{W}_M, \\
\mathbf{H} &= (\mathbf{H}\mathbf{H}^H + \mathbf{I}\sigma_n^2)\mathbf{W}_M, \\
\mathbf{W}_M &= (\mathbf{H}\mathbf{H}^H + \mathbf{I}\sigma_n^2)^{-1}\mathbf{H}, \\
\hat{\mathbf{x}} &= \mathbf{W}_M^H\mathbf{y},
\end{aligned} \tag{2.24}$$

It can be seen that the ZF and MMSE filter solutions have similar forms, with the MMSE filter incorporating the variance of the receive antenna noise. The addition of this variance value improves the accuracy of the MMSE detector at low SNR values, but it should be

noted that at high SNR values, $\sigma_n \to 0$, and so the MMSE filter tends to the ZF filter.

2.5.2 WL Filtering

WL filtering [71], [72], [73] is an extension of the linear filtering discussed in the previous section, and is applicable in systems where the received signal is non-circular, *i.e.* the received signal has an imbalance between the average in-phase and quadrature amplitudes. The more extreme examples of this include modulation schemes that only use either the in-phase of quadrature components, such as BPSK or amplitude shift-keying (ASK) schemes. WL filtering takes advantage of the extra potential diversity present in the I-Q imbalance to improve the accuracy of the estimated data by introducing a second filter that operates on the complex conjugate of the received signal in addition to the standard linear filter.

The cost function of the WL filter follows the same form as the MMSE filter is:

$$\mathcal{E} = E[\|\mathbf{x} - \mathbf{F}^H\mathbf{y} - \mathbf{G}^H\mathbf{y}^*\|^2], \tag{2.25}$$

where $\mathbf{F}$ and $\mathbf{G}$ are the WL filters. The derivation of the WL filters is more complex than that of the linear filters, and so the derivation will be detailed here. The objective is to choose $\mathbf{F}$ and $\mathbf{G}$ such that $\mathcal{E}$ is minimised. If $\mathcal{E}$ is expanded, and the partial derivative of the expansion is taken with respect to $\mathbf{F}^H$ and $\mathbf{G}^H$ separately, the following two expressions are formed:

$$\frac{\partial \mathcal{E}}{\partial \mathbf{F}} = \mathbf{E}[\mathbf{y}\mathbf{y}^H]\mathbf{F} + \mathbf{E}[\mathbf{y}\mathbf{y}^T]\mathbf{G} - \mathbf{E}[\mathbf{y}\mathbf{x}^H] = \mathbf{0}, \tag{2.26}$$

$$\frac{\partial \mathcal{E}}{\partial \mathbf{G}} = \mathbf{E}[\mathbf{y}^*\mathbf{y}^H]\mathbf{F} + \mathbf{E}[\mathbf{y}^*\mathbf{y}^T]\mathbf{G} - \mathbf{E}[\mathbf{y}^*\mathbf{x}^H] = \mathbf{0}. \tag{2.27}$$

It is assumed that $\mathbf{x}$ has entries that are independent, but identically distributed, that $\mathbf{n}$ has independent but identically distributed entries also, with $\mathbf{x}$ and $\mathbf{n}$ being statistically independent from each other. From these assumptions, we can also assume that:

$$\mathbf{E}[\mathbf{x}\mathbf{x}^H] = \mathbf{I}\sigma_x^2, \mathbf{E}[\mathbf{n}\mathbf{n}^H] = \mathbf{I}\sigma_n^2 \tag{2.28}$$

$$\mathbf{E}[\mathbf{x}\mathbf{n}^H] = 0, \mathbf{E}[\mathbf{n}\mathbf{x}^H] = 0 \tag{2.29}$$

Using the above defined expectations, we can now expand and calculate the expectation results in Eq.(2.26) as follows:

$$\mathbf{E}[\mathbf{y}\mathbf{y}^H] = \mathbf{E}[(\mathbf{H}\mathbf{x}+\mathbf{n})(\mathbf{H}\mathbf{x}+\mathbf{n})^H] = \mathbf{H}\mathbf{H}^H + \mathbf{I}\sigma_n^2 \tag{2.30}$$

$$\mathbf{E}[\mathbf{y}\mathbf{y}^T] = \mathbf{E}[(\mathbf{H}\mathbf{x}+\mathbf{n})(\mathbf{H}\mathbf{x}+\mathbf{n})^T] = \mathbf{H}\mathbf{H}^T\sigma_x^2 \tag{2.31}$$

$$\mathbf{E}[\mathbf{y}\mathbf{x}^H] = \mathbf{E}[(\mathbf{H}\mathbf{x}+\mathbf{n})\mathbf{x}^H] = \mathbf{H}\sigma_x^2 \tag{2.32}$$

Similarly, we can expand the expectations from Eq.(2.27) as below:

$$\mathbf{E}[\mathbf{y}^*\mathbf{y}^H] = \mathbf{E}[(\mathbf{H}\mathbf{x}+\mathbf{n})^*(\mathbf{H}\mathbf{x}+\mathbf{n})^H] = (\mathbf{H}\mathbf{H}^T)^*\sigma_x^2 \tag{2.33}$$

$$\mathbf{E}[\mathbf{y}^*\mathbf{y}^T] = \mathbf{E}[(\mathbf{H}\mathbf{x}+\mathbf{n})^*(\mathbf{H}\mathbf{x}+\mathbf{n})^T] = (\mathbf{H}\mathbf{H}^H\sigma_x^2 + \mathbf{I}\sigma_n^2)^* \tag{2.34}$$

$$\mathbf{E}[\mathbf{y}^*\mathbf{x}^H] = \mathbf{E}[(\mathbf{H}\mathbf{x}+\mathbf{n})^*\mathbf{x}^H] = \mathbf{H}^*\sigma_x^2 \tag{2.35}$$

Note that if the modulation scheme used is circular, such as QPSK, then $\mathbf{E}[\mathbf{x}\mathbf{x}^T] = 0$, in which case Eqs.(2.31),(2.33) and (2.35) are reduced to zero.

Now, if Eq.(2.26) and Eq.(2.27) are rearranged to isolate $\mathbf{F}$ and $\mathbf{G}$ respectively, we get:

$$\mathbf{F} = (\mathbf{H}\mathbf{H}^H + \mathbf{I}\frac{\sigma_n^2}{\sigma_x^2})^{-1}(\mathbf{H} - \mathbf{H}\mathbf{H}^T\mathbf{G}) \tag{2.36}$$

$$\mathbf{G} = (\mathbf{H}\mathbf{H}^H + \mathbf{I}\frac{\sigma_n^2}{\sigma_x^2})^{-*}(\mathbf{H}^* - \mathbf{H}^*\mathbf{H}^H\mathbf{F}) \tag{2.37}$$

Then, solving Eq.(2.36) and Eq.(2.37) as simultaneous equations to isolate $\mathbf{F}$ and $\mathbf{G}$, we get the final result:

$$\mathbf{F} = (\mathbf{R}_{hh} - \mathbf{R}_{ht}\mathbf{R}_{hh}^{-*}\mathbf{R}_{ht}^*)^{-1}(\mathbf{H} - \mathbf{R}_{ht}\mathbf{R}_{hh}^{-*}\mathbf{H}^*) \in \mathbb{C}^{RxK} \tag{2.38}$$

$$\mathbf{G} = (\mathbf{R}_{hh} - \mathbf{R}_{ht}\mathbf{R}_{hh}^{-*}\mathbf{R}_{ht}^*)^{-*}(\mathbf{H}^* - \mathbf{R}_{ht}^*\mathbf{R}_{hh}^{-1}\mathbf{H}) \in \mathbb{C}^{RxK} \tag{2.39}$$

where

$$\mathbf{R}_{hh} = \mathbf{H}\mathbf{H}^H\sigma_x^2 + \mathbf{I}\sigma_n^2 \in \mathbb{C}^{KxK} \tag{2.40}$$

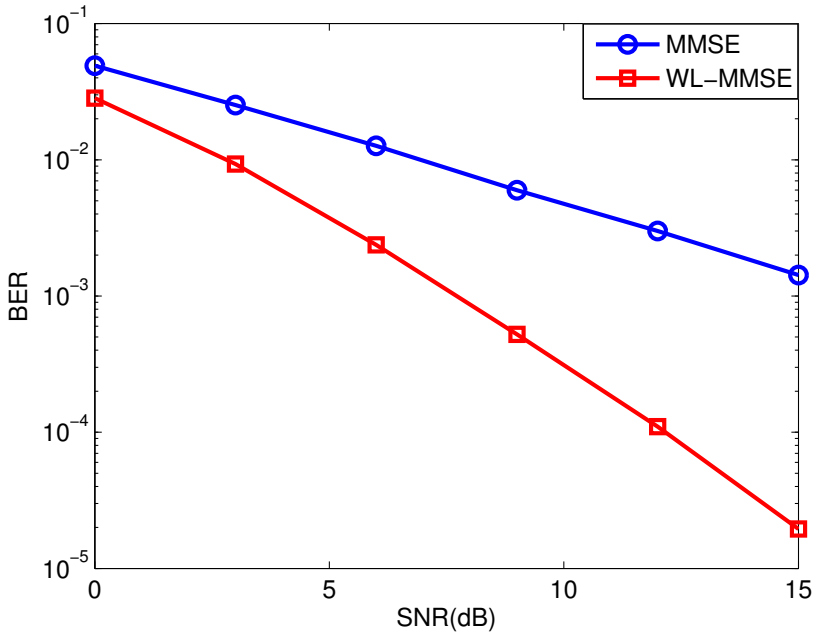

Figure 2.5: Comparison between linear and WL detector in a 4x4 BPSK point-to-point MIMO system

$$\mathbf{R}_{ht} = \mathbf{H}\mathbf{H}^T\sigma_x^2 \in \mathbb{C}^{K\text{x}K} \tag{2.41}$$

As can be seen, the calculation of these filters is more complex than the standard linear filters, but the performance gain over linear techniques in the presence of non-circular data can be significant. Figure 2.5 shows a comparison plot of the BER performances of a linear MMSE and a WL MMSE detector operating in a 4x4 BPSK MIMO system. It can be seen that the WL method gives large SNR gains over the linear detector in this system, even in the low SNR region, which can make the adoption of WL methods in this type of system desirable, despite the increased complexity cost associated with WL methods as compared to linear techniques.

2.5.3 SIC Detection

The method of SIC [6], [74], [75], [76], [77] is based upon the theory that if in a system where multiple signals are interfering with each other, if each signal is estimated individually serially, then the interference effects of an estimated signal can be removed from the signals that have yet to be estimated, thus increasing the reliability of estimation of the remaining signals. The SIC process can increase the accuracy of the transmitted data es-

Table 2.1: Successive Interference Cancellation Algorithm

Initialisation: $\mathbf{y}_0 = \mathbf{y}, \mathbf{H}_0 = \mathbf{H}$

for $i = 1 \rightarrow N_t$ **do**
$\mathbf{W}_i = (\mathbf{H}_i {\mathbf{H}_i}^H + \mathbf{I}\sigma_n^2)^{-1}\mathbf{H}_i$
$\hat{\mathbf{x}}_i = \mathbf{W}_i^H \mathbf{y}_{i-1}$
$\tilde{x}_i = \mathcal{Q}[\hat{x}_i]$
$\mathbf{y}_i = \mathbf{y}_{i-1} - \tilde{x}_i \mathbf{h}_i$
$\mathbf{H}_i = {\mathbf{H}'}_{i-1}^{\langle i \rangle}$
end for

$\mathbf{h}_i$ represents the ith column of $\mathbf{H}$
$\mathbf{H}'^{\langle i \rangle}$ represents $\mathbf{H}$ with the ith column removed
$\mathcal{Q}[\bullet]$ represents the quantise function

timate $\hat{\mathbf{x}}$ as compared with the linear methods. The linear MMSE filter detection method is commonly used within this process to estimate the symbols in the received signal of a MIMO system, the estimate is then quantised appropriately for the modulation scheme being used in the system. Table 2.1 and Figure 2.6 describe the algorithm used for the SIC process.

However, if the quantised estimate $\tilde{x}_i$ is estimated incorrectly within the process, the cancelled interference in the process will be incorrect, and so can increase the likelihood that the subsequent quantised estimates will also be incorrect. This effect is known as error propagation in the SIC algorithm, and can detrimentally affect the performance of the SIC algorithm considerably.

A common method to reduce the likelihood of error propagation occurring is to cancel the signal with the highest received power first, and then the second most powerful and so on. The principle of this method is to remove the signal that causes the most interference first, so that the subsequent estimates have a greater chance of being estimated correctly, and also the signal with the highest power is less likely to be estimated incorrectly due to the interference form the other signal present. The signal with the highest average power can be found by taking the magnitude of the associated channel $\mathbf{h}$ for each signal, and then sorting from the largest to the smallest. This method is known as the ordered SIC (OSIC) or associated with the vertical bell labs space-time architecture (VBLAST) method [78], and can be shown to improve the BER performance of the SIC.

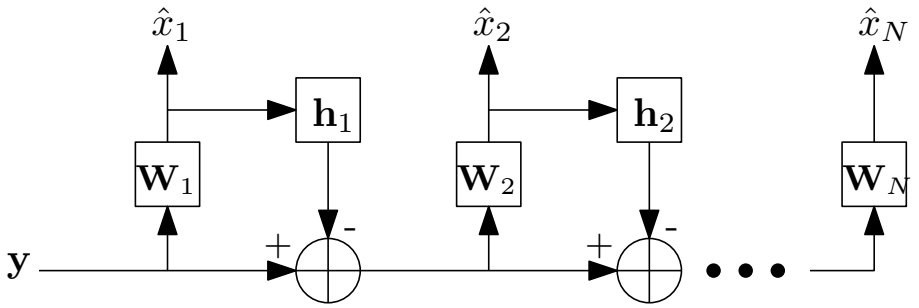

Figure 2.6: SIC Algorithm

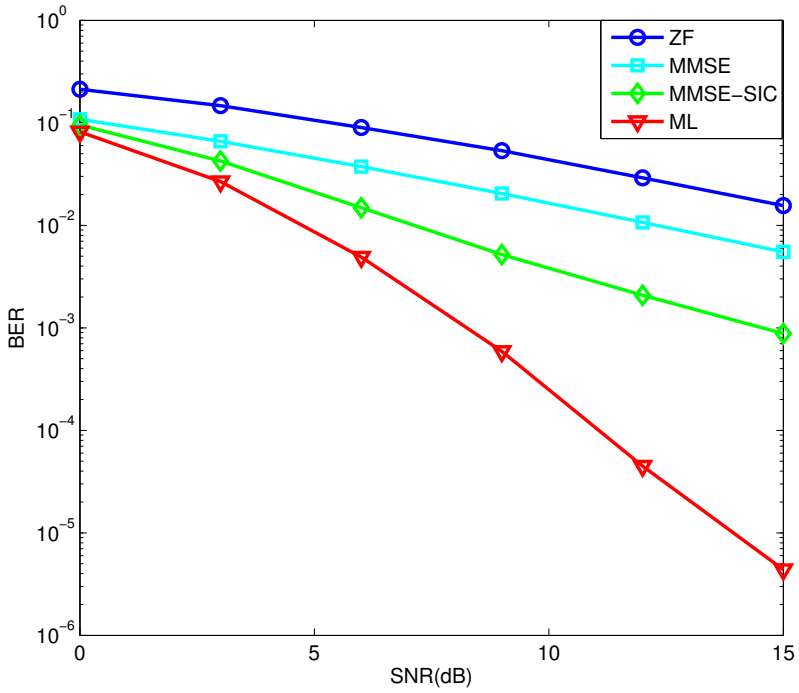

Figure 2.7: Comparison of BER performance of different detectors in a QPSK 4x4 point-to-point MIMO system

2.5.4 ML Detection

ML detection [67], [68] is a high-complexity high-performance technique that is typically used as a benchmark for BER performance when assessing the performance of another detection algorithm in an uncoded hard decision system. ML estimation is a search algorithm that compares every possibility in a set space in a cost function, and returns the possibility that satisfies the cost function to the greatest degree.

In the case of a MIMO communications system, this means testing every possible

symbol combination (and thus bit combination) on every antenna that could have been transmitted, and finding the Euclidean distance of the received signal to the symbol combination multiplied by the channel matrix, as seen below:

$$\hat{\mathbf{x}} = \arg\min_{\mathbf{x}_c \in Z}(\|\mathbf{y} - \mathbf{H}\mathbf{x}_\mathbf{c}\|^2), c = 1 \dots N_t M \tag{2.42}$$

where $\mathbf{x}_c$ is the transmission possibility being tested, M is the number of bits per symbol as according the modulation scheme being used and Z is the set space containing all possible symbol combinations. The symbol combination with the smallest Euclidean distance in the above cost function is then returned as the transmitted symbol estimate.

This method can produce very high accuracy as compared with the other detection methods in this chapter, however the computational complexity of ML estimation is by far the highest of the methods discussed due to having the test every possibility, and the complexity scales exponentially higher when additional bits per symbol are used, or the number of receive antennas is increased, making it impractical to use [79]. Figure 2.7 shows a plot comparing the BER performances of the different detectors discussed in a 4x4 point-to-point MIMO QPSK system (except the WL detector, as the QPSK modulation is a circular signal method, and so the WL method reduces to the linear method). It can be seen that the ML detector has a superior BER performance to the other detectors, but at the cost of a much higher complexity. Also, the gain of the MMSE linear method over the ZF method is clear, and the gain of the SIC method over the linear methods can shows the advantage of the interference cancellation techniques.

Chapter 3

Joint Maximum Likelihood Detection and Link Selection for Cooperative MIMO Relay Systems

Contents

3.1 Introduction

In environments where the point-to-point transmission of signals can be difficult, such as heavily built up urban areas, outages can occur frequently due to shadowing effects, multipath fading and path loss. Through the use of relay nodes, power consumption, outage rates and BER performance can be improved in comparison to the single point-to-point link, as the relay nodes form different transmission paths and increase spatial diversity. Cooperative diversity [13], is a technique that allows transmissions travelling

by multiple routes simultaneously to be combined in an optimal fashion at the destination, increasing the likelihood of the transmission being successfully received [11], [80].

There are three main cooperative strategies at relays that are used for forwarding the transmitted signal, amplify-and-forward (AF) [16], decode-and-forward (DF) [19], [20] and compress-and-forward (CF) [81], each method having its own advantages and disadvantages. However, with the destination receiving many different copies of the same transmitted signal, each with different fading and noise effects applied, the destination needs to use detection techniques that can take advantage of the extra information available, and combine this to reduce the probability of errors as compared to the non-cooperative transmission.

There are many different existing detection techniques in order to perform this combination of signals at the receiver, but the method highlighted in this chapter is based upon the maximum likelihood (ML) receiver, which extends the cooperative ML detector originally proposed by Amiri and Cavallaro [82], [83]. The original cooperative ML detector of Amiri and Cavallaro is limited in the fact that it is formulated for the single relay case, with [84] extending this to the multiple relay case, but within this formulation it is required that the destination have perfect knowledge of each relays retransmission (*i.e.* be able to receive each relays transmission separately from the other relays with no noise or interference), which could not be easily obtained in the system if the relays retransmit simultaneously. In [85] a method was proposed for adapting the multiple relay cooperative ML detector with information that was available within the system, along with a stochastic gradient (SG) [17] power allocation technique that could optimise the global power distribution within the system to the source and relay nodes and their antennas. However, it was seen that the system performance was heavily dependent on the fact that the relays were close to the source and destination and had good channel links to both. If the relays were badly positioned and so had weak channel links to the source and destination nodes, the cooperation at the destination node could actually decrease the performance of the system as compared to the non-cooperative case. It was also shown that if a simple linear detector was used at the DF relay nodes, then the system performance would also degrade.

In this chapter, the AF relay case will be considered in a model that represents multiple

relays with different path loss, and with large scale shadowing effects. A cross-layer cooperative ML detector is derived based upon the expansion and reduction of the ML rules that describe the transmission of signals within the two phase cooperative MIMO system, with considerations and approximations made to utilise the information available to the system effectively. The cooperative ML detector is designed with a summation based simplification of the link channels, which creates an approximation of the combined channels by a simple sum operation, and this is used as a basis for a cross-layer design consideration for link selection in the system.

Techniques for selecting which relays within the system to cooperate with are then considered, with two new link selection strategies proposed, which are based upon the idea of the combination of relay channels as a summation set, in comparison to the prior strategies detailed in this chapter, which only considers the relays individually. The link selection techniques use the power of the channels (*i.e.* the sum of the magnitude of the complex channel values) associated with the links and combination of relays considered, and so can be calculated on a per-packet basis for a quasi-static channel model. The cross-layer design also considers the constraints of a global power limit, in which the available power over the two phases of cooperative transmission is divided between the source and available relays, with the link selection deciding which relays are active within the system, and so which relays are allocated power for transmission. The link selection techniques are also analysed for the computational complexity cost, and how the complexity varies across the number of antennas utilised in the MIMO cooperative system, as well as how the number of relays selected affects the complexity required.

Channel coding and iterative detection are also considered, with a soft information sphere decoder for the cooperative system considered, which is based upon the combination of a list sphere decoder (LSD), which outputs multiple solutions to the ML problem, and maximum *a posteriori* (MAP) bit detection. The iterative detection process can be seen to use *a posteriori*, *a priori* and extrinsic information between the inner soft-information LSD and MAP detector combination and an outer convolutional code decoder, in order to improve the BER performance of the system. The main contributions of this chapter are:

- A cross-layer cooperative ML detection rule is derived for a multiple MIMO relay

two-phase cooperative communication system, with considerations for complexity and available information in the system.

- Two link selection techniques are proposed based upon the idea of the summation of a set of relay channels in different combinations.
- The performance and complexity of the proposed link selection techniques is compared with existing link selection techniques.
- An iterative detection and decoding scheme is integrated into the cross-layer cooperative ML detector with convolutional channel encoding.

In this chapter, the system model being used is described, with the modelling of the various channel effects and how the AF scheme operates, next the Sphere Decoder (SD) ML detector is reviewed, as well as a description of the cooperative ML detector, then the two sets of link selection proposed and used in this system are presented. Then the use of soft decision iterative decoding for the system is described, with the final sections detailing the simulation results and summarising the results of this chapter.

3.2 System Model

The system under consideration is a two-phase MIMO relay system, with a single source node (S), a single destination node (D) and M multiple relay nodes (R). The source node transmits the data in the first phase of the system, which are received by the destination node and the relay nodes, and in the second phase the relay nodes retransmit the received data, through an Amplify-and-Forward (AF) technique, to the destination node. The destination node can use both sets of received signals from each phase to recover the original transmitted data from the source node. For relays using AF, the received signal is not decoded, but instead simply amplified by a determined factor γ before being retransmitted. Using AF eliminates the need for detectors at the relays, but requires the destination to have knowledge of all the channels in the system for both phases of transmission.

Assumptions made in this system are that each node has the same number of antennas per device (N_t), that the system is under a total power constraint, that all relays trans-

mit simultaneously in the second phase, the channels are assumed to be quasi-static for transmissions and so unchanged during a single packet transmission and that nodes that require channel knowledge have this information *a priori* and error-free. Also, the relays are assumed to be linear and the channels are assumed to be frequency independent, and so the amplified noise can be treated as being white Gaussian noise. In the system model, relays are modelled as being at variable distances away from the source and destination nodes, and so path loss is factored into the model, as are large scale shadowing effects, which are modelled by Log-Normal Shadowing (LNS) losses to the power of the received signal.

The first phase ($S \rightarrow R$ and $S \rightarrow D$) of the system model can be represented as follows:

$$\mathbf{y}_{sd} = \alpha_{sd}\beta_{sd}\mathbf{H}_{sd}\mathbf{A}_s\mathbf{x} + \mathbf{n}_d^{(1)} \tag{3.1}$$

$$\mathbf{y}_{sr_m} = \alpha_{sr_m}\beta_{sr_m}\mathbf{H}_{sr_m}\mathbf{A}_s\mathbf{x} + \mathbf{n}_{r_m}^{(1)}, m = 1, \ldots, M \tag{3.2}$$

where $\mathbf{H}_{sd}$ and $\mathbf{H}_{sr_m}$ are $N_t \times N_t$ matrices denoting the $S \rightarrow D$ and $S \rightarrow R$ channels, where the m subscript denotes the relay number that the value is associated with up to M relays and $\mathbf{x}$ is the vector of length N_t that denotes the data symbols that are transmitted from the source. Note that the size of the channel matrices is $N_t \times N_t$ instead of $N_t \times N_r$. For simplification in the following chapter, the scenario being considered is where the number of receive antennas is equal to the number of transmit antennas, and so $N_r = N_t$. The matrix $\mathbf{A}_s$ is the $N_t \times N_t$ diagonal matrix representing the power allocation on each antenna of the source node. The scalars α_{sd}, α_{sr_m} represent the path loss in the channel due to distance and the scalars β_{sd} and β_{sr_m} are the LNS fading channel losses. The N_t length vectors $\mathbf{y}_{sd}$ and $\mathbf{y}_{sr_m}$ represent the received signal at the nodes, and $\mathbf{n}_d$ and $\mathbf{n}_{r_m}$ represent the noise at the receive antennas of the nodes. The superscript $^{(1)}$ on each $\mathbf{n}$ indicates the transmission phase in which the noise vector is applied.

For AF relays, we can describe the second phase of transmission as:

$$\mathbf{y}_{rd} = \sum_{m=1}^{M}(\alpha_{rd_m}\beta_{rd_m}\mathbf{H}_{rd_m}\mathbf{A}_{r_m}\gamma_{r_m}\mathbf{y}_{sr_m}) + \mathbf{n}_d^{(2)}. \tag{3.3}$$

The vector $\mathbf{y}_{rd}$ is the sum of the relay transmissions in the second phase plus the additive noise contribution at the destination receiver in the second phase.

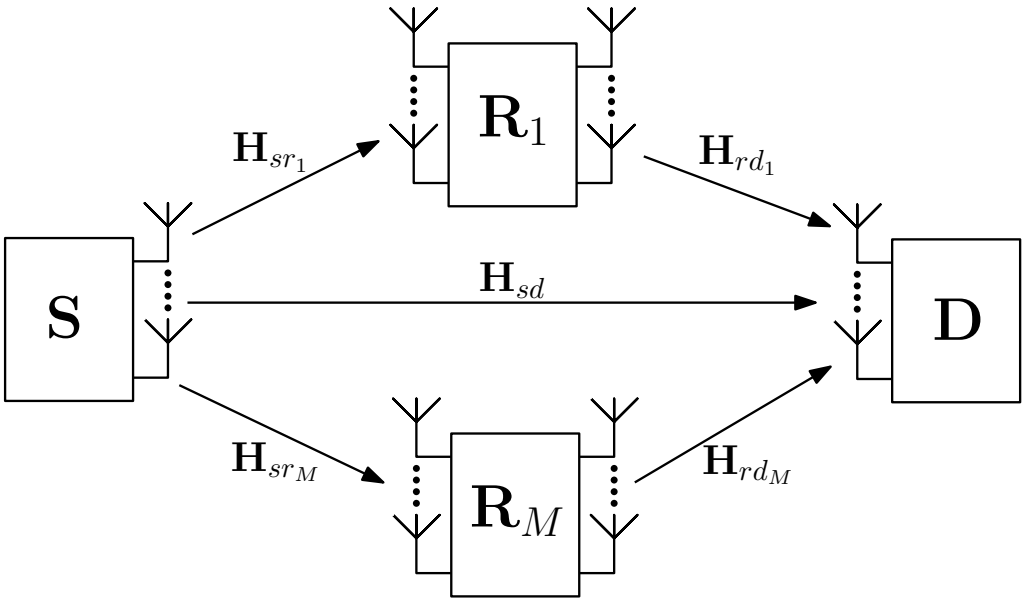

Figure 3.1: MIMO cooperative multiple relay two-phase system model

Fig. 3.1 gives a representation of this system in a block diagram. It is assumed that the statistics of the channels in the system are complex Gaussian distributed with fading applied on a block basis. The distance dependent path loss variable α for the relay links is defined by the relative distances of R from S and D, and so relative to the path loss of the S to D link, similarly to [86]:

$$\alpha_{sd} = \sqrt{L}, \tag{3.4}$$

$$\alpha_{sr_m} = \frac{\alpha_{sd}}{\sqrt{(d_{sr_m})^{\rho}}}, m = 1, \ldots, M, \tag{3.5}$$

$$\alpha_{rd_m} = \frac{\alpha_{sd}}{\sqrt{(d_{rd_m})^{\rho}}}, m = 1, \ldots, M, \tag{3.6}$$

where L is the power path loss of the S to D link, d_{sr_m} and d_{rd_m} are the relative distances of each R from the S and D as compared to the S to D link and ρ is the path loss exponent, usually between 2 and 4 depending on the environment.

The channel LNS is modelled by a log-normal random distribution [87], produced from the logarithmic representation of a normal distribution with a standard deviation of σ_s, which is known as the shadowing spread, given in dB. $\beta_{p,q}$ is a linear log-normal variable, representing shadowing between generic transmitter p and generic receiver q, calculated by:

$$\beta_{p,q} = 10^{\left(\frac{\sigma_s \mathcal{N}(0,1)}{10}\right)} \tag{3.7}$$

where $\mathcal{N}(0,1)$ represents a normal distribution with mean 0 and variance 1, and it is assumed that each channel LNS is characterised by the same shadowing spread.

The AF amplification factor γ_{r_m} for relay m is chosen as to normalise the received signal to unit power 1, [88], [89], in order to keep the AF relay at a mean transmission power over time and this can be expressed as:

$$\gamma_{r_m} = \sqrt{\frac{1}{\|\alpha_{sr_m}\beta_{sr_m}\mathbf{H}_{sr_m}\mathbf{A}_s\|_F^2 + N_t\sigma_n^2}}, m = 1, \ldots, M, \tag{3.8}$$

where $\|\bullet\|_F$ is the Frobenius norm and σ_n^2 is the noise variance.

3.3 Cooperative ML Detection and Sphere Decoding

In this section an overview of the Sphere Decoder (SD) ML detection algorithm for MIMO systems is provided and how we can adapt our cooperative system to efficiently operate using the SD is discussed. For convenience, the scalar terms $\alpha_{p,q}$ and $\beta_{p,q}$ will be grouped into a single term along with the channel matrix $\mathbf{H}_{p,q}$, as in practice a channel estimation technique will estimate these values as part of the channel matrix. The overall channel matrix will be represented by $\tilde{\mathbf{H}}_{p,q} = \alpha_{p,q}\beta_{p,q}\mathbf{H}_{p,q}$.

3.3.1 Sphere Decoder

The SD is designed to give the ML solution to the search problem

$$\hat{\mathbf{x}} = \arg\min_{\mathbf{x}\in\mathcal{X}} ||\mathbf{y} - \tilde{\mathbf{H}}\mathbf{x}||^2 \tag{3.9}$$

where $\mathbf{y}$ is the N_t length observation column vector of the N_t transmitted symbol column vector $\mathbf{x}$ through the $N_t \times N_t$ channel matrix, and where $\mathcal{X}$ is the set of every possible permutation of the symbol vector $\mathbf{x}$ with $\hat{\mathbf{x}}$ as the ML estimate of $\mathbf{x}$. The ML solution involves testing every $\mathbf{x}$ in $\mathcal{X}$ to find the optimum solution of the ML rule, and for large values of N_t or a complex modulation scheme with multiple bits per symbol, testing every

solution quickly becomes computationally prohibitive.

The SD operates on the idea of a constrained search set, instead of the full vector set $\mathcal{X}$, pruning away poor decision options through the algorithm before they get fully processed. Firstly, the ML rule is factorised, so that the solution set relies on an upper-triangular channel matrix equivalent, simplifying the multiplications of the lower values in the column vector $\mathbf{y}$. This factorisation can be done by means of a Cholesky factorisation or a QR decomposition. For the purposes of this description, we shall use the QR decomposition. The QR decomposition of $\tilde{\mathbf{H}}$ produces:

$$\mathbf{QR} = \tilde{\mathbf{H}} \tag{3.10}$$

where $\mathbf{Q}$ is an orthogonal matrix (such that $\mathbf{Q}^H\mathbf{Q} = \mathbf{I}$, and $\mathbf{R}$ is an upper-triangular matrix. Given this decomposition, the ML solution in Eq.(3.9) can be rewritten as:

$$\hat{\mathbf{x}} = \arg\min_{\mathbf{x}\in\mathcal{X}} ||\mathbf{z} - \mathbf{R}\mathbf{x}||^2 \tag{3.11}$$

where the effective observation vector $\mathbf{z} = \mathbf{Q}^H\mathbf{y}$.

The SD effectively searches within a multi-dimensional sphere (a hypersphere) of Euclidean distance radius r in the set space $\mathcal{X}$ around the observation vector $\mathbf{z}$, by checking the ML distance between each partial solution at each layer sequentially, with partial solutions falling outside the Euclidean distance radius r being discarded, along with the subset of solutions that include the discarded partial solution.

The partial Euclidean distance solution can be found as below:

$$d^{n,c,b} = \left| z(n) - \sum_{\eta=n}^{N_t} \mathbf{R}(n,\eta)\chi^{n,c,b}(\eta) \right|^2 + d^{n+1,b}, c = 1, ..., C, n = N_t, ..., 1, \tag{3.12}$$

where $d^{n,c,b}$ is the partial Euclidean distance for the bth possible solution branch (*i.e.* a candidate solution for $\hat{\mathbf{x}}$), on the nth signal layer for the cth constellation point, $d^{n+1,b}$ is the previous partial Euclidean distance (as n decrements from $N_t \rightarrow 1$) for the bth possible solution branch, and $\chi^{n,c,b}$ is the solution set being considered, expressed as below:

$$\chi^{n,c,b} = \begin{bmatrix} Z(c) & \chi^{(n+1,b)} \end{bmatrix}^T, \tag{3.13}$$

where $\chi^{(n+1,b)}$ is the partial solution set from the previous layer in the solution set b and $Z(c)$ is the cth symbol of the constellation set Z being considered for the SD solution. If a partial solution is found to satisfy the radius constraint, then the partial solution is stored, so that for the next layer, the partial solution can have the next solution possibilities appended to it and tested again under the radius constraint. This continues until the last layer, when the complete solution that has the lowest Euclidean distance (if there is more than one solution at this layer) is taken as the ML solution.

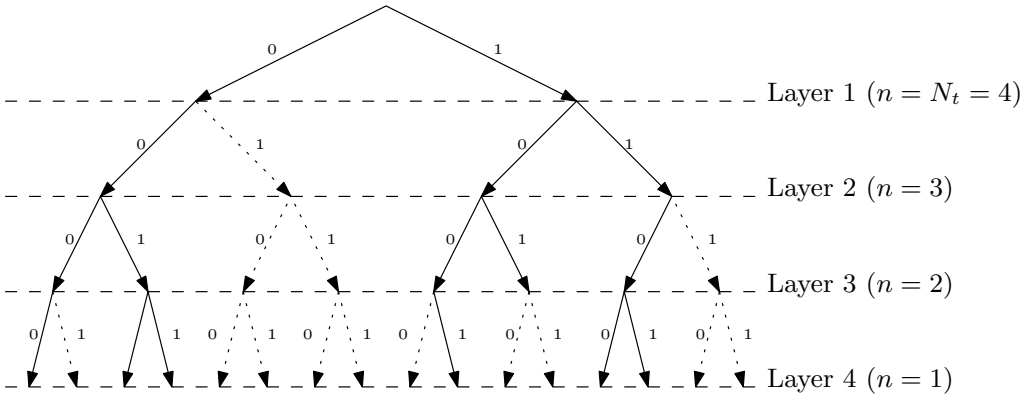

Figure 3.2: SD example tree diagram for $N_t = 4$ and BPSK modulation. Solid lines are branches processed by the SD, dotted lines are pruned branches that are not processed

Fig.3.2 represents the SD process as a tree diagram for a $N_t = 4$ antenna BPSK modulation system, with the permutations of χ represented as a single branch from the top downwards. However, it is possible that the SD will discard every possible solution before the end of the algorithm, in which case the SD has failed to find a solution. This is usually due to the radius r being set too small. However, if the radius is too large, then an unnecessary amount of solutions will be tested, increasing the computational complexity without gain. Also, whilst the SD has a lower computational complexity than the complete ML search, it is generally time-variant for each transmission, and the complexity is high $\mathcal{O}(N_t^3)$, with also the modulation scheme affecting complexity, as the amount of possible symbols per transmission directly affects the number of branches the SD has in the tree diagram.

3.3.2 Cooperative ML Detection

As detailed in the previous subsection, the SD is less complex to solve than the ML search, but the complexity still scales greatly with the number of information streams transmitted. One method of potentially adapting the receive signals at the destination node in the cooperative system considered in Section II is to simply stack the received transmissions from the source and relays as below:

$$\begin{aligned} \mathbf{y}_t &= \tilde{\mathbf{H}}_t \mathbf{x} + \mathbf{n}_t \\ \begin{bmatrix} \mathbf{y}_{sd} \\ \mathbf{y}_{rd} \end{bmatrix} &= \begin{bmatrix} \tilde{\mathbf{H}}_{sd} \mathbf{A}_s \\ \sum_{m=1}^{M} \tilde{\mathbf{H}}_{rd_m} \mathbf{A}_{r_m} \gamma_{r_m} \tilde{\mathbf{H}}_{sr_m} \mathbf{A}_s \end{bmatrix} \mathbf{x} + \begin{bmatrix} \mathbf{n}_{\mathbf{d}}^{(\mathbf{1})} \\ \sum_{m=1}^{M} (\tilde{\mathbf{H}}_{rd_m} \mathbf{A}_{r_m} \gamma_{r_m} \mathbf{n}_{r_m}) + \mathbf{n}_{\mathbf{d}}^{(\mathbf{2})} \end{bmatrix}. \end{aligned} \tag{3.14}$$

However, the stacked received vector $\mathbf{y}_t$ is a $2N_t$ length column vector, which appears as an overloaded system (*i.e.* more transmit antennas than receive antennas), and this is a problem for the standard SD. In the SD algorithm, the QR factorisation of the channel takes place, which is now part of an overloaded system, which means the channel matrix doesn't have full column rank. When a matrix doesn't have full column rank, the QR factorisation for that matrix doesn't exist, and so the SD would not be able to operate on this overloaded scenario. So instead we manipulate the incoming signals and the knowledge of the channel matrices into a form suitable for the cooperative ML detector.

In prior work by Amiri and Cavallaro [82], [83], a cooperative version of the ML detector is designed by pre-processing the received signals and communication channels into a single ML rule form that the SD can easily operate on. However, this is only formulated for the case of a single DF relay. The multiple relay case is described in [84], including AF relays, but does not consider how the information required for this expansion may be obtained from the system information available.

The cooperative ML AF detection problem can be described as the following optimisation:

$$\hat{\mathbf{x}} = \arg \min_{x_n \in Z} (\|\mathbf{y}_{sd} - \tilde{\mathbf{H}}_{sd} \mathbf{A}_s \mathbf{x}\|^2 + \sum_{m \epsilon \Omega_s} \|\mathbf{y}_{rd_m} - \tilde{\mathbf{H}}_{rd_m} \mathbf{A}_{r_m} \gamma_{r_m} \mathbf{y}_{sr_m}\|^2) \tag{3.15}$$

where Z represents the constellation set for the modulation scheme used, Ω_s is the relay set which is selected by a link selection method, such as in Section IV, and x_n is the nth element of $\mathbf{x}, n = 1, ..., N_t$.

The proposed ML rule that is desired is formed by combining the two ML rules of the first and second phase transmissions to the destination, to produce an equivalent ML rule of the form:

$$\hat{\mathbf{x}} = \arg\min_{x_n \in S} \|\mathbf{y}_e - \tilde{\mathbf{H}}_e \mathbf{A}_e \mathbf{x}\|^2, \tag{3.16}$$

where $\mathbf{y}_e$ is the N_t length equivalent received signal column vector, $\tilde{\mathbf{H}}_e$ is the equivalent $N_t \times N_t$ channel matrix and $\mathbf{A}_e$ is the $N_t \times N_t$ equivalent power allocation matrix. The quantities $\mathbf{y}_e$ and $\mathbf{H}_e\mathbf{A}_e$ can be found as below, noting that $\mathbf{H}_e\mathbf{A}_e$ are jointly estimated and substituted in $\mathbf{y}_{sr_m}$ from Eq.(3.2):

$$\tilde{\mathbf{H}}_e \mathbf{A}_e = (\mathbf{A}_s^H \tilde{\mathbf{H}}_{sd}^H \tilde{\mathbf{H}}_{sd} \mathbf{A}_s + \sum_{m \epsilon \Omega_s} \mathbf{A}_s^H \tilde{\mathbf{H}}_{sr_m}^H \gamma_{r_m}^H \mathbf{A}_{r_m}^H \tilde{\mathbf{H}}_{rd_m}^H \tilde{\mathbf{H}}_{rd_m} \mathbf{A}_{r_m} \gamma_{r_m} \tilde{\mathbf{H}}_{sr_m} \mathbf{A}_s)^{1/2} \tag{3.17}$$

$$\mathbf{y}_e = (\tilde{\mathbf{H}}_e \mathbf{A}_e)^{-1} (\mathbf{A}_s^H \tilde{\mathbf{H}}_{sd}^H \mathbf{y}_{sd} + \sum_{m \epsilon \Omega_s} \mathbf{A}_s^H \tilde{\mathbf{H}}_{sr_m}^H \gamma_{r_m}^H \mathbf{A}_{r_m}^H \tilde{\mathbf{H}}_{rd_m}^H \mathbf{y}_{rd_m}) \tag{3.18}$$

Unfortunately, since the system will only have knowledge of the summed second phase received signal $\mathbf{y}_{rd}$ and not the individual relay transmissions $\mathbf{y}_{rd_m}$, we need to reformulate the equations to use the available information. By defining the summed channel relation $\mathbf{S}$

$$\mathbf{S} = \sum_{m \epsilon \Omega_s} \tilde{\mathbf{H}}_{rd_m} \mathbf{A}_{r_m} \gamma_{r_m} \tilde{\mathbf{H}}_{sr_m} \mathbf{A}_s, \tag{3.19}$$

an approximation of the equivalent ML rule can be derived (See the Appendix for details):

$$\tilde{\mathbf{H}}_e \mathbf{A}_e \approx (\mathbf{A}_s^H \tilde{\mathbf{H}}_{sd}^H \tilde{\mathbf{H}}_{sd} \mathbf{A}_s + \mathbf{S}^H \mathbf{S})^{1/2} \tag{3.20}$$

$$\mathbf{y}_e \approx (\tilde{\mathbf{H}}_e \mathbf{A}_e)^{-1} (\mathbf{A}_s^H \tilde{\mathbf{H}}_{sd}^H \mathbf{y}_{sd} + \mathbf{S}^H \mathbf{y}_{rd}) \tag{3.21}$$

3.4 Link Selection

There have been some proposed link selection techniques in the literature [90], [91], [92], [93], [94] that are employed to improve the BER performance of the system, however these link selection techniques only consider each relay link individually. By considering the relay links as sets instead we can use this extra knowledge to make better selections, and we can propose two new link selection strategies based upon the combination of relay channels sets instead of individual relays. The application of these techniques to the cooperative MIMO system will be examined in the case of the destination node having knowledge of all channels in the system, and in the case of the destination node having only $\tilde{\mathbf{H}}_{sd}$ and $\tilde{\mathbf{H}}_{rd_m}$ channel knowledge.

3.4.1 Limited Channel Knowledge

In the limited channel knowledge scenario, a simple scheme is to choose the relays with the greatest second phase channel power p_{rd_m}. This channel power (CP) link selection, if given the number of relays to be selected (R_L), chooses the relay set $\hat{\Omega}_s$ associated with the R_L greatest p_{rd_m}.

$$p_{rd_m} = \sum_{j=0}^{j=N_t} \sum_{k=0}^{k=N_t} (\tilde{\mathbf{H}}_{rd_m} \tilde{\mathbf{H}}_{rd_m}^H)_{j,k}, m = 1, \ldots, M \tag{3.22}$$

$$\hat{\Omega}_s = \{\hat{m}_1, ..., \hat{m}_{R_L}\} = \underset{m \in [1,M] \subset \mathbb{Z}}{\operatorname{argmax}} \; p_{rd_m}, \tag{3.23}$$

where $\hat{m}_1$ is the value of m that returns the largest value of p_{rd_m} and similarly $\hat{m}_{R_L}$ is the value of m that returns the R_Lth largest value of p_{rd_m}. Using the assumption that $\tilde{\mathbf{H}}_{rd_m}$ is static over a single packet, this link selection can be performed once before each packet transmission. Another advantage is that it only requires knowledge of the second phase of the cooperative channels, which is useful for scenarios of limited system knowledge, such as DF systems.

3.4.2 Knowledge of All Channels

If the system has knowledge of all the channels associated with the relays in the system, there are a number of link selection strategies that can be utilised, based upon the channel's powers, as in Eq.(3.22), with the source to relay channel power p_{sr_m} defined as:

$$p_{sr_m} = \sum_{j=0}^{j=N_t} \sum_{k=0}^{k=N_t} (\tilde{\mathbf{H}}_{sr_m} \tilde{\mathbf{H}}_{sr_m}^H)_{j,k}, m = 1, \ldots, M \tag{3.24}$$

The maximum sum channel power (MS-CP) link selection strategy uses the summation of the channel powers from both the first and second phase channels, giving the set:

$$\hat{\Omega}_s = \{\hat{m}_1, ..., \hat{m}_{R_L}\} = \underset{m \in [1,M] \subset \mathbb{Z}}{\operatorname{argmax}} (p_{sr_m} + p_{rd_m}) \tag{3.25}$$

The maximum minimum channel power (MM-CP) link selection strategy [90], [91], [92] finds the least powerful channel associated with each relay and places these channel powers into a set, as the least powerful channel will be the performance limiter for each link, then finds the link with the most powerful channel from this set, as below:

$$\hat{\Omega}_s = \{\hat{m}_1, ..., \hat{m}_{R_L}\} = \underset{m \in [1,M] \subset \mathbb{Z}}{\operatorname{argmax}} (\min(p_{sr_m}, p_{rd_m})) \tag{3.26}$$

The maximum harmonic mean channel power (MH-CP) selection strategy [93], [94] relies on taking the modified harmonic mean of the two channels associated with a relay as the link metric as below:

$$\hat{\Omega}_s = \{\hat{m}_1, ..., \hat{m}_{R_L}\} = \underset{m \in [1,M] \subset \mathbb{Z}}{\operatorname{argmax}} ((p_{sr_m}^{-2} + p_{rd_m}^{-2})^{-1}) \tag{3.27}$$

This metric can however be rearranged so that the amount of division required is reduced, as division operations typically are computationally expensive in a real system as compared to addition and multiplication. The rearrangement of the maximum harmonic mean is below:

$$\hat{\Omega}_s = \{\hat{m}_1, ..., \hat{m}_{R_L}\} = \underset{m \in [1,M] \subset \mathbb{Z}}{\operatorname{argmax}} \left(\frac{p_{sr_m} p_{rd_m}}{p_{sr_m} + p_{rd_m}} \right) \tag{3.28}$$

3.4.3 Proposed Combinatorial Link Selection Strategies

The link selection strategies discussed above consider the power of the channels associated with the relays in the system, but do not take into account the structure of the individual values in the MIMO channel. This would be adequate for selecting a single link or relay within the system, but in this work multiple relays can be utilised together as part of the summation approximation in the cross-layer ML detector in Section II.

As the system model described in Section II shows, the second phase of the cooperative system has the relays transmitting simultaneously, and so the signals from each relay will interfere. It is then possible that the signals from different relays will interfere destructively, producing a small signal at the destination, even if the individual channels have large powers.

The cooperative ML detector in Section III also makes use of a summed channel approximation in Eq.(3.19), and so it is logical to apply the idea of summing the channels into the link selection strategies. Therefore, we define the sum of the relay to destination channels $\tilde{\mathbf{H}}_{rdt}$ of a set of considered relays Ω_c as:

$$\tilde{\mathbf{H}}_{rdt} = \sum_{k=1}^{R_L} \tilde{\mathbf{H}}_{rd_{\Omega_c(k)}}, \tag{3.29}$$

where $\Omega_c(k)$ is the kth relay of the considered relay set, and the power of this summed channel is described as:

$$p_{rdt} = \sum_{j=0}^{j=N_t} \sum_{k=0}^{k=N_t} (\tilde{\mathbf{H}}_{rdt} \tilde{\mathbf{H}}_{rdt}^{H})_{j,k}, m = 1, \ldots, M \tag{3.30}$$

Using these definitions we can now propose link selection strategies based upon the combination of relays, not just individual relays.

Firstly, we propose a maximum minimum combinatorial channel power (MMC-CP) link selection strategy for combinations of relays, that considers the relay sets Ω_c which contain relay combinations of R_L relays in every possible unique combination. The number of possible Ω_c sets for R_L of M relays being selected is $\frac{M!}{(M-R_L)!R_L!}$, where ! denotes the factorial function.

The channel powers to consider for a single Ω_c using the summed second phase channel can then be described as:

$$p_{\Omega_c} = [p_{sr\Omega_c(1)}, ..., p_{sr\Omega_c(R_L)}, p_{rdt}], \tag{3.31}$$

and so the maximum minimum criteria becomes:

$$\hat{\Omega}_s = \{\hat{m}_1, ..., \hat{m}_{R_L}\} = \underset{m \in \left[1, \frac{M!}{(M-R_L)!R_L!}\right] \subset \mathbb{Z}}{\operatorname{argmax}} (\min(p_{\Omega_{cm}})) \tag{3.32}$$

Similarly, we can propose a maximum harmonic mean combinatorial channel power (MHC-CP) selection strategy, using a generalised form of the modified harmonic mean for multiple values:

$$\hat{\Omega}_s = \{\hat{m}_1, ..., \hat{m}_{R_L}\} = \underset{m \in \left[1, \frac{M!}{(M-R_L)!R_L!}\right] \subset \mathbb{Z}}{\operatorname{argmax}} \left(\frac{\prod_{k=1}^{R_L+1} p^2_{\Omega_c}(k)}{\sum_{j=1}^{R_L+1} \prod_{\substack{l=1 \\ l \neq j}}^{R_L+1} p^2_{\Omega_c}(l)} \right) \tag{3.33}$$

Table 3.1 summarises the complex multiplication and addition operations required for each relay selection algorithm, and Fig. 3.3a shows how the number of complex operations varies with the number of available relays, with each complex addition or multiplication counted as 1 unit. It can be seen that the CP link selection that uses limited channel information requires much less complexity than the link selection strategies that require all channel information associated with the relays, but the CP link selection strategy performance will be reduced as compared to the other link selection strategies due to the limited information available. It should also be noted that the proposed combinatorial variants of the link selection strategies have a complexity also reliant on R_L, not just N_t and M as with the other link selection strategies, as shown in Fig.3.3b.

Table 3.1: Link Selection Strategies Complexity

Selection Method	Complex Additions	Complex Multiplications
CP	$M(N_t^3 - 1)$	MN_t^3
MS-CP	$2(M(N_t^3 - 1)) + M$	$2MN_t^3$
MM-CP	$2(M(N_t^3 - 1))$	$2MN_t^3$
MH-CP	$2(M(N_t^3 - 1)) + M$	$2MN_t^3 + 3M$
MMC-CP	$\left(\frac{M!}{(M-R_L)!R_L!} + M\right) N_t^3$	$\frac{M!(N_t^3 + N_t^2(R_L - 1) - 1)}{(M-R_L)!R_L!} + M(N_t^3 - 1)$
MHC-CP	$\left(\frac{M!}{(M-R_L)!R_L!} + M\right) N_t^3 + R_L^2 + 3R_L + 2$	$\frac{M!(N_t^3 + N_t^2(R_L - 1) - 1)}{(M-R_L)!R_L!} + M(N_t^3 - 1) + R_L$

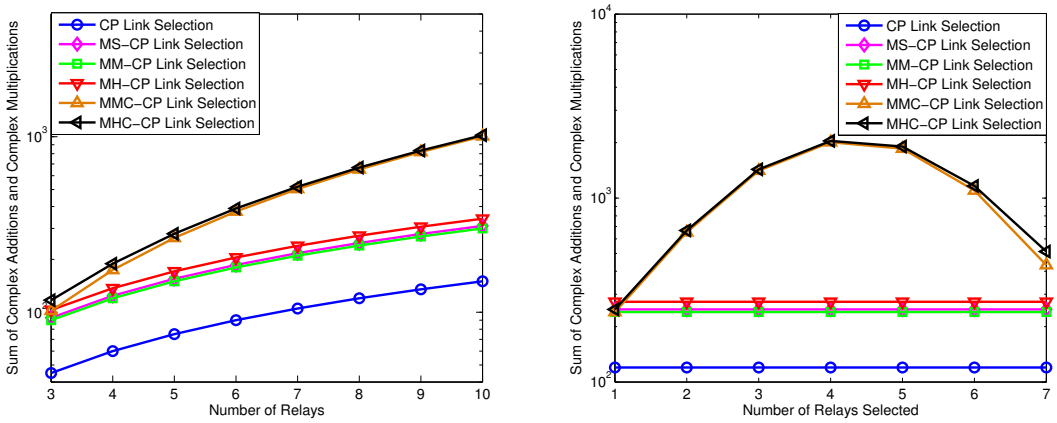

(a) $R_L = 2$, variable M

(b) $M = 8$, variable R_L

Figure 3.3: Number of complex operations for each link selection strategy, with $N_t = 2$

3.5 Iterative and Cooperative Detection and Decoding

Here a brief overview of a simple convolutional code soft-input soft-output (SISO) decoder [33], [95–98] and detector incorporating a List Sphere Decoder (LSD) will be covered, for use in comparing how the proposed iterative cooperative detection and decoding scheme performs with an iterative processing detector at the destination node. The subscripts 1 and 2 will be used in this section to denote the variables associated with the inner mapping and detection operations, and the outer encoding and decoding sections, respectively.

3.5.1 Iterative Processing

The transmission of the individual data symbols is as described in Section II, but the data symbols themselves are not directly converted from the binary data ($\mathbf{b}$) source by the constellation mapper. A channel encoder is applied to the data which encodes them into $\boldsymbol{\lambda}_2$, according to the code chosen to be used in the system, adding redundant and correlated data bits, then the data are interleaved to $\boldsymbol{\lambda}_1$, before mapping to data symbols by the constellation set chosen. It will be assumed that the relays operate as described in Section II, with the major difference being in the destination node, which consists of a detector and a decoder that exchange soft information between each other in an iterative manner of fashion, refining the estimate of the transmitted symbols for a number of iterations.

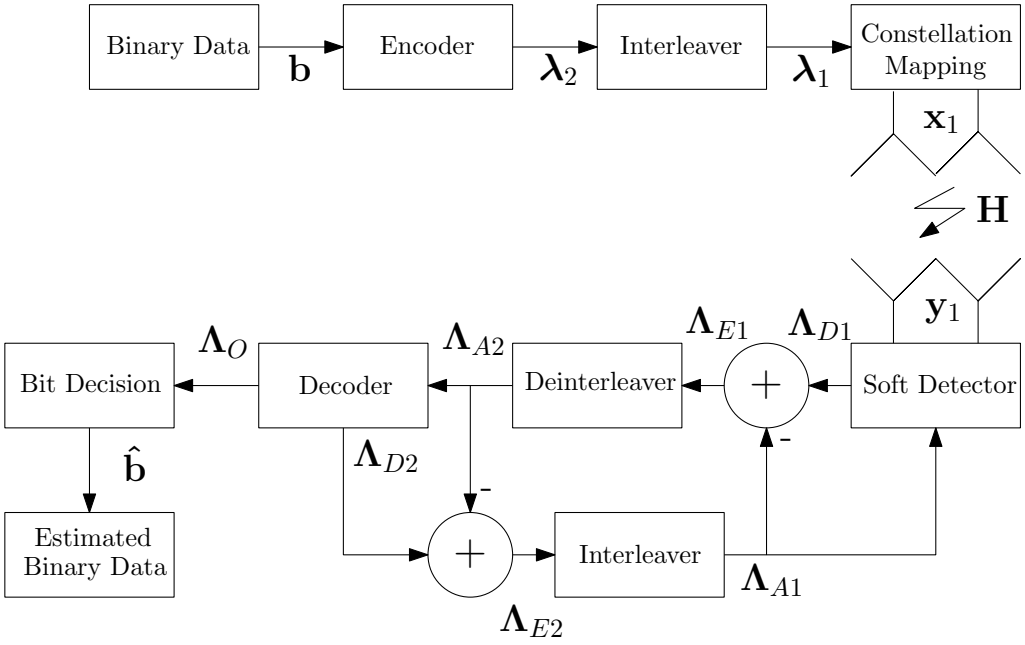

Figure 3.4: Iterative Decoding System Layout

Fig. 3.4 illustrates the SISO iterative processing model, with the following definitions: $\boldsymbol{\Lambda}_D$ represents the *a posteriori* log-likelihood ratio value (LLRV) of the bit b_k of the bit vector $\mathbf{b}$, $\boldsymbol{\Lambda}_A$ is the *a priori* LLRV of b_k, $\boldsymbol{\Lambda}_E$ is the extrinsic information LLRV and the output LLRV $\boldsymbol{\Lambda}_O$, which is the output of each iteration that is used for the bit estimation.

An iteration of the iterative decoder starts with the soft detector producing the inner *a posteriori* LLRV of the estimated solution $\boldsymbol{\Lambda}_{D1}$. If the inner *a priori* LLRV of $\mathbf{b}^{c,n}$, $\boldsymbol{\Lambda}_{A1}$ is available, this is taken into consideration by the LSD. The estimated LLRV is

then deinterleaved and decoded into the output LLRV $\mathbf{\Lambda}_O$. The difference between the outer *a posteriori* LLRV $\mathbf{\Lambda}_{D2}$ from the decoder and the outer *a priori* LLRV $\mathbf{\Lambda}_{A2}$ is then interleaved into the inner *a priori* LLRV $\mathbf{\Lambda}_{A1}$, for use in the next iteration of detection.

For the purposes of the cooperative ML detector, an ML detector that uses and outputs soft information is needed, to take the place of the soft detector in Fig. 3.4. The List Sphere Decoder [99] can be used for this purpose, which outputs a set of most likely solutions to the ML rule, rather than a single solution as in the hard decision SD, and calculates the LLRVs for each solution in the set. The set size can be varied to increase performance, but this has the trade-off of increasing the detection complexity. As the LSD operates on the same ML rule as the hard decision SD, Eq.(3.16-3.21) are usable in the iterative detection system, as the manipulation involved takes place before the detection process takes place.

3.5.2 MAP Detection for an Iterative Cooperative Detector

For maximum *a posteriori* (MAP) bit detection, maximising the *a posteriori* probability (APP) for a given bit reduces the probability of making an incorrect detection decision on that bit. The APP is usually expressed as a LLRV, which is convenient to use, as the iterative detection process in Fig. 3.4 uses LLRVs to describe the iterative algorithm. The LLRVs are used in detection to determine the bit decision, the sign of the LLRV is used to determine whether the bit is a one or zero, and the magnitude of the LLRV indicates the reliability of this decision, the larger the magnitude, the more confident the estimation is. Correspondingly, LLRVs with a magnitude near zero are considered unreliable. The cth bit of the nth symbol in a symbol vector $\mathbf{b}$ for $n = 1, ..., N_t, c = 1, ..., C$ (where C is the number of bit per symbol for the modulation scheme used), will be referenced as $b^{n,c}$ in this chapter, and the logical zero is represented by an amplitude level of $b^{n,c} = -1$, with the logical one amplitude level described as $b^{n,c} = +1$. The assumption is also made that although the bits in the system are encoded in the encoder block with a channel code, the interleaver will randomly shuffle the bits such that we can assume that the bits are statistically independent from each other.

The inner APP LLRV (Λ_{D1}) of the bit $b^{n,c}$, given the received signal symbol vector $\mathbf{y}$

can be expressed as:

$$\Lambda_{D1}(b^{n,c}|\mathbf{y}) = \ln \frac{P(b^{n,c}=+1|\mathbf{y})}{P(b^{n,c}=-1|\mathbf{y})}, n = 1, ..., N_t, c = 1, ..., C, \tag{3.34}$$

which describes the ratio of the probability that the bit $b^{n,c}$ is a logical one to the probability that the bit $b^{n,c}$ is a logical zero. Using Bayes theorem, and using the bit independence assumption to split up the joint probabilities into probability products, Eq.(3.34) can be expressed as:

$$\Lambda_{D1}(b^{n,c}|\mathbf{y}) = \Lambda_{A1}(b^{n,c}) + \underbrace{\ln \frac{\sum_{\mathbf{b}\in\mathcal{X}_{+1}} \left(p(\mathbf{y}|\mathbf{b}) \exp \prod_{j\in\mathcal{J}_{\mathbf{b}}} P(b^j) \right)}{\sum_{\mathbf{b}\in\mathcal{X}_{-1}} \left(p(\mathbf{y}|\mathbf{b}) \exp \prod_{j\in\mathcal{J}_{\mathbf{b}}} P(b^j) \right)}}_{\Lambda_{E1}(b^{n,c}|\mathbf{y})}, \tag{3.35}$$

where $\mathcal{X}_{+1}$ is the set of possible transmitted bit vectors $\mathbf{b}$ where $b^{n,c} = +1$, and likewise $\mathcal{X}_{-1}$ is the set of possible transmitted encoded bit vectors where $b^{n,c} = -1$, as below:

$$\mathcal{X}_{+1} = \{\mathbf{b}|b^{n,c} = +1\}, \mathcal{X}_{-1} = \{\mathbf{b}|b^{n,c} = -1\}, \tag{3.36}$$

and $\mathcal{J}_{\mathbf{b}}$ is the set of indices that can reference every bit in the bit vector set $\mathbf{b}$, except the bit under consideration $\mathbf{b}^{n,c}$, as below:

$$\mathcal{J}_{\mathbf{b}} = \{j|j = 0, ..., N_tC - 1, b^j \neq b^{n,c}\}. \tag{3.37}$$

Also, the inner *a priori* probability LLRV of a bit, $\Lambda_{A1}(b^{n,c})$ can be expressed as:

$$\Lambda_{A1}(b^{n,c}) = \ln \frac{P(b^{n,c}=+1)}{P(b^{n,c}=-1)}, \tag{3.38}$$

which is usually obtained from the previous iteration of processing in the iterative detector, or if the current iteration is the first, the inner *a priori* probability LLRV of a bit is set to zero. It is also shown that the second half of Eq.(3.35) is referred to as the inner extrinsic information LLRV ($\Lambda_{E1}(b^{n,c}|\mathbf{y})$), giving the result that the inner APP LLRV is the sum of the inner *a priori* probability LLRV and the inner extrinsic information LLRV.

If the *a priori* probability of b^j is expressed as a function of the LLRV $\Lambda_{A1}(b^j)$ then:

$$\begin{aligned} P(b^j) &= \frac{\exp(\pm\Lambda_{A1}(b^j))}{\exp(1+\pm\Lambda_{A1}(b^j))} \\ &= \left(\frac{\exp(-\Lambda_{A1}(b^j)/2)}{1+\exp(-\Lambda_{A1}(b^j))}\right)\exp(\Lambda_{A1}(b^j)b^j/2) \\ &= \mathcal{F}\exp(\Lambda_{A1}(b^j)b^j/2). \end{aligned} \tag{3.39}$$

It is possible to rewrite Eq.(3.35) with the right side summation as a vector multiplication with some manipulation, to give:

$$\Lambda_{D1}(b^{n,c}|\mathbf{y}) = \Lambda_{A1}(b^{n,c}) + \underbrace{\ln \frac{\sum_{\mathbf{b}\in\mathcal{X}_{+1}}\left(p(\mathbf{y}|\mathbf{b})\exp\left(\frac{1}{2}\mathbf{b}^{[n,c]T}\mathbf{\Lambda}_{A1}^{[n,c]}\right)\right)}{\sum_{\mathbf{b}\in\mathcal{X}_{-1}}\left(p(\mathbf{y}|\mathbf{b})\exp\left(\frac{1}{2}\mathbf{b}^{[n,c]T}\mathbf{\Lambda}_{A1}^{[n,c]}\right)\right)}}_{\Lambda_{E1}(b^{n,c}|\mathbf{y})}, \tag{3.40}$$

where $\mathbf{b}^{[n,c]}$ is the bit vector $\mathbf{b}$ with the bit $b^{n,c}$ removed, and $\mathbf{\Lambda}_{A1}^{[n,c]}$ is the vector of all *a priori* probability LLRV Λ_{A1} values associated with $\mathbf{b}$, also excluding the Λ_{A1} of the bit $b^{n,c}$. Note that as $\mathcal{F}$ is reliant solely on the *a priori* LLRV $\Lambda_{A1}(b^j)$, it can be factorised out of the product and summation, and so cancelled in the LLRV Λ_{E1}.

3.5.3 Obtaining the MAP Detection Values

In Eq.(3.40), the function $(p(\mathbf{y}|\mathbf{b})$ is required to be known, and this is found with the following definition:

$$p(\mathbf{y}|\mathbf{b}) = \frac{\exp\left(-\frac{1}{2\sigma_n^2}|||\mathbf{y}-\mathbf{H}\mathbf{x}||^2\right)}{(2\pi\sigma_n^2)^{N_t}}, \tag{3.41}$$

where $\mathbf{H}$ is the equivalent channel matrix that through which $\mathbf{x}$ is transmitted with $\mathbf{x}$ representing the bit vector $\mathbf{b}$ mapped to constellation points governed by the modulation scheme used in the system. However, it should be noted that the denominator of the equation will be cancelled out during the calculation of the LLRV, and so can be discarded from the calculation of $p(\mathbf{y}|\mathbf{b})$.

It can also be seen that the numerator and denominator of the inner extrinsic informa-

tion $\Lambda_{E1}(b^{n,c}|\mathbf{y})$ might be computationally complex to calculate, due to the large amount of exponential values that must be calculated, but this can be avoided by using a Max-log approximation. The Max-log approximation is a simplification of a sum of exponentials within a logarithm, and can be expressed as:

$$\ln\left(\sum_{i}\exp(a^i)\right) \approx \max_{i}(a^i), \tag{3.42}$$

and so this simplification can be used to reduce the computational complexity of the inner extrinsic information LLRV calculation $\Lambda_{E1}(b^{n,c}|\mathbf{y})$ to give:

$$\begin{aligned}\Lambda_{E1}(b^{n,c}|\mathbf{y}) \approx \frac{1}{2}\max_{\mathbf{b}\in\mathcal{X}_{+1}}\left(-\frac{1}{\sigma_n^2}|||\mathbf{y}-\mathbf{H}\mathbf{x}||^2+\mathbf{b}^{[n,c]^T}\mathbf{\Lambda}_{A1}^{[n,c]}\right)\\ -\frac{1}{2}\max_{\mathbf{b}\in\mathcal{X}_{-1}}\left(-\frac{1}{\sigma_n^2}|||\mathbf{y}-\mathbf{H}\mathbf{x}||^2+\mathbf{b}^{[n,c]^T}\mathbf{\Lambda}_{A1}^{[n,c]}\right)\end{aligned} \tag{3.43}$$

Unfortunately, despite the complexity reductions given above, for each $b^{n,c}$ there 2^{N_tC-1} possible encoded bit vectors $\mathbf{b}$ to test, which can result in a high complexity for higher order modulation schemes and a large number of antennas.

3.5.4 Cooperative List Sphere Decoder

The cooperative LSD is a variant of the SD, which instead of attempting to reach a single ML optimal solution, produces a list of the most likely ML solutions, as the solution to Eq.(3.11) may not be the optimal solution to satisfy Eq.(3.34). If we are given a desired list size L of list $\mathcal{L}$, then the LSD needs to return L solutions. To this end, we can alter the procedure of the SD so that if a partial solution satisfying the radius constraint is found, it is added to $\mathcal{L}$ if $\mathcal{L}$ is not full, and if $\mathcal{L}$ is full, the partial Euclidean distance of the partial solution is compared to the largest partial Euclidean distance in $\mathcal{L}$, replacing the existing partial solution if the new partial Euclidean distance is smaller.

When the cooperative LSD has completed its processing, $\mathcal{L}$ contains the ML solution (given that the radius constraint is appropriately large), and the $L-1$ next closest solutions. The list $\mathcal{L}$ can then be used as a constrained set for Eq.(3.43), reducing the search size for

the $\max$ function:

$$\begin{aligned}\Lambda_{E1}(b^{n,c}|\mathbf{y}) \approx \frac{1}{2}\max_{\mathbf{b}\in\mathcal{L}\cap\mathcal{X}_{+1}}\left(-\frac{1}{\sigma_n^2}|||\mathbf{y}-\mathbf{H}\mathbf{x}||^2+\mathbf{b}^{[n,c]T}\mathbf{\Lambda}_{A1}^{[n,c]}\right)\\ -\frac{1}{2}\max_{\mathbf{b}\in\mathcal{L}\cap\mathcal{X}_{-1}}\left(-\frac{1}{\sigma_n^2}|||\mathbf{y}-\mathbf{H}\mathbf{x}||^2+\mathbf{b}^{[n,c]T}\mathbf{\Lambda}_{A1}^{[n,c]}\right)\end{aligned} \tag{3.44}$$

If the size of the list L is set to the maximum possible size 2^{N_tC}, then this is equivalent to full MAP detection, and if $L = 1$, then this is equivalent to ML detection, as the LSD will only return the ML solution (assuming appropriate constraint radius size).

It should be noted that for iterations of the iterative MAP detection process, the cooperative LSD only relies on the observed received signal vector $\mathbf{y}$ and the channel matrix $\mathbf{H}$, and does not use any extra information from the iterative process, such as the *a priori* LLR Λ_{A1}, and so the list $\mathcal{L}$ will not change between iterations on the same $\mathbf{y}$, consequently the list $\mathcal{L}$ can be generated once for the first iteration using the LSD, and used for each iteration without reprocessing.

3.6 Simulations

In this section, the results of the simulations performed using the techniques set out in this chapter are presented. In the simulation environment, the assumption is made that the relays are arranged pseudo-randomly in an area defined by a set of polar coordinates, i.e. a radius length and an angle, that is centred on the source node which is defined as being a relative distance of unit 1 for the S to D link for the purposes of the path loss fading calculations in Eqs.(3.4)-(3.6). The radius length of the polar positioning $d_{sr_m}$is determined as a uniform random variable between a minimum $r_{\min}$ and maximum radius $r_{\max}$ limit, and the angular component θ_{sr_m} is a uniform random angle between 0 and 2π. The distance of the relay nodes to the destination node d_{rd_m} is then calculated using trigonometrical identities, as below:

$$d_{rd_m} = \sqrt{d_{sr_m}^2 + 1 - 2d_{sr_m}\cos(\theta_{sr_m})} \tag{3.45}$$

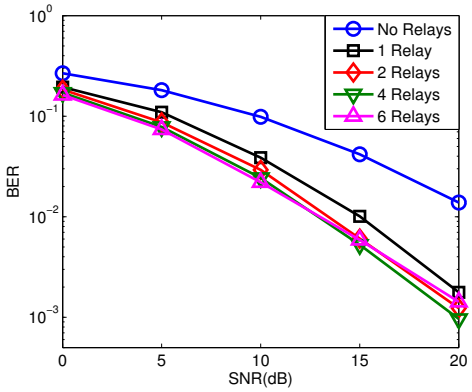

(a) System model used in this chapter

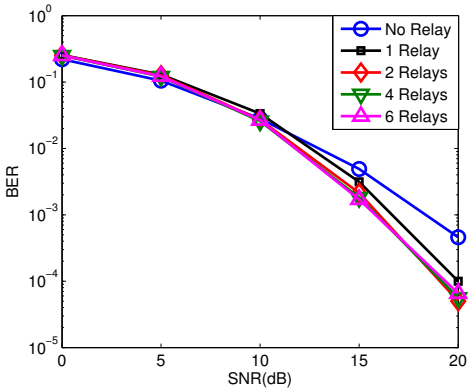

(b) Rayleigh system model commonly used in literature

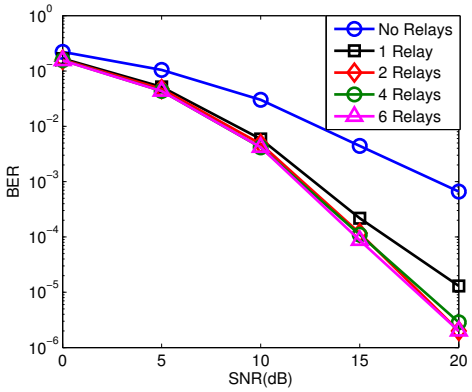

(c) System model used in [82]

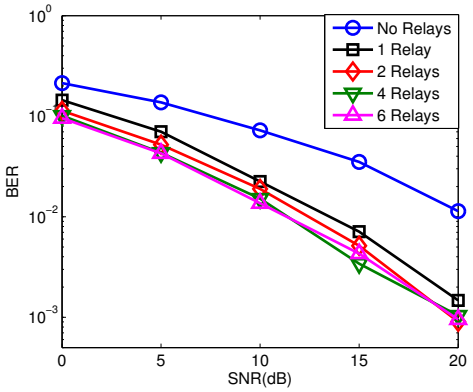

(d) System model used in [86]

Figure 3.5: 2x2 MIMO System, QPSK modulation with a variable number of relays

For the numerical results, $r_{\min}$ is set to 0.1 and $r_{\max}$ is set to 0.9. For the power allocation matrices $\mathbf{A}_s$, the system allocates half of the global power constraint (across both phases) to the source node, and the other half spread evenly across the relay nodes. The global power constraint is set to 1 for the obtained results, and so the source node power allocation matrix $\mathbf{A}_s$ is set as:

$$\mathbf{A}_s = \sqrt{\frac{0.5}{N_t}}\mathbf{I} \tag{3.46}$$

and the relay power allocation matrices $\mathbf{A}_{r_m}$ are set as:

$$\mathbf{A}_{r_m} = \sqrt{\frac{0.5}{N_t R_L}}\mathbf{I} \tag{3.47}$$

If the system is operating without using relay selection (i.e. all relays are used), then the number of selected relays value R_L in Eq.(3.47) is replaced with the number of relays in the system M. For the fading effects associated with the channel $\tilde{\mathbf{H}}$, the path loss fading

for the channels associated with each relay is defined by the distances d_{sr_m} and d_{rd_m}, and the base power loss of the S to D link, L. For the simulations, L is set as a 20dB power loss. The large scale LNS is randomised per packet according to a log-normal random distribution, with the shadowing spread set at 6dB for all channels.

Within the system, we assume that the channel values are perfectly known at the relay and destination nodes, and that the relays in the second phase all transmit with perfect synchronisation. Fig.3.5a shows the results of a 2x2 MIMO system with no channel coding or link selection, with a hard decision ML SD detector at the destination, using a QPSK modulation scheme with Gray coding to minimise bit errors when adjacent symbols are incorrectly detected. The system model used is the model described in Section II. The number of relays in the system is varied, from no relays (non-cooperative case), to 6 relays (cooperative case). It can be seen that the addition of a single relay to the system can improve BER performance by up to 7dB at a BER of 10^{-2}, but the gains of adding extra relays quickly diminish. Adding two relays to the system gives approximately an extra 2dB of BER gain at the same BER level, but four relays only give another $\sim$1dB of gain.

Increasing the number of relays beyond four appears to give no gains, and it can be observed that for six relays, there is actually a BER performance loss at high values of SNR as compared to the four relay case. This can be attributed to the relays causing destructive interference amongst each other, and the power constraint causing the relays to have less and less transmission power as the number of relays increases. So it can be seen that if the extra relays do not contribute gains to the BER performance, then a method of selecting relay links that are beneficial whilst discarding relay links that do not contribute gains may save resources in the system (such as freeing up relays for other potential users), and possibly increase the BER gains.

Fig.3.5b represents the BER results for a similar system to Fig.3.5a, but with the system model instead having Rayleigh channel modelling, with no path loss or LNS fading, as is common in literature on cooperative systems. Only the channel modelling is changed for fair comparison with the system described in this chapter. It can be seen that unlike Fig.3.5a, adding relays to the system does not appear to contribute much BER gain, until a high SNR value, and at that point, adding more than one relay does not give much BER

gain.

Fig.3.5c shows the BER results for the channel model and relay placement scheme from [82], which proposed the single relay cooperative ML detector. This model takes into account path loss, but the relay(s) are placed very close to the source node, and so is in an advantageous position. Adding the relays to the system gives a very large BER gain as the relays are well placed and fixed in position, and so the performance is much greater than Fig.3.5a.

Fig.3.5d shows the BER results for a system with path loss and 8dB of shadowing, which is similar to the system model described in this chapter, but the relays are fixed in position midway between the source and destination nodes, and so are well placed for relaying signals. The performance is similar to Fig.3.5a, due to the similarity of the system model used, but the static, well placed relays give this system reliability and a slight performance gain over Fig.3.5a.

The system models compared and contrasted in Fig.3.5a-d show that the system models in previous literature tend to not take into account all the features of the system model described in this chapter, such as the path loss or LNS, or for considering non-static relays, that may not be well placed for relaying signals.

Fig.3.6 shows the comparison of the different relay link selection schemes in a system with no channel coding or soft information, using the hard decision ML SD for detection at the destination. The 2x2 MIMO system is using a QPSK modulation scheme with Gray coding, with 6 relays available in the system. The scenarios presented in Fig.3.6 show the BER versus SNR for 1,2 and 3 relay links being selected from the 6 relays available in the system. It can be seen that the MH-CP and MM-CP link selection strategies perform much better than the MS-CP and CP link selection strategies, and the proposed MHC-CP and MMC-CP outperforms the other link selection strategies. For the single relay selected case, the proposed combinatorial strategies are seen to perform exactly as the non-combinatorial versions, as with only 1 relay being selected, there are no combinations as such, and so the combinatorial schemes reduce to the non-combinatorial cases. For 2 relays selected in the system, the gains of the combinatorial strategies over the non-combinatorial strategies are seen to be 2-3dB at a BER level of 10^{-3}, and similarly for

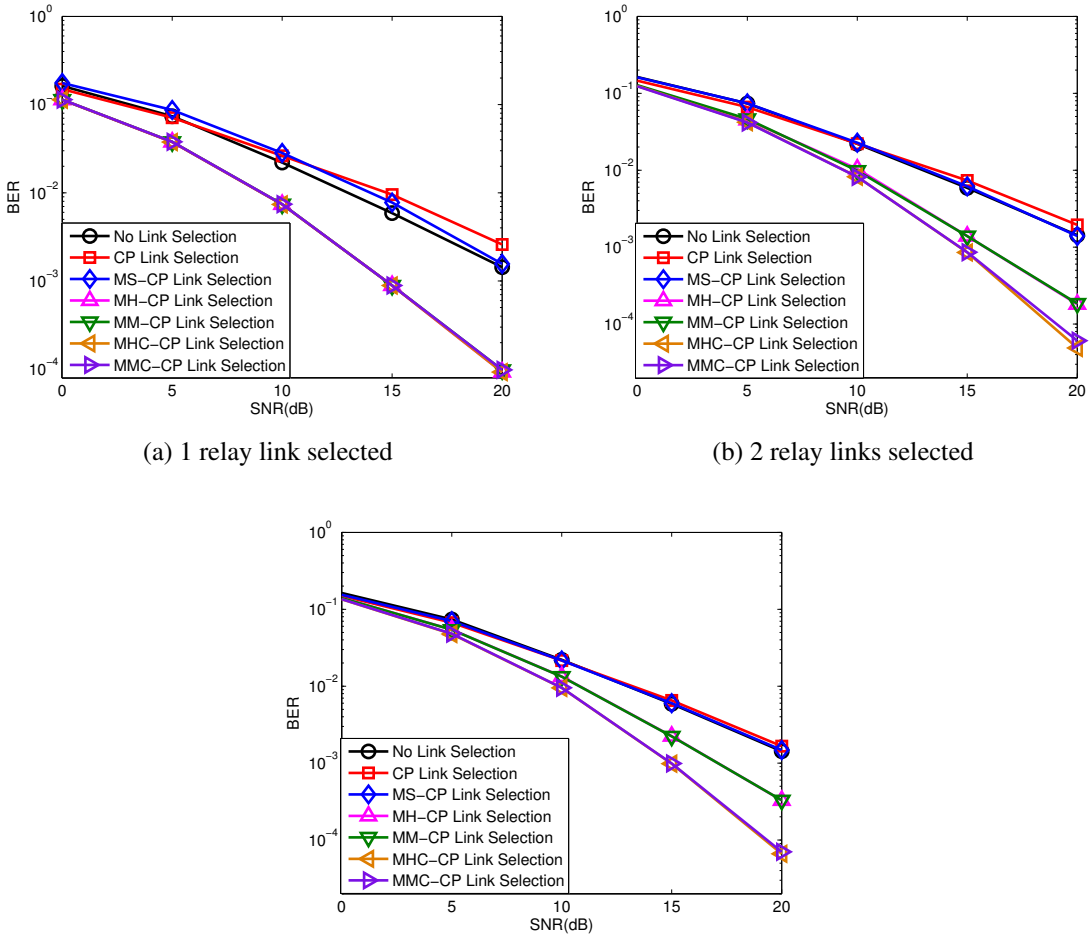

(a) 1 relay link selected

(b) 2 relay links selected

(c) 3 relay links selected

Figure 3.6: BER vs $S \rightarrow D$ SNR for the 2x2 MIMO relay system with QPSK modulation and no channel coding with a hard-decision SD, 6 relays, with 1,2 or 3 relay links selected for different relay selection schemes

3 relays selected, the difference between the non-combinatorial and the combinatorial is $\sim$3dB at a BER level of 10^{-3}. This is expected for the CP link selection, as this only uses limited channel information from the system, but the MS-CP strategy has full knowledge, and still has very little gain over the simpler CP strategy. The performance of the MH-CP and MM-CP link selection strategies is extremely similar for this setup, and so the MM-CP link selection could be seen as preferable, as it has a lower cost than the MH-CP. The proposed combinatorial MHC-CP and MMC-CP are seen to provide superior BER performance in the system as compared to the other link selection strategies considered, but at a higher computational complexity.

Fig.3.7a shows the system with an iterative detection and decoding scheme at the des-

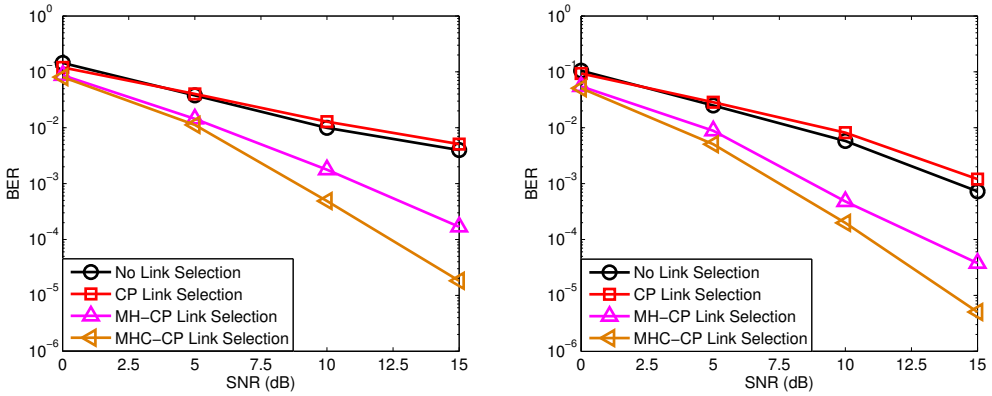

(a) Rate 1/2 code, generator [7,5] (b) Rate 1/3 code, generator [7,7,5]

Figure 3.7: BER vs $S \rightarrow D$ SNR for the 2x2 channel coded MIMO relay system with QPSK modulation and iterative detection and decoding, 6 relays, 2 relay links selected and 3 iterations of detection and decoding with a list size of 8 for the LSD

tination and convolutional channel coding at rate 1/2. The 2x2 MIMO system is using Gray coded QPSK, 6 relays, with 2 relays selected by the link selection methods. The presented plots are the numerical results from the 3rd iteration of decoding in the iterative detection and decoding scheme, with a list size of 8 for the LSD. It can be seen that the CP link selection is not very effective in this system setup, with a slight performance loss over no link selection scheme being implemented. However, the MH-CP and MHC-CP schemes have up to 7.5dB and 9dB of SNR gain at a BER level of $10^{-2.5}$ respectively over no link selection scheme being used. At higher SNR values, the MHC-CP link selection method has up to 3.5dB of gain over the non-combinatorial MH-CP link selection scheme at a BER level of 10^{-4}. Comparing the coded system from Fig.3.7a with the uncoded system from Fig.3.6(b), the MH-CP link selection scheme can been seen to have a decade of BER gain in the coded system over the equivalent uncoded system at 15dB SNR, and similarly the MHC-CP link selection scheme in the coded system can be seen to have a decade and a half of BER gain over the MHC-CP link selection scheme in the uncoded system at 15dB SNR. Fig.3.7b represents the results for the same system setup, but with a rate 1/3 code. The rate 1/3 code can be seen to give up to 2dB of gain over the rate 1/2 code for the MHC-CP link selection, with the gains between the different link selection techniques being similar to that for the rate 1/2 code.

In the case of the system setup being simulated for these numerical results, it can be seen that selecting more than 2 relays out of the 6 available reduces the BER performance

of the harmonic channel power and maximum minimum channel channel power link selection, whilst channel power and sum channel power link selection strategies slightly increase in performance. This suggests that on average for the relay setup considered, that only 1-2 relays will be in a position that benefits the transmission from the source to the relay in terms of BER performance.

3.7 Summary

In this chapter, we have defined a two phase cooperative system incorporating path-loss based and large scale shadowing based fading, with variable positioning of MIMO AF relays for a MIMO source and destination under a power constraint. In this system we have demonstrated cooperative ML detection that incorporates both phases of the received signal from the source and relays expressed as a single cooperative ML rule that can be processed by a SD detector, taking into account available information in the system and making appropriate substitutions so that the results can be numerically calculated. Also considered is the use of soft decision information and iterative processing for MAP detection, utilising the LSD as a soft decision detector that can be incorporated into a channel coded iterative processing detector. Several relay link selection strategies are also considered for the system, with limited channel information and full channel information scenarios considered. The proposed combinatorial link selection strategies have been shown to have BER performance gains over existing link selection schemes in both coded and uncoded cooperative MIMO systems. It has also been shown that adding relays to the system may not necessarily give BER gains, depending on the positioning and the number of relays present in the system model, and so the relay link selection strategies can be shown to give gains in BER performance over a full relay case, even when using less relays. It is also shown that some relay link strategies do not necessarily give BER gains, but it can be considered that the relay link selection can still maintain the BER performance, whilst releasing some relay resources that could be used by other potential users.

Chapter 4

Multi-Feedback Successive Interference Cancellation with Dynamic Reliability Ordering

Contents

4.1 Introduction

The SIC detector is a well-known technique for the detection of data symbols at the receiving device in a multi-user or MIMO system, and typically to improve the performance of the SIC detector, the data streams with the greatest power are cancelled first, thus re-

moving the greatest source of interference first, which is known as the VBLAST technique [100], and is implemented by considering the powers of the channels associated with each user or antenna. However, as shown in [103], although the VBLAST cancellation order within the SIC is the optimal for the vast majority of detected symbols, other cancellation orders can outperform the VBLAST ordering on a given occasion, which could result in performance gains.

In this chapter, dynamic reliability ordering (RO) based upon log-likelihood-ratios (LLR) [70] is considered in conjunction with a method of multiple-feedback (MF), [104], [105, 106] which is designed to provide alternative cancellation candidates for data symbols, to compensate for and correct potentially erroneous detected symbols. These methods are integrated into the proposed MF-RO-SIC detector, which utilises both methods and makes considerations for reducing the computational complexity associated with these methods, whilst increasing the BER performance. A discussion on the complexity of the proposed detector with comparisons to existing methods, and a method for integrating the proposed detector with iterative detection and decoding in a channel coded system is also considered.

This chapter is organised as follows, firstly the point-to-point MIMO system model on which this chapter's work is based will be described, followed by an in-depth look at interference cancellation techniques, including SIC, RO and MF techniques, and an explanation of Voronoi diagrams. In the next section, the proposed MF-RO-SIC detector is detailed, and the integration of the methods involved is developed to produce an algorithm with reduced computational complexity. After this, an iterative detection and decoding system for the proposed MF-RO-SIC detector is detailed, which includes a method of hard decision feedback. Finally, the results of simulations in the point-to-point system model are presented, for both the proposed detector and the iterative detection and decoding methods, ending with a summary of this chapters main results.

4.2 System Model

The system under consideration is a point-to-point spatial multiplexing MIMO link, consisting of N_t transmit antennas and N_r receive antennas. At each time instant, the N_t length column vector $\mathbf{x}$ consisting of N_t data symbols taken from the constellation set V that is appropriate for the modulation scheme being used, is transmitted through the $N_r \times N_t$ channel matrix $\mathbf{H}$. At the N_r receive antennas at the destination, the transmitted signal vector is received, processed and organised as the N_r length column vector $\mathbf{y}$. This can be described as:

$$\mathbf{y} = \mathbf{H}\mathbf{x} + \mathbf{n}, \tag{4.1}$$

where **n** is the circular complex additive white Gaussian noise (AWGN) vector representing noise at the receive antennas with a variance given by

$$\sigma^2 = 1/(2\gamma), \tag{4.2}$$

where γ is the signal-to-noise ratio (SNR) per antenna. The channel $\mathbf{H}$ is modelled as a complex Rayleigh distributed channel, and can be expressed as the horizontal concatenation of the individual channel vector associated with each transmit antenna,

$$\mathbf{H} = [\mathbf{h}_1, ..., \mathbf{h}_i, ..., \mathbf{h}_{N_t}]. \tag{4.3}$$

The linear MMSE detection technique described in Chapter 2 will be used in this chapter as the basis for the proposed interference cancellation method developed in this chapter. The MMSE filter detection can be described as below:

$$\hat{\mathbf{x}} = \mathbf{W}_{MMSE}^{H}\mathbf{y}, \tag{4.4}$$

where $\hat{\mathbf{x}}$ is the N_t length vector of the estimated transmitted data, which can also be described as per-antenna values $[\hat{x}_1, \ldots, \hat{x}_i, \ldots, \hat{x}_{N_t}]$. It is possible to estimate the distribution of the bits ($b_i \in \{-1, +1\}$) of the elements of $\hat{\mathbf{x}}$ as Gaussian random variables, as shown in [60], with a probability density function (PDF) of:

$$f(\hat{x}_i|b_i) = \frac{1}{\sqrt{2\pi}\sigma_i}\exp\left[-\frac{(\hat{x}_i - m_i)^2}{2\sigma_i^2}\right], i = 1, ..., N_t, \tag{4.5}$$

where m_i and σ_i^2 are the mean and variance, respectively,

$$m_i = \frac{\bar{\gamma}_i}{1+\bar{\gamma}_i} b_i, \tag{4.6}$$

$$\sigma_i^2 = \frac{\bar{\gamma}_i}{2(1+\bar{\gamma}_i)^2}, \tag{4.7}$$

with $\bar{\gamma}_i$ representing the instantaneous SINR of receive antenna i. The fact that the elements of $\hat{\mathbf{x}}$ can be accurately modelled as Gaussian random variables is important as this makes the analysis of the MMSE detection output convenient, thus making it easier to derive useful results for determining cancellation ordering in later sections.

4.3 Interference Cancellation Techniques

In this section, we shall review the interference cancellation techniques that are involved in our proposed MF-RO-SIC detector, with an overview of the importance of the order of interference cancellation, a look at the idea of dynamic ordering and a method of ordering based on the reliability of estimated symbols using the LLR values of the estimated symbols. Finally the technique of MF is discussed with consideration for computational complexity.

4.3.1 Cancellation Order

The order in which a SIC process cancels the estimated signals can make a significant difference to the overall error rate performance of the detection algorithm, as some signals will have a greater effect on the level of interference than others. If the signal being estimated has a high level of interference, the symbol estimate produced has a greater chance of being inaccurate. If this inaccuracy is then used for cancellation in the algorithm, this may cause the other signals to also be estimated incorrectly, in an effect known as error propagation.

To reduce the impact of this effect, we can order the signals by the greatest associated channel power first, and the weakest last, as this ensures that the signals with a good SINR

are estimated first, and are thus less likely to be unreliably estimated. This also means the interferer with the greatest power is cancelled first, improving the SINR of the remaining signals by the greatest amount, and this is known as Ordered SIC (OSIC) or the VBLAST algorithm. In a quasi-static channel environment, this can be calculated once per packet, and the resultant ordering used for every time instant in that packet.

4.3.2 Log Likelihood Ratio Based Reliability Ordering

As the well-known VBLAST technique is based on the average channel power per antenna, which does not consider the received signal and the effect of noise in a given time instant, it does not take into consideration the per-time instant values of SINR at the receive antennas, which will vary over time around the average SINR due to the random properties of the values used to calculate it, like noise. The SINR at each antenna is affected by multiple factors, including the channel state and the random noise at the antennas, as well as other possible interference effects, such as other transmissions from other systems. Thus, just considering the channel state once per packet of data transmission, and resorting to an interference cancellation ordering decision based on this information could lead to accuracy loss when computing the SIC algorithm. So a possibility for the SIC method is to consider the cancellation order on a per-time instant basis, possibly resulting in the ordering changing at each time instant, giving the SIC method a dynamic ordering.

To calculate the dynamic ordering, we could consider the SINR at each time instance, and directly derive a method to calculate the ordering, however this would likely require accurate knowledge of the nature of interference, and so could be difficult to obtain. However, if we consider the LLR at each time instant of transmission, it is possible to derive a dynamic ordering of the SIC process [70], [107]. First, let us consider the LLR of a bit of a received BPSK symbol given the estimate $\hat{x}_i$:

$$L_i = \left| \ln \left[\frac{f(\hat{x}_i | b_i = +1)}{f(\hat{x}_i | b_i = -1)} \right] \right|. \tag{4.8}$$

The magnitude of L_i can be considered a measurement of how certain the detector can be that the estimated symbol is correct when the quantisation of $\hat{x}_i$ is performed, and thus can

be considered a measure of the reliability of the estimated bit. Now, if the filter $\mathbf{W}_{MMSE}$ of the linear MMSE detector is considered:

$$\mathbf{W}_{MMSE} = (\mathbf{H}\mathbf{H}^H + \mathbf{I}\sigma_n^2)^{-1}\mathbf{H} = \mathbf{R}_y^{-1}\mathbf{H}, \tag{4.9}$$

the filter for each individual antenna $\mathbf{w}_i$ can be rewritten as a product of the auto-correlation matrix of the interference plus noise $\mathbf{R}_i$:

$$\mathbf{w}_i = (1 + \mathbf{h}_i^H \mathbf{R}_i^{-1}\mathbf{h}_i)^{-1}\mathbf{R}_i^{-1}\mathbf{h}_i, \tag{4.10}$$

$$\mathbf{R}_i = \left(\sum_{\substack{l=1 \\ l \neq i}}^{N_r} \mathbf{h}_l \mathbf{h}_l^H + \mathbf{I}\sigma_n^2 \right). \tag{4.11}$$

If Eq.(4.10) is substituted into Eq.(4.4), the Gaussian PDF Eq.(4.5) of $\hat{\mathbf{x}}$ can give us the instantaneous SINR $\bar{\gamma}_i$ as:

$$\bar{\gamma}_i = \mathbf{h}_i^H \mathbf{R}_i^{-1}\mathbf{h}_i. \tag{4.12}$$

Now, if the Gaussian approximation for $\hat{x}_i$ in Eq.(4.5) is substituted into Eq.(4.8), the reliability L_i is equivalent to:

$$L_i = 4(1 + \bar{\gamma}_i)|\hat{x}_i| \simeq (1 + \bar{\gamma}_i)|\hat{x}_i|. \tag{4.13}$$

However, $\bar{\gamma}_i$ requires $\mathbf{R}_i^{-1}$, which may be complex to acquire in the system. In [107], the matrix inversion lemma may be applied to $\mathbf{R}_i^{-1}$, resulting in:

$$\bar{\gamma}_i = \frac{\mathbf{h}_i^H \mathbf{R}_y^{-1}\mathbf{h}_i}{1 - \mathbf{h}_i^H \mathbf{R}_y^{-1}\mathbf{h}_i}, \tag{4.14}$$

which only uses $\mathbf{R}_y$, which is the autocorrelation of the received signal already calculated for use in the MMSE filter. Substituting this result into Eq.(4.13) and simplifying gives:

$$L_i = (1 - \mathbf{h}_i^H \mathbf{R}_y^{-1}\mathbf{h}_i)^{-1}|\hat{x}_i|, \tag{4.15}$$

which is referred to as the Type-L reliability [107] for b_i. If we are using a modulation scheme with multiple bits per symbol (for example Quadrature Phase Shift Keying

Table 4.1: Reliability Ordering Successive Interference Cancellation Algorithm

Initialisation: $\mathbf{y}_0 = \mathbf{y}, \mathbf{H}_0 = \mathbf{H}$, $\mathbf{R}_{y,0} = \mathbf{H}\mathbf{H}^H + \mathbf{I}\sigma_n^2$

for $i = 1 \rightarrow N_t$ **do**
- $\mathbf{W}_i = \mathbf{R}_{y,i-1}^{-1}\mathbf{H}_{i-1}$
- $\hat{\mathbf{x}}_i = \mathbf{W}_i^H \mathbf{y}_{i-1}$
- **for** $j = 1 \rightarrow (N_t + 1 - i)$ **do**
  - $L_j = (1 - \mathbf{h}_j^H \mathbf{R}_{y,i-1}^{-1}\mathbf{h}_j)^{-1}|\hat{x}_j|$
- **end for**
- $j = \arg\max_{L_j}(L_1, ..., L_{N+1-i})$
- $\tilde{x}_j = \mathcal{Q}[\hat{\mathbf{x}}_i(j)]$
- $\mathbf{y}_i = \mathbf{y}_{i-1} - \tilde{x}_j \mathbf{h}_j$
- $\mathbf{H}_i = \mathbf{H'}_{i-1}{}^{\langle j \rangle}$
- $\mathbf{R}_{y,i} = \mathbf{R}_{i-1} - \mathbf{h}_j \mathbf{h}_j^H$

end for

$\hat{\mathbf{x}}_i(j)$ represents the jth value of $\hat{\mathbf{x}}_i$
$\mathbf{H'}_{i-1}{}^{\langle j \rangle}$ represents $\mathbf{H}_{i-1}$ with the jth column removed

(QPSK)), then a simple extension to Eq.(4.15) is:

$$L_i = (1 - \mathbf{h}_i^H \mathbf{R}_y^{-1}\mathbf{h}_i)^{-1}(|\Re(\hat{x}_i)| + |\Im(\hat{x}_i)|). \tag{4.16}$$

This reliability L_i can be incorporated into the SIC algorithm, as at every stage of the SIC procedure for each antenna's signal that has not yet been estimated, the reliability can be calculated, and the signal with the highest reliability measurement will be the next estimated signal. This results in a dynamic ordering that is not predetermined before the SIC is processed, and can change with every time instant. Table 4.1 shows the algorithm used for the RO-SIC process.

4.3.3 Multiple Feedback Cancellation

The method of MF [104–106] in a SIC process is based on the idea of reliable and unreliable symbol estimates, and how alternative symbol quantisation decisions can affect the cancellation results. During the SIC cancellation process, the quantised estimated symbol $\tilde{x}_i$, is defined as $\tilde{x}_i = \mathcal{Q}[\hat{x}_i]$, where $\mathcal{Q}[]$ is the quantisation function appropriate for the modulation scheme being used in the system, and the quantisation operates by choosing the constellation point c with the smallest Euclidean distance to the estimated symbol as

described by

$$\tilde{x}_i = \arg\min_{c \in V} \|\hat{x}_i - c\|^2. \tag{4.17}$$

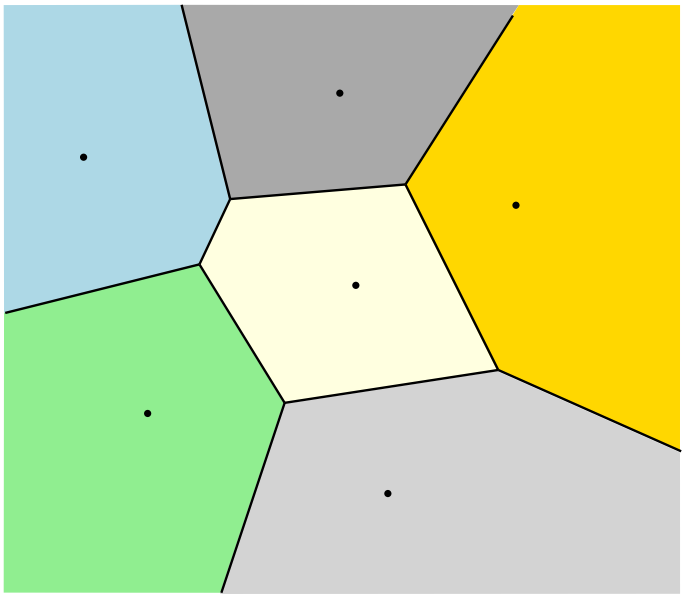

Figure 4.1: Example of a Voronoi diagram

This operation can be represented by a Voronoi diagram [108–110], which is a method of dividing an area up into regions around a set of points placed in the area. Each point in the diagram has a Voronoi cell associated with it, and the area within each Voronoi cell is defined as the space which has the Voronoi cell's point as its closest point in Euclidean distance. Fig. 4.1 shows an example of a Voronoi diagram with 6 points on a flat plane. The area is divided up into 6 regions around the 6 points, and if any position on the plane is chosen, the region in which the position is located shows which point is closest. The boundaries between the Voronoi regions can be called Voronoi boundaries, and represent the threshold at which a position can be considered to be close to two or more points.

The Voronoi diagram can thus be shown to correspond to how the quantisation function quantises estimated symbols to constellation points on a constellation diagram, with the Voronoi points representing the constellation points, the Voronoi regions showing where an estimated symbol will be quantised to and the Voronoi boundaries showing where the decision boundaries are located. Fig. 4.2a and 4.2b show the Voronoi diagrams for QPSK and 16-QAM modulation schemes, and so show how estimated symbols will be quantised.

However, if the estimated symbol is close to the Voronoi boundaries of two or more

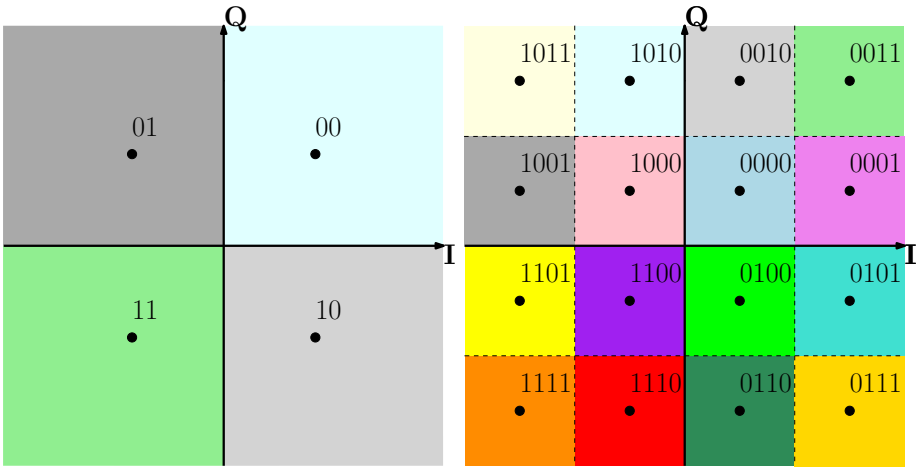

(a) QPSK (b) 16-QAM

Figure 4.2: Voronoi diagrams for QPSK and 16-QAM modulation schemes

constellation points, then the estimated symbol could conceivably be attributed to a constellation point that does not have the smallest Euclidean distance from the estimated symbol, as the effects of noise and interference are likely to cause the estimate to cross a Voronoi boundary.

Therefore, an area surrounding the Voronoi boundaries can be described as a scenario in which it is possible that the standard quantisation process may give inaccurate results. And so, a shadowing region on the constellation diagram is created, which defines an area in which an estimated symbol may be considered for alternative quantisation results. If $\hat{x}_i$ falls within this region, then the C alternative constellation points with the smallest Euclidean distances ($U \subset V, [u_1, ..., u_C]$) to $\hat{x}_i$ are considered for SIC processing, instead of just the closest. Fig. 4.3 shows how the shadowing region is defined by a shadowing criterion value S for QPSK modulation, which defines how far from the constellation axes (which are the Voronoi boundaries for a QPSK constellation) the shadowing region is set.

When these alternative candidates for $\tilde{x}_i$ are considered, the MF algorithm processes the SIC to completion for the C possible candidates, to produce an estimated symbol vector for all transmitted antennas $\tilde{\mathbf{x}}_c, c = 1, ..., C$. Then using the ML rule, the MF technique chooses the $\tilde{\mathbf{x}}_c$ that produces the smallest Euclidean distance as described by:

$$\tilde{\mathbf{x}} = \arg\min \|\mathbf{y} - \mathbf{H}\tilde{\mathbf{x}}_c\|^2, c = 1, ..., C. \tag{4.18}$$

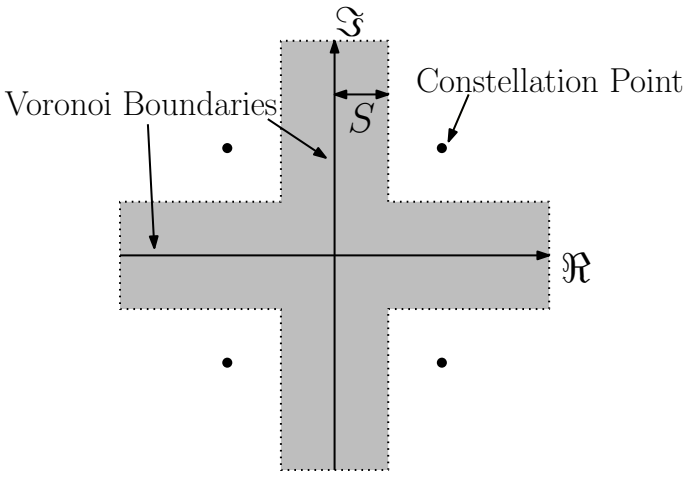

Figure 4.3: Shadow region for QPSK modulation

Table 4.2: Multiple Feedback Successive Interference Cancellation Algorithm

Initialisation: $\mathbf{y}_0 = \mathbf{y}, \mathbf{H}_0 = \mathbf{H}$
$\mathbf{w}_i = (\bar{\mathbf{H}}_i \bar{\mathbf{H}}_i^H + \mathbf{I}\sigma_n^2)^{-1}\mathbf{h}_i, \qquad i = 1, ..., N_t$

for $i = 1 \rightarrow N_t$ **do**
  $\hat{x}_i = \mathbf{w}_i^H \mathbf{y}_{i-1}$
  if $|\Re[\hat{x}_i]|$ and $|\Im[\hat{x}_i]| > S$ **then**
    $\tilde{x}_i = \mathcal{Q}[\hat{x}_i]$
  else
    for $k = 1 \rightarrow C$ **do**
      $\tilde{\mathbf{x}}^k = \tilde{\mathbf{x}}$
      $\mathbf{y}_i^k = \mathbf{y}_{i-1} - u_k \mathbf{h}_i$
      for $l = i + 1 \rightarrow N_t$ **do**
        $\tilde{x}_l^k = \mathcal{Q}[\mathbf{w}_l^H \mathbf{y}_{l-1}^k]$
        $\mathbf{y}_l^k = \mathbf{y}_{l-1}^k - \tilde{x}_l^k \mathbf{h}_l$
      end for
    end for
    $\tilde{x}_i = \arg\min_{k=1,...,C} \|\mathbf{y} - \mathbf{H}_0 \hat{\mathbf{x}}_k\|^2$
  end if
  $\mathbf{y}_i = \mathbf{y}_{i-1} - \tilde{x}_i \mathbf{h}_i$
  $\mathbf{H}_i = \mathbf{H'}_{i-1}{}^{\langle i \rangle}$
end for

$\bar{\mathbf{H}}_i$ represents the matrix formed by taking the columns $i, i+1, ..., N_t$ of $\mathbf{H}$
Assuming QPSK data is transmitted

The symbol candidate u_c associated with the chosen $\tilde{\mathbf{x}}_c$ is then chosen as $\tilde{x}_i$ for that cancellation stage, and the MF-SIC continues from the ith stage. Table 4.2 shows the MF-SIC algorithm.

4.4 Proposed Multiple Feedback Reliability Ordering Successive Interference Cancellation

Our proposed MF-RO-SIC detector combines the ideas of dynamic ordering within the SIC process, the multiple candidates feature for unreliable cancellation estimates, and overcomes the drawbacks of existing SIC detectors by minimising the extra computational complexity required.

A possibility for the combination of the MF-SIC and RO-SIC is to have the MF process taking place after the RO algorithm has decided which signal to estimate for this current iteration of the main SIC for loop. But, as may be noted in the algorithm in Table 4.2, the MF-SIC adds only a small amount of extra complexity over the SIC, as the cancellation filters for each stage $\mathbf{W}_n$ can be precalculated and reused within the MF process:

$$\mathbf{w}_i = (\bar{\mathbf{H}}_i \bar{\mathbf{H}}_i^H + \mathbf{I}\sigma^2)^{-1}\mathbf{h}_i, i = 1, ..., N_t, \tag{4.19}$$

eliminating the requirement to use a matrix inverse at each stage for a filter calculation, but this is only true if the cancellation order is known before the SIC is processed. In the case of the RO-SIC, the ordering dynamically changes with each cancellation stage so that the order is not predetermined, and so the MF filters cannot be precalculated for each time instant. For this reason, the filters would have to be recalculated for each stage in the MF, introducing a matrix inversion operation at each cancellation stage, every time $\hat{x}_i$ falls within the MF shadowing region, as well as determining the dynamic RO. This would involve a large increase in complexity over the standard MF-SIC, and this should be avoided.

In order to avoid this large increase in required complexity, we can split the MF-RO-SIC into two sections. Firstly, the RO-SIC can be calculated as in Table 4.1, in order to give a base estimate of $\tilde{\mathbf{x}}$, and to also determine the cancellation order taken by the dynamic ordering algorithm for this time instant. This cancellation order can then be returned to the MF-SIC.

This returned ordering can then be used as a predetermined ordering for the MF-SIC

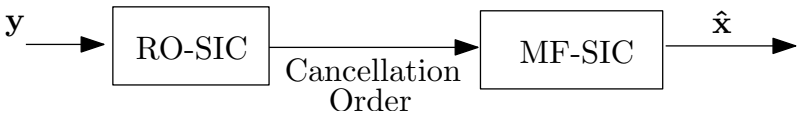

Figure 4.4: Structure of piece-wise MF-RO-SIC

process, and so the filters can be precalculated as in Table 4.2, with the new predetermined ordering, which means the filters only have to be calculated once per time instant for the MF-SIC, reducing the complexity of the MF-SIC process to the original level. This piece-wise approach is shown in Fig.4.4.

This piece-wise approach to the MF-RO-SIC does save complexity over the exhaustive ordering algorithm, but the filters are still calculated for the MF-SIC, and in effect the complexity of the RO-SIC and the MF-SIC is additive, roughly doubling the complexity over either individual algorithm.

However, greater reductions in complexity can be achieved by further integrating the two stages together intelligently. The MF-SIC filters $\mathbf{g}_i$ can be extracted from each stage of the RO-SIC, by taking and storing the jth column of the RO-SIC filter associated with the chosen cancellation, thus these values can be reused for the MF-SIC, so that the filters do not need to be calculated at all for the MF-SIC, reducing the complexity as no extra matrix inversions have to be performed. The MF-SIC filter $\mathbf{g}_i$ is given by:

$$\mathbf{g}_i = \mathbf{w}_{i,j}, \tag{4.20}$$

where $\mathbf{w}_{i,j}$ is the jth column of the filter $\mathbf{W}$ calculated for the ith cancellation stage of the RO-SIC. Also, whilst the MF-SIC cannot be directly integrated into the RO-SIC with low complexity due to the dynamic ordering restriction, the shadow criterion test for each $\hat{x}_i$ can still be carried out within the RO-SIC process, as below assumming QPSK data:

$$|\Re[\hat{x}_i]| < S \text{ and } |\Im[\hat{x}_i]| < S \tag{4.21}$$

If no $\hat{x}_i$ falls within the shadow criterion area during the RO-SIC, then logically the MF-SIC will not give a different $\tilde{\mathbf{x}}$ than the RO-SIC, as the MF technique will never be performed, and so the MF-SIC stage can be skipped for that time instant, reducing complexity further. Fig. 4.5 shows the structure of the MF-RO-SIC with these considerations,

Table 4.3: Multiple Feedback Reliability Ordering Successive Interference Cancellation Algorithm

Initialisation: $\mathbf{y}_0 = \mathbf{y}, \mathbf{H}_0 = \mathbf{H}, \mathbf{R}_{y,0} = \mathbf{H}\mathbf{H}^H + \mathbf{I}\sigma_n^2, m = 0$

for $i = 1 \rightarrow N_t$
- $\mathbf{W}_i = \mathbf{R}_{y,i-1}^{-1}\mathbf{H}_{i-1}$
- $\hat{\mathbf{x}}_i = \mathbf{W}_i^H \mathbf{y}_{i-1}$
- **for** $j = 1 \rightarrow (N_t + 1 - i)$
  - $L_j = (1 - \mathbf{h}_j^H \mathbf{R}_y^{-1} \mathbf{h}_j)^{-1} |\hat{x}_j|$
- **end for**
- $j = \arg\max_{L_j}(L_1, ..., L_{N_t+1-i})$
- $\mathbf{g}_i = \mathbf{w}_{i,j}$
- $\tilde{x}_j = \mathcal{Q}[\hat{\mathbf{x}}_i(j)]$
- **if** $|\Re[\hat{\mathbf{x}}_i(j)]|$ or $|\Im[\hat{\mathbf{x}}_i(j)]| < S$
  - $m = 1$
- **end if**
- $\mathbf{y}_i = \mathbf{y}_{i-1} - \tilde{x}_j \mathbf{h}_j$
- $\mathbf{H}_i = \mathbf{H'}_{i-1}{}^{\langle j \rangle}$
- $\mathbf{R}_{y,i} = \mathbf{R}_{i-1} - \mathbf{h}_j \mathbf{h}_j^H$

end for

if m = 1

for $i = 1 \rightarrow N_t$
- $\hat{x}_i = \mathbf{g}_i^H \mathbf{y}_{i-1}$
- **if** $|\Re[\hat{x}_i]$ and $|\Im[\hat{x}_i] > S$
  - $\tilde{x}_i = \mathcal{Q}[\hat{x}_i]$
- **else**
  - **for** $k = 1 \rightarrow C$
    - $\tilde{\mathbf{x}}^k = \tilde{\mathbf{x}}$
    - $\mathbf{y}_i^k = \mathbf{y}_{i-1} - u_k \mathbf{h}_i$
    - **for** $l = i + 1 \rightarrow N_t$
      - $\tilde{x}_l^k = \mathcal{Q}[\mathbf{g}_l^H \mathbf{y}_{l-1}^k]$
      - $\mathbf{y}_l^k = \mathbf{y}_{l-1}^k - \tilde{x}_l^k \mathbf{h}_l$
    - **end for**
  - **end for**
  - $k_{opt} = \arg\min_{k=1,...,C} \|\mathbf{y}_0 - \mathbf{H}_0 \hat{\mathbf{x}}_k\|^2$
  - $\tilde{x}_i = u_{k_{opt}}$
- **end if**
- $\mathbf{y}_i = \mathbf{y}_{i-1} - \tilde{x}_i \mathbf{h}_i$
- $\mathbf{H}_i = \mathbf{H'}_{i-1}{}^{\langle i \rangle}$

end for

end if

Assumes that QPSK is transmitted

and Table 4.3 shows the complete algorithm for the proposed MF-RO-SIC detector.

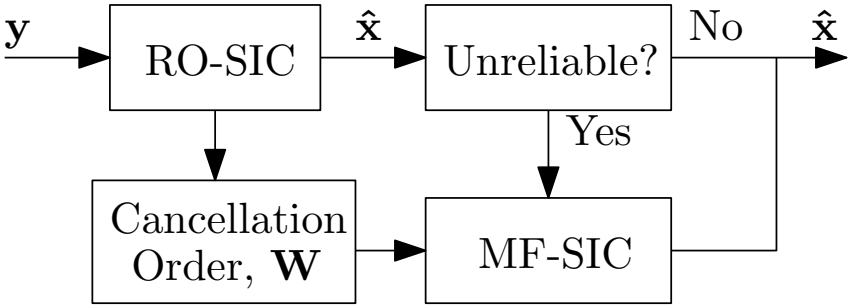

Figure 4.5: Structure of proposed MF-RO-SIC

4.5 Computational Complexity

The proposed MF-RO-SIC MIMO detector was designed in the previous section to reduce the extra complexity required as compared to the methods which the proposed detector is derived from. In order to fairly compare the algorithms in terms of computational complexity, it is required that the four methods (SIC, RO-SIC, MF-SIC and MF-RO-SIC) are analysed in terms of the number of complex additions and multiplications (collectively called operations) that are needed to run the algorithms per time instant.

As the MF-SIC and MF-RO-SIC use the conditional shadow criterion, directly analysing the complexity will be extremely difficult as the probability of the operations dependent on the shadow criterion result being run will change with each time instant. To easily assess the computational complexity, the complexity analysis will include some empirical variables, which are obtained by running simulations of the algorithms to be analysed in the system model detailed in Section 4.2. These empirical variables negate the need for complex statistical analysis of the conditional portions of the algorithms, and will be defined as follows:

- F will represent the average number of shadow criterion tests that are failed (*i.e.* . alternative candidates are considered) per time instant.
- T will represent the average number of alternative candidates that are calculated per time instant.
- Z will represent the average percentage of time instants that require the MF section of the MF-RO-SIC to be processed.

Table 4.4: Computational Complexity of Interference Cancellation Algorithms

Algorithm	Complex Additions	Complex Multiplications
SIC	$\frac{N_t}{2}(N_r{}^2 N_t + 3N_r{}^2 + 2N_r - 2) + N_t(\frac{N_r{}^3}{3} + \frac{N_r{}^2}{2} - \frac{5N_r}{6})$	$\frac{N_r N_t}{2}(N_r N_t + 3N_r + 4) + N_t(\frac{N_r{}^3}{3} + \frac{N_r{}^2}{2} + \frac{N_r}{3})$
RO-SIC	$\frac{N_r N_t}{2}(5N_r N_t - 4N_t + 5N_r + 2) + N_t(\frac{N_r{}^3}{3} + \frac{N_r{}^2}{2} - \frac{5N_r}{6})$	$\frac{N_t}{2}(3N_r{}^2 N_t + 3N_r N_t + N_t + 5N_r{}^2 + 3N_r + 1) + N_t(\frac{N_r{}^3}{3} + \frac{N_r{}^2}{2} + \frac{N_r}{3})$
MF-SIC	$\frac{N_t}{2}(N_r{}^2 N_t + 3N_r{}^2 + 2N_r - 2) + N_t(\frac{N_r{}^3}{3} + \frac{N_r{}^2}{2} - \frac{5N_r}{6}) + T(2N_r - 1) + CN_r{}^2 F$	$\frac{N_r N_t}{2}(N_r N_t + 3N_r + 4) + N_t(\frac{N_r{}^3}{3} + \frac{N_r{}^2}{2} + \frac{N_r}{3}) + N_r(2T + CN_r F)$
MF-RO-SIC	$\frac{N_r N_t}{2}(5N_r N_t - 4N_t + 5N_r + 2) + +N_t(\frac{N_r{}^3}{3} + \frac{N_r{}^2}{2} - \frac{5N_r}{6}) + T(2N_r - 1) + CN_r{}^2 F + Z(2N_r - 1)$	$\frac{N_t}{2}(3N_r{}^2 N_t + 3N_r N_t + N_t + 5N_r{}^2 + 3N_r + 1) + N_t(\frac{N_r{}^3}{3} + \frac{N_r{}^2}{2} + \frac{N_r}{3}) + N_r(2T + CN_r F + 2Z)$

Using these variables, it is possible to express the computational complexity of the four methods as shown in Table 4.4, and form comparisons of the relative computational cost. For the purpose of this analysis, it has been assumed that for matrix inversion operations that the Gauss-Jordan elimination method has been used. For practical systems, more efficient methods may be used, but this has little impact on the relative complexity of the algorithms as each method requires N_t inversions of an $N_r \times N_r$ matrix per time instance to operate.

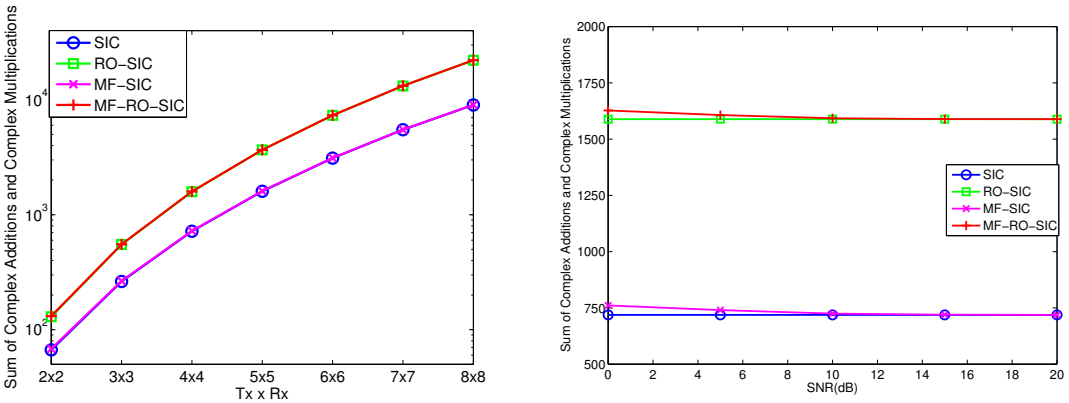

(a) $SNR = 10$dB, variable $N_r \times N_t$

(b) $N_r, N_t = 4$, variable SNR

Figure 4.6: Number of complex operations for each algorithm for a QPSK MIMO system, $S = 0.2, C = 4$

Fig. 4.6 shows plots of the computational complexity for different sizes of a MIMO system, and over different SNR values. For these simulations, QPSK was used as the

Table 4.5: Average Complexity Cost for RO-SIC and MF-RO-SIC

SNR	RO-SIC Operations	MF-RO-SIC Operations	Average % Increase
0	1588.7	1627.3	2.4288
5	1588.7	1607.1	1.1576
10	1588.7	1592.6	0.2459
15	1588.7	1589.1	0.0266
20	1588.7	1588.8	0.0036

modulation scheme, with the shadow criterion S set to 0.2, and the number of alternative candidates considered C to 4. Fig. 4.6a shows how the complexity changes as the size of the MIMO system increases, at an SNR of 10dB. It can be seen that adding the MF method to the SIC and RO-SIC adds very little complexity compared to the original methods, and that using the RO method roughly doubles the complexity as compared to the SIC. This is due to the amount of reliabilities that have to be calculated per time instant for the RO method. Fig. 4.6b shows how the complexity varies over a range of SNR values for a 4x4 system. The only terms dependent on the SNR are the empirical variables obtained (S, T and Z), and so the SIC and RO-SIC have no variance in their complexity over the SNR range, whereas the MF-SIC and MF-RO-SIC do have some variance. At high SNR values, the MF-SIC and MF-RO-SIC converge towards the SIC and RO-SIC complexity costs, respectively, due to the shadow criterion test failing only rarely. At low SNR values, the difference between the MF and non-MF methods can be seen, but the increase in complexity is only a small percentage. Table 4.5 shows the average percentage increase in complexity between the RO-SIC and proposed MF-RO-SIC algorithm. At a 0dB SNR, the MF-RO-SIC only increases the complexity by 2.4%, whereas at 20dB SNR, the MF section of the algorithm is processed so rarely, that the increase is less than a hundredth of a percent.

4.6 Iterative Detection and Decoding

Here a hard decision feedback IDD system is presented, incorporating the idea of IDD [36, 95, 96, 98] with the proposed MF-RO-SIC detector to improve the BER performance in conjunction with channel coding.

4.6.1 Hard Decision Feedback System

In this scenario, the IDD system is based upon the IDD system in Chapter 3, but in contrast, hard decision detection and feedback are used for the detectors, eliminating the need for a list based MAP algorithm. In the proposed MF-RO-SIC algorithm, the quantised estimated symbols $\tilde{\mathbf{x}}$ are used to refine the received signal to increase the accuracy of subsequent stream detections, but the effectiveness of this interference cancellation is dependent on the accuracy of the $\tilde{\mathbf{x}}$ symbols being cancelled. If the accuracy of $\tilde{\mathbf{x}}$ can be improved, then the BER performance of the MF-RO-SIC detector will improve.

To this end, we can use the detected and decoded bits from an iterative detection system as a substitute for $\tilde{\mathbf{x}}$ in the interference part of a SIC algorithm. The theory behind this idea is that by using channel coding in the IDD system, the estimated decoded bits will have a higher accuracy than the encoded bits that are manipulated and estimated between the encoder stage at the transmitter and the decoder stage at the receiver of the IDD system. Thus, the symbols derived from the decoded bits will have a better BER than the $\tilde{\mathbf{x}}$ symbols in the MF-RO-SIC algorithm. And so the system consists of the layout as seen in Fig. 4.7, with the subscripts 1 and 2 representing the inner and outer coding and mapping functions respectively and $\mathbf{\Lambda}_D$ represents the *a posteriori* LLRV of the inner bits b of the bit vector $\mathbf{b}$, $\mathbf{\Lambda}_A$ is the *a priori* LLRV of b, $\mathbf{\Lambda}_E$ is the extrinsic information LLRV and the output LLRV $\mathbf{\Lambda}_O$, which is the output of each iteration that is used for the bit estimation.

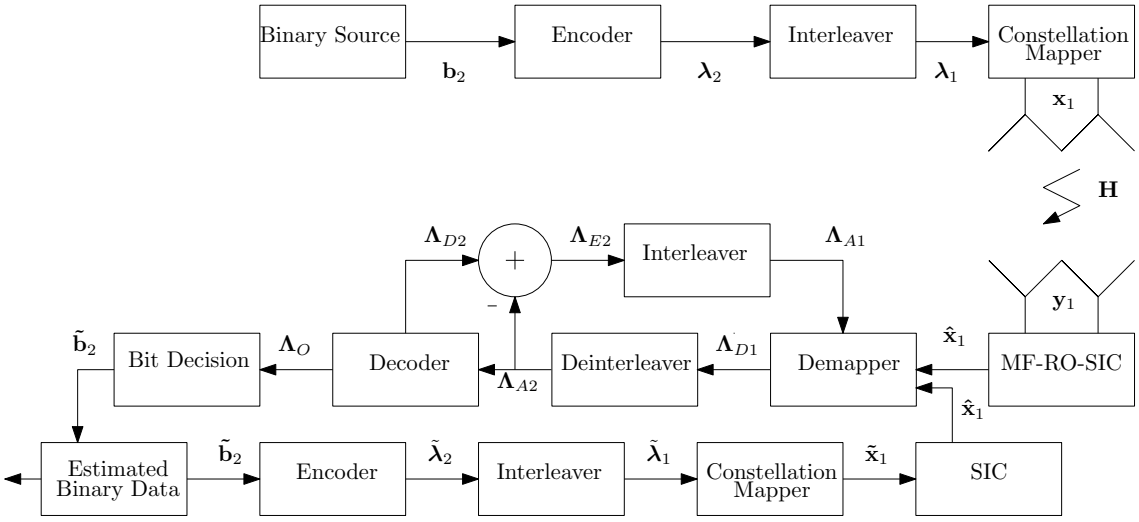

Figure 4.7: Hard decision iterative decoding system layout

The binary source bits $\mathbf{b}_2$ are first encoded by the channel coding scheme used by the IDD system (in this case a convolutional code) to produce the outer coded bits $\boldsymbol{\lambda}_2$, which are then interleaved into the inner coded bits $\boldsymbol{\lambda}_1$. The inner coded bits are then mapped to a constellation diagram to produce the symbols for MIMO transmission $\mathbf{x}_1$. The coded transmitted symbols are received as the received coded signal vector $\mathbf{y}_1$, and then the proposed MF-RO-SIC detector performs the algorithm to produce the inner estimated coded transmitted symbols $\hat{\mathbf{x}}_1$. The demapper then will estimate the inner *a posteriori* bit LLRV $\boldsymbol{\Lambda}_{D1}$ using a MAP method and then this result is deinterleaved to the outer *a priori* LLRV $\boldsymbol{\Lambda}_{A2}$, which is given to the decoder which produces the output LLRV $\boldsymbol{\Lambda}_O$. A bit decision process then takes place on $\boldsymbol{\Lambda}_O$ to produce the outer estimated binary data bits $\tilde{\mathbf{b}}_2$, which is our result for this first iteration of detection.

Now two types of feedback take place, firstly in a similar fashion to Chapter 3's IDD system, the decoder also produces the outer *a posteriori* bit LLRV $\boldsymbol{\Lambda}_{D2}$, which has the $\boldsymbol{\Lambda}_{A2}$ subtracted from it to give the outer extrinsic information LLRV $\boldsymbol{\Lambda}_{E2}$. This is then interleaved to give the inner *a priori* LLRV $\boldsymbol{\Lambda}_{A1}$, which is an input to the demapper for the next iteration of processing.

Secondly, in order to refine the estimated binary data bits, we now feedback these bits to the SIC algorithm for a refinement of the estimated symbols $\hat{\mathbf{x}}_1$, but this first requires some manipulation. The outer estimated binary data bits are re-encoded and interleaved using the same convolutional code and interleaver as the transmitter, to produce the estimated inner coded bits $\boldsymbol{\lambda}_1$, which are then mapped to the estimated inner coded transmitted symbols $\tilde{\mathbf{x}}_1$. A standard SIC detector will then use this re-encoded result in place of the quantised estimated symbols $\mathcal{Q}[\hat{x}_i]$ in the SIC process. The SIC process will then produce the inner estimated coded transmitted symbols $\hat{\mathbf{x}}_1$ instead of the MF-RO-SIC, which then are processed in the second iteration as in the first iteration. Each iteration subsequently is processed using the same method as the second iteration, producing refined and more accurate versions of $\tilde{\mathbf{b}}_2$.

4.6.2 Demapping Estimated Symbols

The demapper in Fig. 4.7 is a two-stage process that relies on the MAP method to produce individual bit LLRVs from the estimated symbols $\hat{\mathbf{x}}_1$. A difference from the MAP method in Chapter 3 is that the MAP method here will not have a list of potential symbols candidates produced by the detector, but only a single vector. In order to calculate the MAP, the probability of getting the estimate $\hat{x}_1$ for each possible constellation point is required. This probability is calculated by:

$$p(\hat{x}_1|x_k) = \frac{1}{2\pi\sigma^2} \exp\left(\frac{-|\hat{x}_1 - x_k|^2}{2\sigma^2}\right), k = 1...K, \tag{4.22}$$

where K is the number of constellation points in the modulation scheme used, and x_k is the kth symbol in the modulation scheme. To get the symbol log-likelihood this is then arranged as:

$$\log f(\hat{x}_1|x_k) = \frac{-|\hat{x}_1 - x_k|^2}{2\sigma^2}, k = 1...K. \tag{4.23}$$

To obtain the inner bit LLRV $\Lambda_{1,b}$, where b is the bit index for each symbol, $b = 1...\log_2 K$, we use the above result in a MAP algorithm [111]:

$$\Lambda_{1,b} = \log\left(\frac{\sum\limits_{x_k \in \mathcal{X}_1} f(\hat{x}_{1,b}|x_k)p(x_k)}{\sum\limits_{x_k \in \mathcal{X}_0} f(\hat{x}_{1,b}|x_k)p(x_k)}\right), \tag{4.24}$$

where $p(x_k)$ is the *a priori* probability of x_k, which is obtained from the decoder after each iteration. For the first iteration process this LLRV is set to 0 for all symbols, which represents no initial assumption about the bit data. The MAP can then be approximated using the Max-Log approximation detailed in Chapter 3 to give:

$$\Lambda_{1,b} \approx \max_{x_k \in \mathcal{X}_1} \log\left(f(\hat{x}_{1,b}|x_k)p(x_k)\right) - \max_{x_k \in \mathcal{X}_0} \log\left(f(\hat{x}_{1,b}|x_k)p(x_k)\right) \tag{4.25}$$

4.7 Simulation Results

For the simulation results presented in this chapter, a MIMO system was considered with either a QPSK or a 16-QAM scheme, and with perfect knowledge of the channel state information, the SIC detectors considered are based upon linear MMSE filtering, and the individual channel elements are modelled as having Rayleigh distributions. Extensions to other modulation schemes and propagation channels is straightforward.

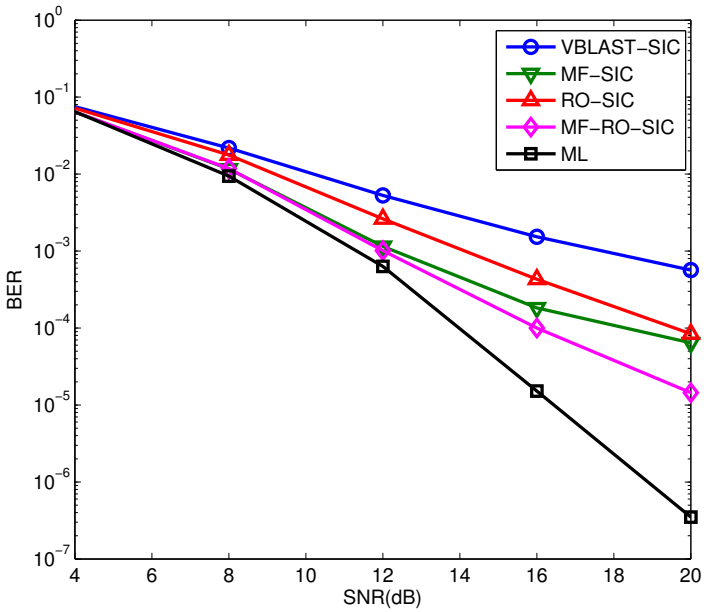

Figure 4.8: 4x4 MIMO with QPSK modulation, $C = 4, S = 0.2$

Fig. 4.8 shows how the proposed MF-RO-SIC detector compares with the VBLAST-SIC, RO-SIC, MF-SIC and the ML detector in terms of BER in a 4x4 MIMO system. The number of candidates for the MF (C) is set to 4, with the shadow criterion S set to 0.2. The MF-RO-SIC can be seen to have up to 4dB in BER performance improvement over the MF-SIC at a BER level of 10^{-4}, just over 4dB over the RO-SIC at a BER level of 10^{-4} and up to 8dB of gain over the VBLAST-SIC at a BER level of 10^{-3}. In this scenario, it appears that the MF method is the major contributor to the MF-RO-SIC detectors performance in the lower SNR region, with the dynamic RO providing the extra gains at the higher SNR level.

Fig. 4.9 similarly shows how the proposed MF-RO-SIC detector compares with the VBLAST-SIC, RO-SIC, MF-SIC and the ML detector in terms of BER in an 8x8 MIMO

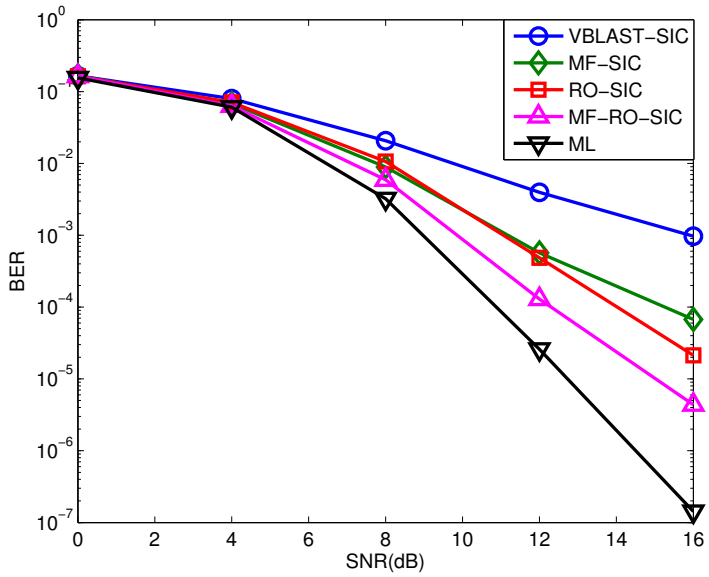

Figure 4.9: 8x8 MIMO with QPSK modulation, $C = 4, S = 0.2$

system. The number of candidates for the MF (C) is set to 4, with the shadow criterion S set to 0.2. The MF-RO-SIC can be seen to have up to 4dB BER performance over the MF-SIC at a BER level of 10^{-4}, just over 2dB over the RO-SIC at a BER level of $10^{-4.7}$ and up to 8dB of gain over the VBLAST-SIC at a BER level of 10^{-3}, with the MF-RO-SIC approaching the ML performance with a 2dB loss at a BER level of $10^{-5.4}$. It can be noted that in Fig. 4.8, the MF-SIC had better performance than the RO-SIC, but in Fig. 4.9, the RO-SIC outperformed the MF-SIC, suggesting that for larger MIMO systems, the RO in the MF-RO-SIC provides the major contribution to the performance gains of the MF-RO-SIC over the VBLAST SIC, whilst for smaller MIMO systems, the MF provides the greater performance gains.

Fig. 4.10 shows how the BER performance of the MF-RO-SIC changes as the shadow criterion is varied, as compared to the RO-SIC and the ML solution. As the shadow criterion is increased, the BER performance varies from the RO-SIC performance and tends towards the ML performance. It can be seen that for each 0.1 increase of S, the BER performance of the MF-RO-SIC has another 1-2dB of gain added at a BER level of $10^{-3.7}$. This however, is at the cost of complexity, as the larger the shadow criterion, the more likely an estimated symbol is to fall within the shadow area, and thus the MF process is calculated more often. It should be noted that a degradation in BER performance was observed if S was set too high ($\sim 0.4 > S$). These values of S represent the shadow

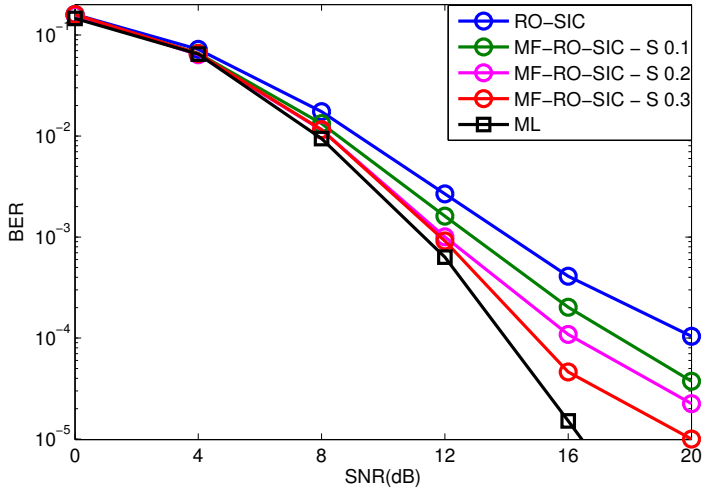

Figure 4.10: 4x4 MIMO with QPSK modulation, $C = 4$, variable S

criterion boundary being closer to the constellation point than the constellation axis, as for QPSK, the constellation point is at a value of 0.7071. This is possibly due to the MF-RO-SIC testing a large amount of alternative constellation points in the MF process, increasing the likelihood that false positive solutions are found for the ML rule due to noise and self-interference.

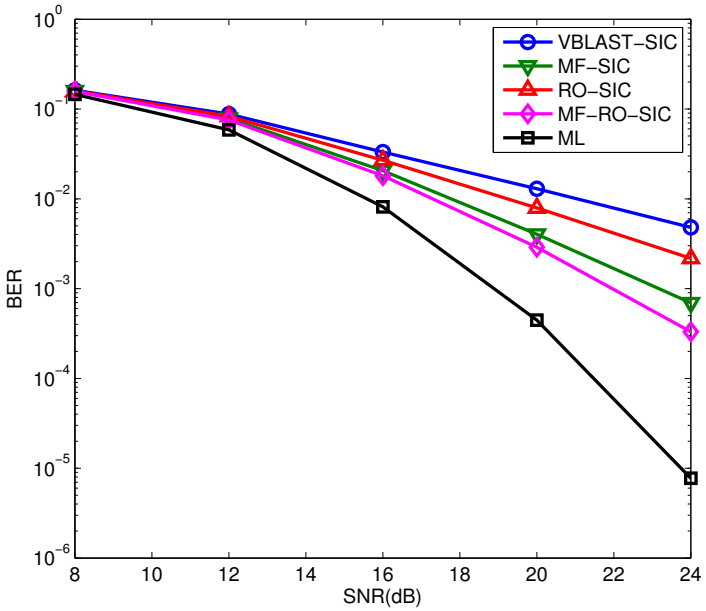

Figure 4.11: 4x4 MIMO with 16-QAM modulation, $C = 4, S = 0.1$

Fig. 4.11 shows the performance of proposed MF-RO-SIC detector as compared with the VBLAST-SIC, RO-SIC, MF-SIC and the ML detector in terms of BER in a 4x4 MIMO

system, in a system using 16-QAM. The number of candidates for the MF (C) is set to 4, with the shadow criterion S set to 0.1. The shadow criterion is set lower for 16-QAM than QPSK, as the constellation points for 16-QAM are closer together than for QPSK, and so the shadow criterion is scaled down to account for this. For this system, the MF-RO-SIC has 1dB of gain over the MF-SIC at a BER level of 10^{-3}, 4dB of gain over the RO-SIC at a BER level of $10^{-2.5}$ and up to 6dB of gain over the VBLAST-SIC at a BER level of 10^{-2}. The MF-RO-SIC has about 4dB of loss from the ML detector at a BER level of $10^{-3.2}$, which is a greater loss than for QPSK, which suggests that the shadow criterion and number of candidates can be further optimised.

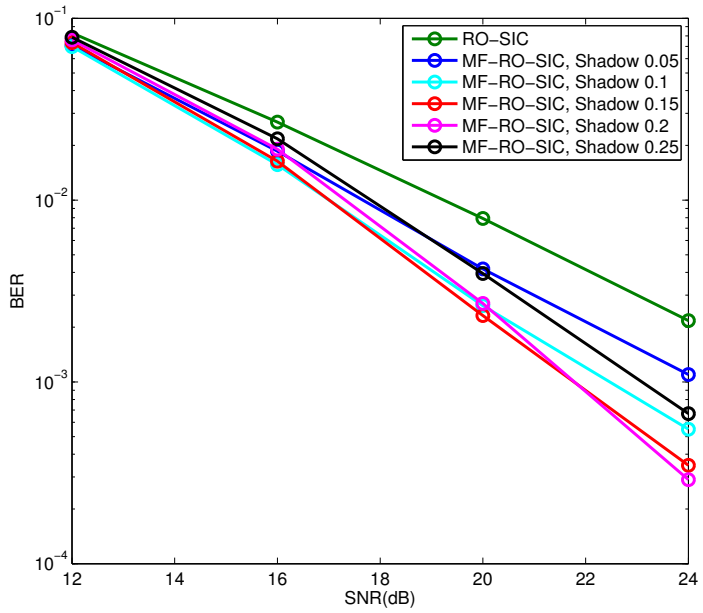

Figure 4.12: 4x4 MIMO with 16-QAM modulation, $C = 4$, variable S

Fig. 4.12 shows the BER performance of the proposed MF-RO-SIC detector as the shadow criterion is varied. It can be seen that increasing the shadow criterion increases the BER performance, until at $S = 0.15$ the performance starts decreasing, as the number of false positives starts degrading the accuracy of the detector. The value at which the shadow criterion increase degrades performance is smaller than for QPSK, due to the smaller separation between the constellation points and the Voronoi boundaries.

Fig. 4.13 shows how varying the candidate limit C affects the BER performance of the MF-RO-SIC for a 16-QAM modulation. It can be seen that adding extra candidates (which increases the complexity of the MF section of the algorithm) beyond 4 candidates

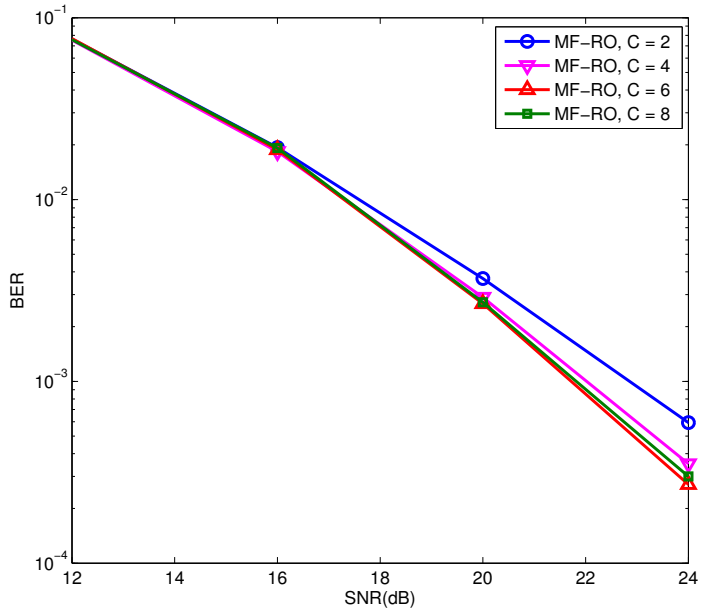

Figure 4.13: 4x4 MIMO with 16-QAM modulation, variable C, $S = 0.1$

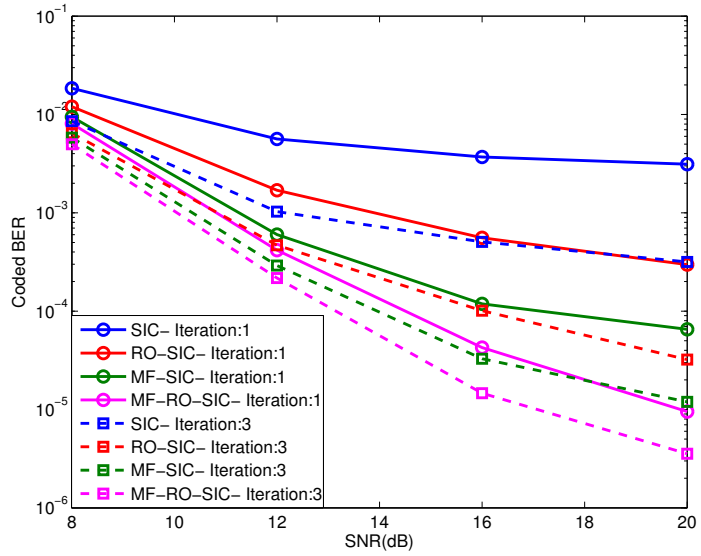

Figure 4.14: 4x3 MIMO with QPSK modulation, $C = 4, S = 0.2$

has diminishing gains. The gain from using 2 candidates to 4 candidates is approximately 1dB, but the gain from 4 to 6 candidates is less than 0.5dB, similarly from 6 to 8 candidates. This suggests that for this scenario, a choice of 4 candidates in the MF algorithm offers a very attractive complexity to gain ratio.

Fig. 4.14 shows how the hard decision iterative feedback version of the proposed MF-

RO-SIC performs in terms of coded BER, in a 4x3 MIMO QPSK system. The plots shown are the results of the 1st and 3rd iteration of decoding and detection. It can be seen that the 3rd iteration of the MF-RO-SIC outperforms the 3rd iteration of the MF-SIC by up to 4dB at a BER level of 10^{-5}, and the 3rd iteration of the RO-SIC by up to 6dB at a BER level of $10^{-4.4}$. It can also be seen that from the 1st to 3rd iteration of the hard decision feedback system, the MF-RO-SIC gains up to 3.5dB in BER performance at a BER level of 10^{-5}.

4.8 Summary

In this chapter, a new MF-RO-SIC detector has been proposed, utilising the ideas of dynamic cancellation stage reliability ordering and multiple candidates for estimated symbol decisions, with consideration given to the complexity of the resultant detector and how this can be reduced. An analysis of the complexity shows that the proposed detector adds very little complexity to the RO-SIC, but that simulation results have shown up to 4dB of gains over previously established SIC detectors and 8dB gains over the VBLAST-SIC, for 4x4 and 8x8 MIMO systems with QPSK modulation, and up to 4dB of gain over established detectors for a 16-QAM modulation scheme system. It has also been shown how the BER performance of the MF-RO-SIC detector is altered as the parameters of the detector are altered, and how this can approach the ML detector performance. Also considered is an iterative version with channel decoding, utilising hard feedback that is re-encoded to provide greater accuracy for the interference cancellation process. It is seen that this IDD method is effective in accurately detecting the transmitted data.

Chapter 5

Multi-Branch Interference Cancellation with Widely-Linear Processing for Multiuser Cooperative MIMO Systems

Contents

5.1 Introduction

In systems using real-valued constellations such as Binary Phase Shift Keying (BPSK), Widely Linear (WL) filtering techniques [61, 112, 113] can produce much superior Bit Error Rate (BER) performances as compared with standard linear Minimum Mean Squared Error (MMSE) filters by exploiting the non-circularity of the received data to give extra degrees of freedom. Although WL techniques have been shown to perform well in point-to-point MIMO systems [62, 114], the scenarios of overloaded multi-user detection (MUD), where there are more transmit antennas at the users than receiver antennas at the destination [115] or cooperative communication cases [13, 17] have seen very little development.

As WL techniques are applicable particularly in modulation schemes where there is only one dimension used (BPSK, Amplitude Shift keying (ASK) etc.), or in modulation schemes where there is an imbalance between the average power of the in-phase and quadrature dimensions, such as offset QPSK and offset QAM, it is possible to overload the system by using more transmit antennas than receive antennas, and still maintain an acceptable error performance as compared with standard linear techniques. This can be applied to situations where multiple users are transmitting data simultaneously to a multiple antenna destination, and the destination is able to receive more data streams/user transmissions than receive antennas at the destination. This is similar to the up-link scenario of a system with multiple users and a base station.

WL MUDs can potentially resolve twice the number of users than that of antenna elements at the receiver, without significant loss of error performance in the system [116], assuming real valued modulation schemes are used, unlike linear receivers, which can only resolve the same number of users as that of antenna elements at the receiver without error performance loss. This is due to the WL Wiener filtering techniques taking advantage of the covariance matrix of the received signal as well as the pseudo-covariance matrix of the received signal, which is non-zero for non-circular signals. This setting gives the WL filter extra degrees of freedom as compared with the linear filter, which only uses the covariance matrix of the received signal [117]. Cooperative systems can also be considered for this scenario, with some user devices acting as relays for the other

devices, retransmitting the received signals for the other users in a different time frame to the destination. These relayed signals can give the destination an extra source of spatial diversity, and so potentially improve the error performance.

In this chapter, we shall propose a technique in which a WL Successive Interference Cancellation (SIC) algorithm [71] is enhanced with the Multi-Branch (MB) method [69, 103, 118, 119], and show how this method can be applied to the design of receivers of an overloaded multi-user cooperative scenario using simple Amplify-and-Forward (AF) relays [16]. The results shown will demonstrate that the introduction of relays into the system can improve the BER performance at the destination, and that the introduction of the MB method can improve performance even further.

5.2 System Model

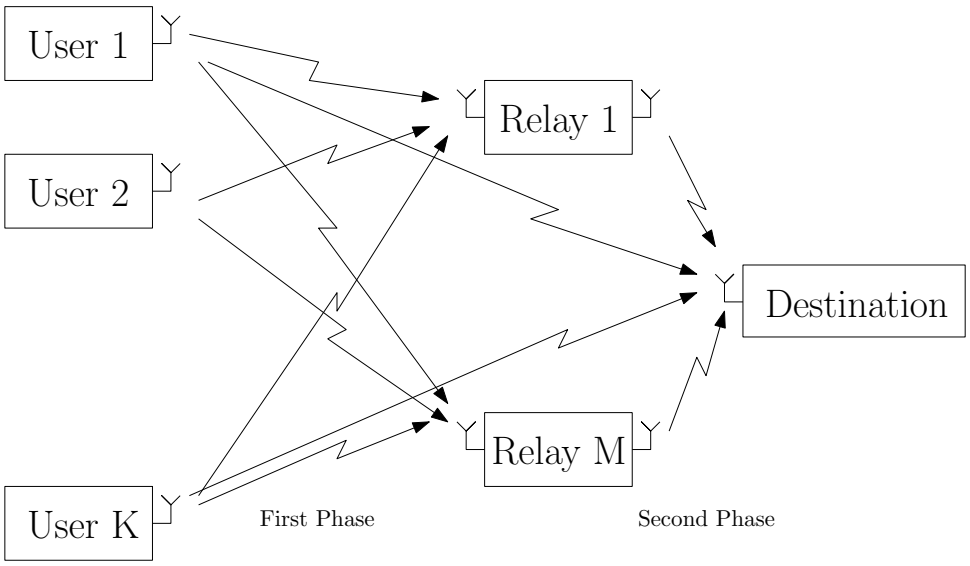

Figure 5.1: Two-Phase MIMO Multiuser Cooperative System Model

The system under consideration is a two-phase multi-relay scenario, with K single-antenna source users and a destination node with R antenna elements. The first phase of transmission originates from the K source users to the M single-antenna AF relays and the destination node, with the second phase consisting of the relay nodes retransmitting

to the destination node. The first phase of transmission is described by:

$$\mathbf{y}_{sd} = \sum_{k=1}^{K} \mathbf{h}_{sd_k} x_{s_k} + \mathbf{n}_d^{(1)} \in \mathbb{C}^{R\text{x}1}, \tag{5.1}$$

$$y_{sr_m} = \sum_{k=1}^{K} h_{sr_{m,k}} x_{s_k} + n_{r_m}^{(1)}, m = 1, \ldots, M, \tag{5.2}$$

and the second phase of transmission by:

$$\mathbf{y}_{rd} = \sum_{m=1}^{M} \mathbf{h}_{rd_m} \gamma_{r_m} y_{sr_m} + \mathbf{n}_d^{(2)} \in \mathbb{C}^{R\text{x}1}. \tag{5.3}$$

The quantities $\mathbf{y}$ and y denote the received signal vector or scalar, $\mathbf{x}$ and x are the transmitted symbol vector and scalar, the channels are represented by the $\mathbf{h}$ vector or h scalar, and $\mathbf{n}$ and n represent the Additive White Gaussian Noise (AWGN) vector or scalar at the receive antennas, whose samples are drawn from a complex Gaussian distribution with mean zero and variance σ_n^2, which is given by:

$$\sigma_n^2 = 1/(\zeta), \tag{5.4}$$

where ζ is each user's signal-to-noise ratio (SNR).

The s,d and r subscripts denote the variable's relation to the system, source, destination and relay, respectively, and the subscript k represents the user index. For example, the quantity $\mathbf{h}_{sd_k}$ represents the channel between the source user k and the destination. The superscript $^{(1)}$ on each noise term, $\mathbf{n}$ indicates the transmission phase in which the noise vector is applied. The scalar γ is the AF amplification factor at the relays, defined as:

$$\gamma_{r_m} = \sqrt{\frac{1}{|h_{sr_m}|^2 + {\sigma_n}^2}} \tag{5.5}$$

where $|\bullet|$ is the absolute value of the complex scalar. Note that if h_{sr_m} was a vector or matrix (in the case of the users or relays having multiple antennas), the Frobenius norm would be appropriate instead of the absolute value. Fig.5.1 shows the two-phase multiuser cooperative system layout.

The propagation channels between nodes are modelled as Rayleigh distributed chan-

nels, with a path-loss exponential scaling factor [86] and added large scale log-normal shadowing (LNS) [87], as given by

$$\mathbf{h} = \alpha_{p,q}\beta_{p,q}\mathbf{h}_o, \tag{5.6}$$

with $\mathbf{h}_o$ denoting a complex Gaussian distributed channel with a Rayleigh distributed modulus, $\alpha_{p,q}$ representing the distance related path-loss between transmitter p and receiver q and $\beta_{p,q}$ as a log-normal variable, representing shadowing between transmitter p and receiver q. The parameters α and β are calculated as follows:

$$\alpha_{sd} = \sqrt{L}, \tag{5.7}$$

$$\alpha_{sr_{m,k}} = \frac{\alpha_{sd}}{\sqrt{(d_{sr_{m,k}})^{\rho}}}, m = 1, \ldots, M, k = 1, \ldots, K \tag{5.8}$$

$$\alpha_{rd_{m,k}} = \frac{\alpha_{sd}}{\sqrt{(d_{rd_{m,k}})^{\rho}}}, m = 1, \ldots, M, k = 1, \ldots, K \tag{5.9}$$

$$\beta_{p,q} = 10^{\left(\frac{\sigma_s \mathcal{N}(0,1)}{10}\right)} \tag{5.10}$$

where L is the base power path loss of the source to destination link, ρ is the path loss exponent, usually between 2 and 4 depending on the environment, $\mathcal{N}(0,1)$ represents a Gaussian distribution with mean zero and variance 1 and σ_s is the shadowing spread in dB. It is assumed the LNS affecting each channel is subject to similar shadowing spread, but is expressed as independent log-normal variables.

5.3 Proposed Multi-Branch Widely-Linear Successive Interference Cancellation

In this section, the theory and derivation of WL filters and their integration into the SIC process is discussed, and how MB processing can include the WL SIC, along with descriptions of the algorithms required for implementation.

5.3.1 Widely Linear Successive Interference Cancellation

The method of SIC is well established, and operates by estimating each transmitted symbol in a received symbol vector using a receive filter to compute the estimate. Once an estimate for a transmitted symbol has been obtained, the estimate is then refined by attempting to remove the effects of the interference on the desired signal. This allows the remaining symbols to be estimated with a greater accuracy. In traditional SIC methods, the filter applied to extract the received symbols is typically a linear MMSE filter, but in the case of non-circular modulation schemes, it is possible to replace this with a WL MMSE filter as described in Chapter 2. Note that for circular modulation schemes such as QPSK or 16-QAM, the WL MMSE filter reduces to the linear MMSE filter, and its application results in no performance gain.

The WL MMSE filter is based upon a similar form to the linear MMSE filter, but instead of operating solely upon the received signal, it also has a filter applied to the complex conjugate of the received signal, described as below for a complex vector estimate $\mathbf{z}$ of the desired complex vector $\mathbf{x}$:

$$\mathbf{z} = \mathbf{F}^H \mathbf{y} + \mathbf{G}^H \mathbf{y}^* \tag{5.11}$$

where ^{H} represents the Hermitian transformation and * indicates the complex conjugate, and the observation vector $\mathbf{y}$ is modelled as:

$$\mathbf{y} = \mathbf{H}\mathbf{x} + \mathbf{n}, \tag{5.12}$$

which can be described as a single phase of the cooperative transmission, similar to Eq.(5.1) for the first phase of transmission, if the K users are instead viewed as K transmit antennas, and similar to Eq.(5.3) if the M relays are M transmit antennas, with $\gamma_{r_m} y_{sr_m}$ replacing the complex vector $\mathbf{x}$. In both cases, the definition of $\mathbf{n}$ remains as in Section 5.2.

The design of the WL MMSE filters $\mathbf{F}$ and $\mathbf{G}$ corresponds to solving the following minimisation problem:

$$\mathcal{E} = \mathbf{E}[\|\mathbf{x} - \mathbf{F}^H \mathbf{y} - \mathbf{G}^H \mathbf{y}^*\|^2], \tag{5.13}$$

Table 5.1: Widely Linear Successive Interference Cancellation Algorithm

Initialisation: $\mathbf{y}(0) = \mathbf{y}, \mathbf{H}(0) = \mathbf{H}$

for $i = 1 \rightarrow K$ **do**
$\mathbf{z}(i) = \mathbf{F}^H(i)\mathbf{y}(i-1) + \mathbf{G}^H(i)\mathbf{y}^*(i-1)$
$\tilde{\mathbf{x}}(i) = \mathcal{Q}[\mathbf{z}(i)]$
$\mathbf{y}(i) = \mathbf{y}(i-1) - \tilde{\mathbf{x}}(i)\mathbf{H}(i-1)^{\langle i \rangle}$
$\mathbf{H}(i) = \mathbf{H}'(i-1)^{\langle i \rangle}$
end for

$\mathbf{H}^{\langle i \rangle}$ represents the ith column of $\mathbf{H}$ $\mathbf{H}'^{\langle i \rangle}$ represents $\mathbf{H}$ with the ith column removed $\mathcal{Q}[\bullet]$ represents the quantise function

where $\mathbf{E}[\bullet]$ is the expectation operator, and this can give the cost function of the mean squared error ($\mathcal{E}$) between the desired signal $\mathbf{x}$ and the estimate $\mathbf{z}$ given by

$$[\mathbf{F}_{opt}, \mathbf{G}_{opt}] = \arg\min_{\mathbf{F},\mathbf{G}} \mathcal{E}. \tag{5.14}$$

Using the derivation of the WL filters as described in Chapter 2 (Eq.2.26-2.41), Eq.(5.13) can be solved using simultaneous equations to isolate $\mathbf{F}$ and $\mathbf{G}$, obtaining the final result:

$$\mathbf{F} = (\mathbf{R}_{hh} - \mathbf{R}_{ht}\mathbf{R}_{hh}^{-*}\mathbf{R}_{ht}^{*})^{-1}(\mathbf{H} - \mathbf{R}_{ht}\mathbf{R}_{hh}^{-*}\mathbf{H}^{*}) \in \mathbb{C}^{RxK} \tag{5.15}$$

$$\mathbf{G} = (\mathbf{R}_{hh} - \mathbf{R}_{ht}\mathbf{R}_{hh}^{-*}\mathbf{R}_{ht}^{*})^{-*}(\mathbf{H}^{*} - \mathbf{R}_{ht}^{*}\mathbf{R}_{hh}^{-1}\mathbf{H}) \in \mathbb{C}^{RxK} \tag{5.16}$$

where

$$\mathbf{R}_{hh} = \mathbf{H}\mathbf{H}^H + \mathbf{I}\sigma^2 \in \mathbb{C}^{KxK} \tag{5.17}$$

$$\mathbf{R}_{ht} = \mathbf{H}\mathbf{H}^T \in \mathbb{C}^{KxK} \tag{5.18}$$

where $^{-*}$ represents the inverse conjugate, and so gives definitions for the WL MMSE filters, $\mathbf{F}$ and $\mathbf{G}$. Table 5.1 shows the algorithm used for the WL SIC process.

5.3.2 Multi-Branch Successive Interference Cancellation

The order of cancellation within a SIC process is important, and can affect the performance of the SIC method, as an incorrectly estimated symbol at an early cancellation

stage may cause other symbols to be incorrectly estimated also, resulting in error propagation.

An often used scheme is to estimate the symbol with the greatest associated channel power first, and then the next greatest power symbol and so on. This is sometimes referred to as the Ordered SIC (OSIC) or the VBLAST scheme [78], [100], [101]. The principle behind VBLAST being that the symbol with the greatest channel power will be the least prone to being estimated incorrectly, thus reducing error propagation. However, the VBLAST ordering is not guaranteed to be the best cancellation order for each received symbol vector due to noise and other interference effects. In addition, the use of SIC limits the diversity order achieved by the detector as compared to the full receive diversity attained by the ML detector.

The MB scheme [102] operates by altering the order of cancellation in the SIC process, by default the VBLAST scheme, and running this altered order separately from the original order. Each different order permutation process is known as a branch, thus the MB scheme runs several different cancellation order branches in parallel. The results of the branches are processed by an ML decision rule using the Euclidean distance as a metric, which chooses the most likely symbol for each user amongst the candidates available in the branches. This strategy allows the MB scheme to attain a superior diversity order to the standard SIC algorithm and closer to that of the ML detector. The ML rule used is as described below:

$$\tilde{\mathbf{x}} = (\tilde{x}_1, ..., \tilde{x}_K)^T = \min_{b=1,..,B} \|(\mathbf{y} - \mathbf{H}(\hat{x}_{1,b}, ..., \hat{x}_{K,b})^T\|^2, \tag{5.19}$$

where B is the number of branches being considered by the ML rule, and b is the index of the branch currently being considered, with $\tilde{\mathbf{x}}$ representing the final answer of the MB-WL-SIC.

Each branch, and thus cancellation order, has an associated permutation matrix $\mathbf{T}$ which alters the branch's cancellation order. The permutation matrix $\mathbf{T}_i$ is a binary matrix which is applied to the base VBLAST ordering vector c_0 to create a new ordering vector for branch i, c_i, as below:

$$\mathbf{c}_i = \mathbf{T}_i \mathbf{c}_0, \tag{5.20}$$

Table 5.2: Multiple Branch Algorithm

for $i = 1 \rightarrow B$ **do**
$\mathbf{y}_t = (\mathbf{y}_{sd}^T, \mathbf{y}_{rd}^T)^T$
$\mathbf{h}_{sd} = (\mathbf{h}_{sd_1}, ..., \mathbf{h}_{sd_K})$
$\mathbf{h}_{ur} = (\mathbf{h}_{sr_1,m}, ..., \mathbf{h}_{sr_K,m})$
$\mathbf{h}_{srd} = \sum_{m=1}^{M} (\mathbf{h}_{rm} \gamma_{r_m} \mathbf{h}_{ur})$
$\mathbf{H}_t = (\mathbf{h}_{sd}^T, \mathbf{h}_{srd}^T)^T$
$(\hat{x}_{s_1,i}, ..., \hat{x}_{s_K,i})^T =$WL-SIC$(\mathbf{y}_t, \mathbf{H}_t, \mathbf{T_i}, \sigma_n)$
end for
$(\tilde{x}_{s_1}, ..., \tilde{x}_{s_K})^T = \min_{j=1,..,B} \|(\mathbf{y}_t - \mathbf{H}_t(\hat{x}_{s_1,j}, ..., \hat{x}_{s_K,j})^T\|^2$

where $\mathbf{T}_i$ starts as a $K \times K$ matrix of zeros, with entries corresponding to the desired permutation changed to 1's. To determine which entries are 1's, each row of $\mathbf{T}_i$ is related to a single entry in the desired ordering c_i. And so for the kth row of $\mathbf{T}_i$, the value of $c_i(k)$ determines which column in this row is set to 1. For example, if the desired ordering c_i was $[2, 3, 1, 4]$ for $K = 4$, then $\mathbf{T}_i$ would be:

$$\mathbf{T}_i = \begin{pmatrix} 0 & 1 & 0 & 0 \\ 0 & 0 & 1 & 0 \\ 1 & 0 & 0 & 0 \\ 0 & 0 & 0 & 1 \end{pmatrix} \tag{5.21}$$

Within this MB system, each branch performs a WL-SIC process, with the cancellation order altered by $\mathbf{T}$. The algorithm operates as in Table 5.2 for B branches, and is represented in Fig.5.2:

5.4 Branch Selection

Choosing which permutation branches to run is important, as there are $K!$ different possible permutations, so running every possible branch would be computationally prohibitive. Fig.5.3 shows the possible permutations of a system with 4 transmitted data streams (by individual antennas or users), with the default ordering defined as the VBLAST ordering, which will order the cancellation by the norm of the channel associated with each

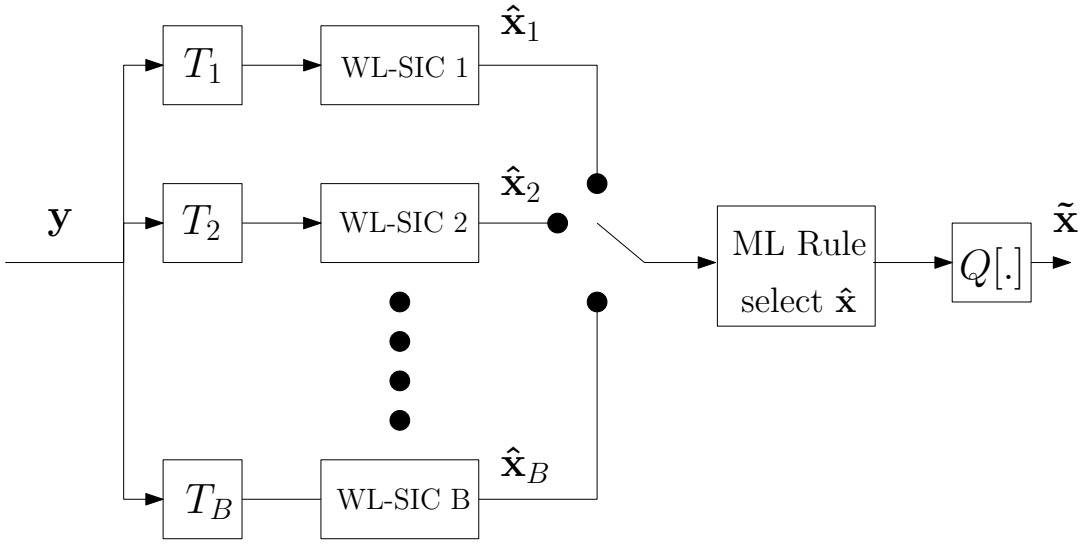

Figure 5.2: Multi-Branch System

transmitted data stream. It can be seen how different cancellation orders create branches from the initial cancellation stage within the SIC at the top of the diagram, and as the algorithm progresses it moves down the cancellation stages from top to bottom, with each branch describing a different cancellation order, potentially giving different results for the symbol detection.

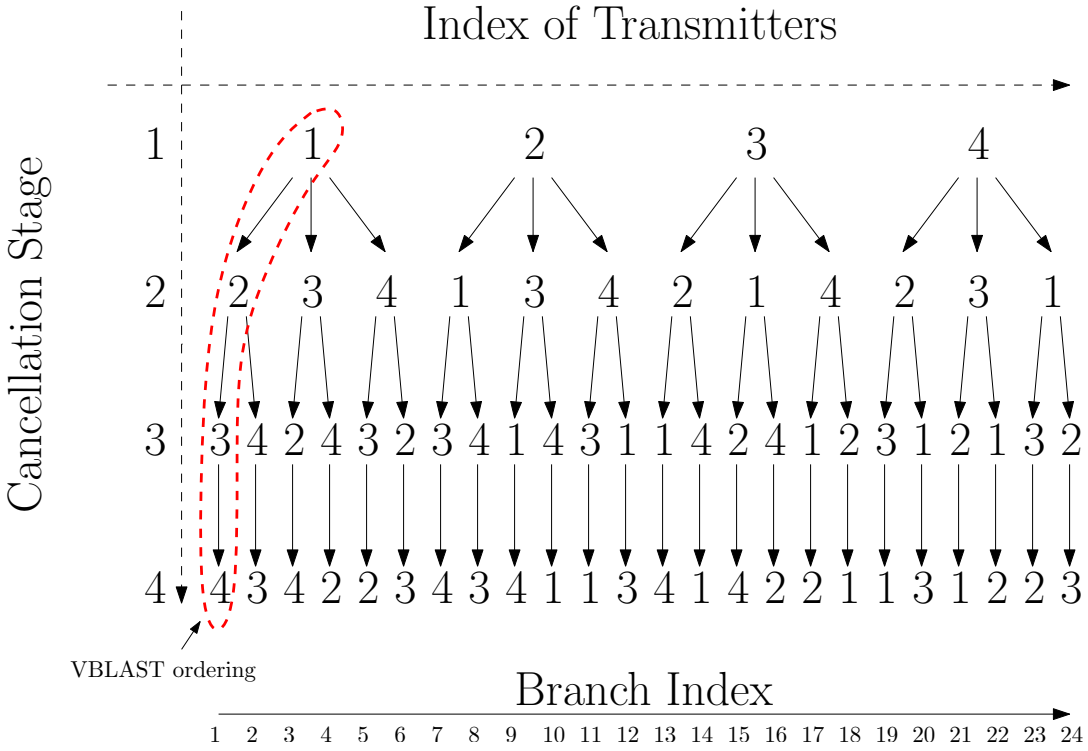

Figure 5.3: Multi-Branch Permutation Possibilities for a MIMO system with 4 transmitters

A proposed strategy for branch selection is to choose $B \leq K, b = 1, ..., B$ branches (including the original VBLAST branch), where b is the branch index, with the bth branch altering the cancellation order by initially processing the bth cancellation stage first, and then processing the remaining stages in order. For example, in a 4-user system, the cancellation orders for $B = 4$ branches would be $[1, 2, 3, 4]$, $[2, 1, 3, 4]$, $[3, 1, 2, 4]$ and $[4, 1, 2, 3]$, or referring to Fig.5.3, branch indices 1,7,15 and 24. This gives the 4 permutation matrices $\mathbf{T}_1 ... \mathbf{T}_4$ as:

$$\mathbf{T}_1 = \begin{pmatrix} 1 & 0 & 0 & 0 \\ 0 & 1 & 0 & 0 \\ 0 & 0 & 1 & 0 \\ 0 & 0 & 0 & 1 \end{pmatrix}, \mathbf{T}_2 = \begin{pmatrix} 0 & 1 & 0 & 0 \\ 1 & 0 & 0 & 0 \\ 0 & 0 & 1 & 0 \\ 0 & 0 & 0 & 1 \end{pmatrix}$$

$$\mathbf{T}_3 = \begin{pmatrix} 0 & 0 & 1 & 0 \\ 1 & 0 & 0 & 0 \\ 0 & 1 & 0 & 0 \\ 0 & 0 & 0 & 1 \end{pmatrix}, \mathbf{T}_4 = \begin{pmatrix} 0 & 0 & 0 & 1 \\ 1 & 0 & 0 & 0 \\ 0 & 1 & 0 & 0 \\ 0 & 0 & 1 & 0 \end{pmatrix}$$

Alternatively, it is possible to compile a list of the most commonly selected branches by the ML rule for a system, as these branches are most likely to give better BER performance than the other branches. However, the only way to determine the most commonly selected branches by the ML rule is to empirically run the system over a very large number of packets and time instances in the environment the system is to operate in, calculating every branch for each detection instance, and observe the frequency at which each branch is selected [103]. Unfortunately, for large numbers of transmit antennas or users, this quickly becomes impractical due to the fact that there are $K!$ numbers of possible branches, and would have to be rerun for each different scenario in which the algorithm could operate in.

Therefore, in order to counter the extremely high complexity of calculating each branch for each time instance, without excluding a branch from being processed it is fundamental to find a new way of selecting the ordered branches.

The proposed branch selection strategy consists of a dynamic selection of branches, where during the original VBLAST branch, if a symbol decision in the SIC process is considered unreliable, a new branch is created such that the branches diverge in processing

order at the point of the unreliable symbol estimate, giving rise to a different cancellation order branch, which could also create another new branch in the case of an unreliable symbol estimate arising in the new branch. In order to determine if a symbol estimate is unreliable, the idea of a shadowing area in the constellation diagram from the MF algorithm [104–106] in Chapter 4 can be used. Fig. 5.4 shows the shadow area for QPSK modulation on a constellation diagram. If a symbol estimate falls within the shadow area on the constellation diagram, then the symbol can be considered unreliable, and so an alternative cancellation order can be considered for the MB algorithm, creating a new branch in parallel with the old ordering.

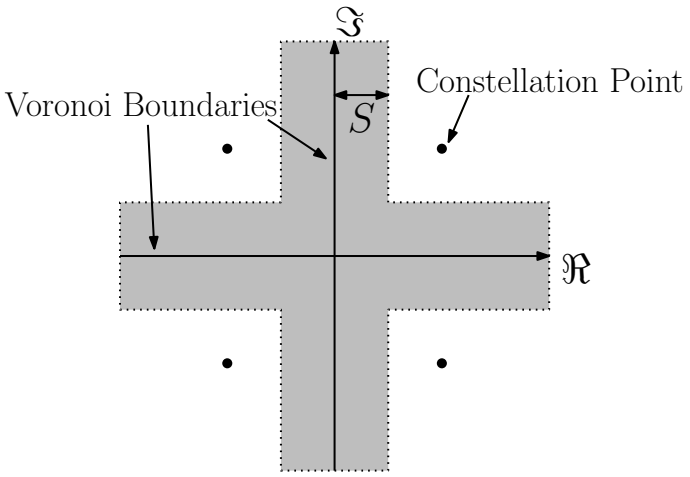

Figure 5.4: Shadow region for QPSK modulation

The rules of operation in the dynamic branching as based upon Fig.5.3 are:

- Start with branch index 1, and process cancellation stage 1
- If at any point during the processing of the branch, a symbol estimate is unreliable, hop right to the next possible alternative **unless** the next cancellation to the right does not share a common root with the current branch, *e.g.* 3rd stage of branch index 6 to 3rd stage of branch index 7 is not allowed.
- If hopping branches, the original branch continues the processing, and the new branch uses the previously processed data from previous stages.
- If the alternative cancellation hopped to is also unreliable, the algorithm can hop again if possible.
- Each newly created branch can spawn new branches.

- The last cancellation stage has no alternatives to hop to, and so the unreliablity test does not need to be processed.

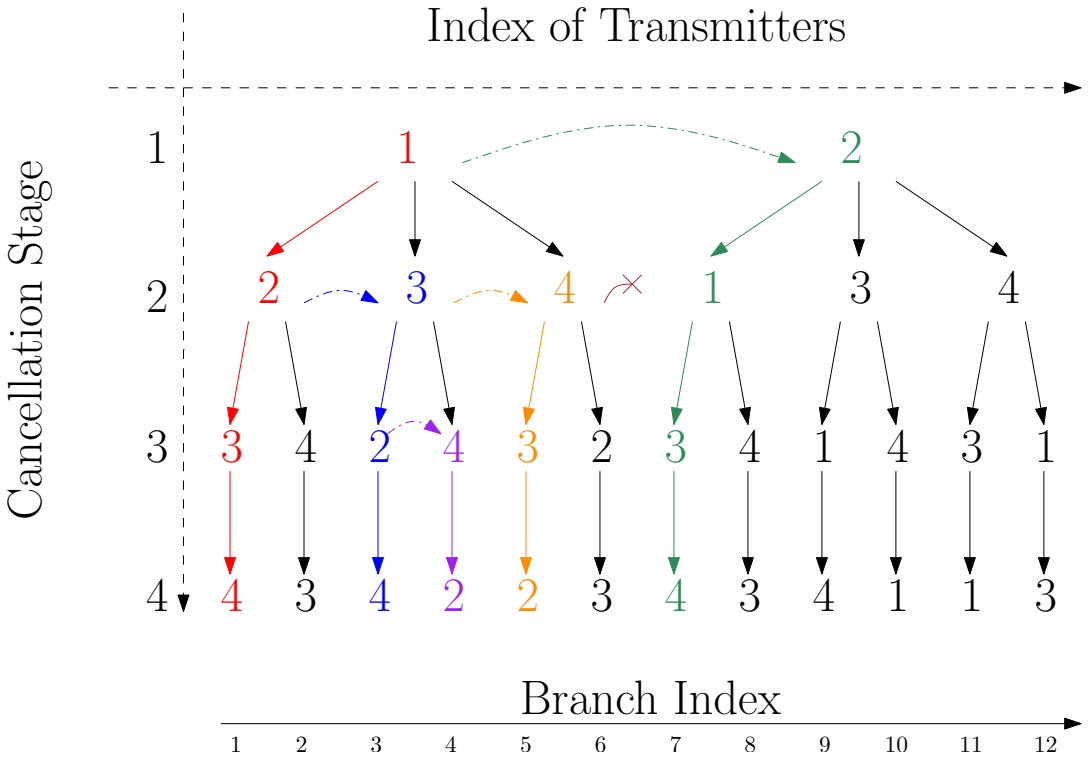

Figure 5.5: Dymanic branching branch selection

Fig.5.5 shows how the dynamic branch selection creates new branches as the SIC operates in a single time instant. (The right half of the orders are not considered, and so omitted from this diagram for the purpose of clarity.) In Fig.5.5, the original branch (highlighted in red) first processes the data stream from transmitter 1. In this case, the symbol is considered unreliable, and so a new branch is created (in green), and instead start by processing transmitter 2's data. The estimate obtained is reliable, and so the branch continues, and completes without any more unreliable symbol estimates. As the red branch continues, in the second stage the symbol estimate is also considered unreliable, and so another new branch is created (blue). The red branch continues without any more unreliable estimates and completes. The blue branch uses the processed data from the first stage, as the roots of the red and blue branches are the same, and continues processing the branch, but the symbol estimate in the second cancellation stage is also unreliable, and so the order hops right (orange). However this estimate is also unreliable, and tries to hop right again, but as this would hop to a branch that does not share a root with this branch, the hop does not happen (represented by the brown line with a cross).

Table 5.3: Dynamic branching and branch hop algorithm

Dynamic Branching
1. Run branch index 1 (VBLAST branch) and during processing note at which stages unreliable symbol estimates occurred, if any 2. If unreliable estimates occurred, calculate which branches to hop to, and queue the branch indices for processing, else go to Step 6 3. If there is a queue of branches to be processed, process the next branch noting at which stages unreliable symbol estimates occurred, if any 4. If unreliable estimates occurred, calculate which branches to hop to, and queue the branch indices for processing 5. If there are branches remaining to be calculated that have not been processed already, go to Step 3 6. Gather results from each processed branch, and determine the best result using the ML rule
Hop Algorithm
$b =$ current branch index, $s =$ stage at which unreliable estimate occurred **if** $s = k$ **then** skip to end **for** $i = 1 \rightarrow s - 1$ Remove columns whose first row does not equal the ith stage of b Remove first row **end for** Remove columns whose first row does equal the sth stage of b Remove columns whose branch index is less than or equal to b Branch to hop to is the lowest remaining branch index **if** no branch indices remain **then** cannot hop

The orange branch then processes to completion without any more unreliable data estimates. In the third cancellation stage, the blue branch has an unreliable symbol estimate, and so a new branch (purple) is created. All remaining branches then complete, as for the last cancellation stage there are no alternatives. The result of this process has thus created 5 branches (indices 1,3,4,5 and 7) that will be compared by Euclidean distance metrics. Alternatively, if there had been no unreliable symbol estimates during the processing, then the only branch processed would have been the original branch index 1, equivalent to the VBLAST WL-SIC.

To describe this algorithm in a way suitable for implementation in computer programming, we can consider the possible branch orders as a table, with each order as a column in the table containing the cancellation order indices, as in Table 5.4. The dynamic branching can then be thought of as manipulating the table and removing rows as necessary. The algorithm for the dynamic branching is described in Table 5.3.

Table 5.4: MB order table

1	1	1	1	1	1	2	2	2	2	2	2	3	3	3	3	3	3	4	4	4	4	4	4
2	2	3	3	4	4	1	1	3	3	4	4	2	2	1	1	4	4	2	2	3	3	1	1
3	4	2	4	3	2	3	4	1	4	3	1	1	4	2	4	1	2	3	1	2	1	3	2
4	3	4	2	2	3	4	3	4	1	1	3	4	1	4	2	2	1	1	3	1	2	2	3
1	2	3	4	5	6	7	8	9	10	11	12	13	14	15	16	17	18	19	20	21	22	23	24
Branch Index																							

5.5 Computational Complexity

The proposed MB-WL-SIC detector is obviously more computationally intense than the WL-SIC detector to process per time instance, due to the multiple branches being processed, but the dynamic branch selection algorithm aims to alleviate this problem somewhat by only processing extra branches when necessary. In order to compare the different detection algorithms, four different detection schemes (SIC, WL-SIC, MB-WL-SIC using B branches and MB-WL-SIC with dynamic branch selection (DMB-WL-SIC)) will be analysed to assess the computational complexity per time instance in terms of complex additions and multiplications.

However, directly analysing the computational complexity of the DMB-WL-SIC is not easy, due to the fact that the dynamic branching relies on the conditional shadow criterion to determine the algorithm's operation. This is similar to the problem in analysing the complexity of the MF-SIC and MF-RO-SIC in Chapter 4, and so a similar solution to calculate the computational complexity is used. A variable C will be used to denote the number of cancellation stages that take place on average per time instant, and this variable will be empirically estimated during the operation of the DMB-WL-SIC in the system model in Section 5.2, along with the average number of branches $\tilde{B}$ that the DMB-WL-SIC processes. As the MB-WL-SIC stacks the received signals from both phases into a single vector, the received signal vector length is $2R$, which is represented by the quantity T. This now allows for the comparison of the complex additions and multiplications required to process each algorithm per time instant, as shown in Table 5.5.

Fig 5.6 shows plots demonstrating the complex operations required to process the algorithm per time instant, with each complex addition or multiplication counted as 1 unit,

Table 5.5: Computational Complexity of Interference Cancellation Algorithms

Algorithm	**Complex Additions**	**Complex Multiplications**
Linear SIC	$\frac{K}{2}(KT^2+3T^2+2T-2)+T(\frac{T^3}{3}+\frac{T^2}{2}-\frac{5T}{6})$	$\frac{KT}{2}(KT+3T+4)+T(\frac{T^3}{3}+\frac{T^2}{2}+\frac{T}{3})$
WL-SIC	$T(2K^2T+KT^2+3KT+K-2T+1)+2K(\frac{T^3}{3}+\frac{T^2}{2}-\frac{5T}{6})$	$KT(2KT+K+2T^2+4T+1)+2K(\frac{T^3}{3}+\frac{T^2}{2}+\frac{T}{3})$
MB-WL-SIC	$B(T(2K^2T+KT^2+3KT+K-2T+1)+2K(\frac{T^3}{3}+\frac{T^2}{2}-\frac{5T}{6})+KT)$	$B(KT(2KT+K+2T^2+4T+1)+2K(\frac{T^3}{3}+\frac{T^2}{2}+\frac{T}{3})+T(K+1))$
DMB-WL-SIC	$T(2KT-2T+1)+CT(2KT+2T^2+T+1+2(\frac{T^3}{3}+\frac{T^2}{2}-\frac{5T}{6}))+\tilde{B}KT$	$2KT^2+CT(4KT+K+2T^2+2T+1+2(\frac{T^3}{3}+\frac{T^2}{2}+\frac{T}{3}))+\tilde{B}T(K+1)$

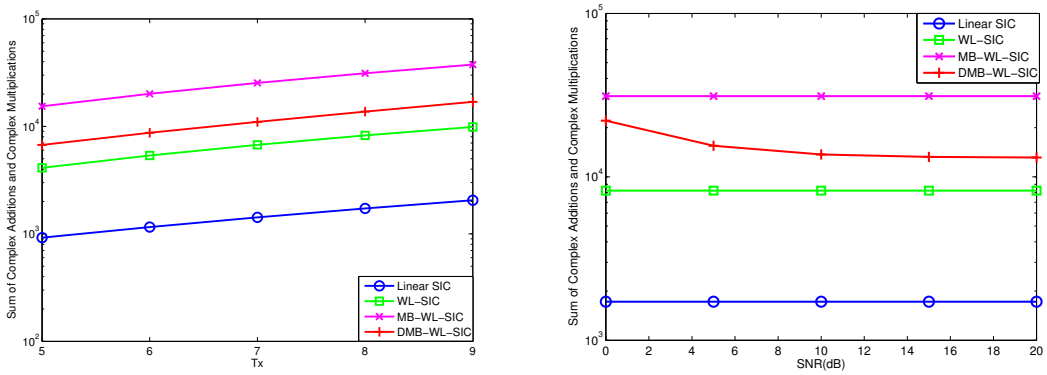

(a) $SNR = 10$dB, variable K

(b) $K = 8$, variable SNR

Figure 5.6: Number of complex operations for each algorithm for a BPSK cooperative MIMO system, $S = 0.2, M = 2, R = 2, B = 4$

Fig. 5.6a shows how the complexity changes as the number of transmitting users is increased at 10dB SNR. The complexity of the different algorithms can be seen to remain proportional in relation to each other as K changes, with the WL-SIC having roughly four times the complexity of the SIC, which is expected due to the extra processing the WL filters require. The MB-WL-SIC also increases the complexity over the WL-SIC by four times, which is due to the MB-WL-SIC using four branches in this case. However, the DMB-WL-SIC has a reduced complexity as compared with the MB-WL-SIC, using over 50% less complexity, meaning that the complexity of the DMB-WL-SIC is roughly double that of the WL-SIC. Fig. 5.6b shows how the complexity changes as the SNR value changes when $K = 8$. As expected, the complexity of the DMB-WL-SIC reduces as the SNR increases, due to the dynamic branching switching branches less often. This gives

the result that the DMB-WL-SIC has between 30% less complexity at 0dB, and 60% less complexity at 20dB than the MB-WL-SIC.

5.6 Iterative Detection and Decoding

Here a list-based IDD system is presented, which extends the proposed MB-WL-SIC to output a list of potential symbol estimate candidates, instead of a single hard decision, and how this principle can also be applied to generate list candidates from the linear SIC and WL-SIC.

5.6.1 IDD List-Based System

The candidate list-based IDD system is very similar to the IDD system presented in Chapter 3, but with a few key differences, as can be seen in Fig. 5.7. Firstly, the list sphere decoder (LSD) that is used as the detector is not appropriate in this setting, as the proposed detector is not directly based upon the ML rule, but instead must be replaced with list-generating algorithm based upon the proposed MB-WL-SIC. This can be easily accomplished with the MB-WL-SIC by eliminating the final ML rule decision from the algorithm, so that the detector instead returns the result from every branch, not just the branch determined to be optimal by the ML rule. The output of the list MB-WL-SIC algorithm is therefore:

$$\tilde{\mathbf{X}} = (\hat{x}_{s_1,j}, ..., \hat{x}_{s_K,j}), j = 1...B, \tag{5.22}$$

instead of just $\tilde{\mathbf{x}}$, where each column vector of $\tilde{\mathbf{X}}$ is a candidate vector in the list.

Secondly, a list $\mathcal{L}$ is generated for every iteration of the IDD system from the inner *a priori* LLRV $\mathbf{\Lambda}_{A1}$, using a list generation algorithm, which can generate a list of candidates from a single vector of symbol estimates. This list is then used in the MAP detector instead of the list from the previous iteration. This is in contrast to the IDD system in Chapter 3, which generates the list using the LSD during the first iteration, and then uses this list for each subsequent iteration.

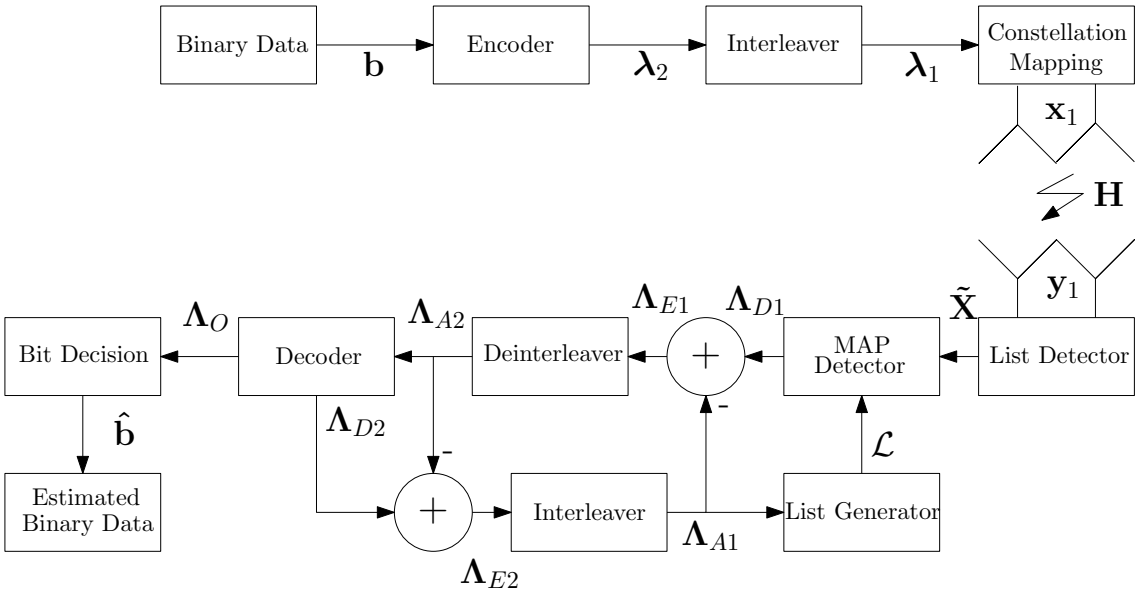

Figure 5.7: List based iterative decoding system layout

5.6.2 List Generator

The list generator algorithm used here is based upon the work in [120, 121]. The algorithm works upon the principle of the reliability of each bit of each symbol estimate, and of swapping the bits of the most unreliable estimates for different bits, and so different symbol estimates. By swapping the bits of the most unreliable symbols, a list of alternative symbol estimate vector is built up, and so this list can be used for the MAP algorithm. The list algorithm is controlled by a maximum list size L_{max} and a reliability threshold V_{th} which sets the maximum reliability sum for a bit vector. The list algorithm works by creating a permutation of a bit vector that is already under V_{th}, and then testing the reliability sum of the new permutation. If the permutation reliability sum ω is below ω_{th}, then the permutation is kept for the next round of permutations. Otherwise the permutation is discarded. If more permutation candidates are created than the maximum list size, then the permutations with the largest ω are discarded until there are L_{max} permutation candidates. Table 5.6 shows the algorithm for the list generator method.

The list generator algorithm can also be used to create candidate lists from the unquantised symbol estimates $\mathbf{z}$ from the SIC, WL-SIC or any other detector that produces only a single set of symbol estimates. In this case, the *a priori* LLRVs $\boldsymbol{\Lambda}_{A1}$ are substituted with $\mathbf{z}$ in the algorithm in Table 5.6 to produce the initial candidate list for the MAP detector in the first iteration of the IDD, and then the list from the *a priori* LLRVs for

Table 5.6: List Generator Algorithm

Initialisation: $b_A = (\text{sgn}[\mathbf{\Lambda}_{A1}] + 1)/2$, $\mathbf{V}(0) = \mathbf{0}_{K\times 1}, \omega(0) = 0$, L = 1

for $i = 1 \rightarrow K$ **do**
  $\mathbf{p} = \mathbf{0}_{K\times 1}$
  $\mathbf{p}(i) = 1$
  for $l = 1 \rightarrow L$ **do**
    $\mathbf{V}_l(i) = \mathbf{V}_l(i-1) + p$
  end for
  $\mathbf{V}_i = [\mathbf{V}(i-1), \mathbf{V}(i)]$
  $L = 2L$
  for $l = 1 \rightarrow L$ **do**
    $\omega_l = \mathbf{V}_l(i)^T |\mathbf{\Lambda}_{A1}|$
  end for
  if 1st iteration of IDD **then**
    for $l = 1 \rightarrow L$ **do**
      if $\omega_l > \omega_{th}$ **then**
        Discard ω_l and $\mathbf{V}_l(i)$
      end if
    end for
    $L =$length(ω)
  end if
  if $L > L_{max}$ **then**
    Sort ω_l and $\mathbf{V}_l(i)$ by $\omega_l, l = 1 \rightarrow L$
    Keep first L_{max} entries of ω_l and $\mathbf{V}_l(i)$
    $L = L_{max}$
  end if
end for
for $l = 1 \rightarrow L$ **do**
  $b = b_A \oplus \mathbf{V}_l$
  $\mathcal{L}_l =$BPSK-Modulate(b)
end for

$\mathbf{V}_l$ is the lth column of $\mathbf{V}$, $\mathbf{0}_{K\times 1}$ represents a K length vector of zeros
$\oplus$ represents the bit-wise XOR operator

subsequent iterations.

5.7 Simulation Results

In the simulations performed, the system is set up as a base pool of $K + M$ sources which are randomly distributed between a distance of 0.75 to 1.25 units away from the destination, where a unit of distance is a generic measure, relative to the average distance

of 1 unit from the destination, which defines the base path loss in Eq.(5.7). For these simulations, the base path loss at a distance of 1 unit is 20dB. From this pool, the M closest sources to the destination are redefined as relays, to ensure the relays are well positioned to transmit to the destination, with the rest of the source pool becoming the user sources. The users distance from the newly defined relays ($d_{sr_{m,k}}$) is similarly modelled as randomly distributed between a relative distance of 0.75 to 1.25 units. The distances of 0.75 and 1.25 are chosen for both the sources and relay to ensure that the relays were close enough to potentially be of use in the system, but not close enough to always dominate.

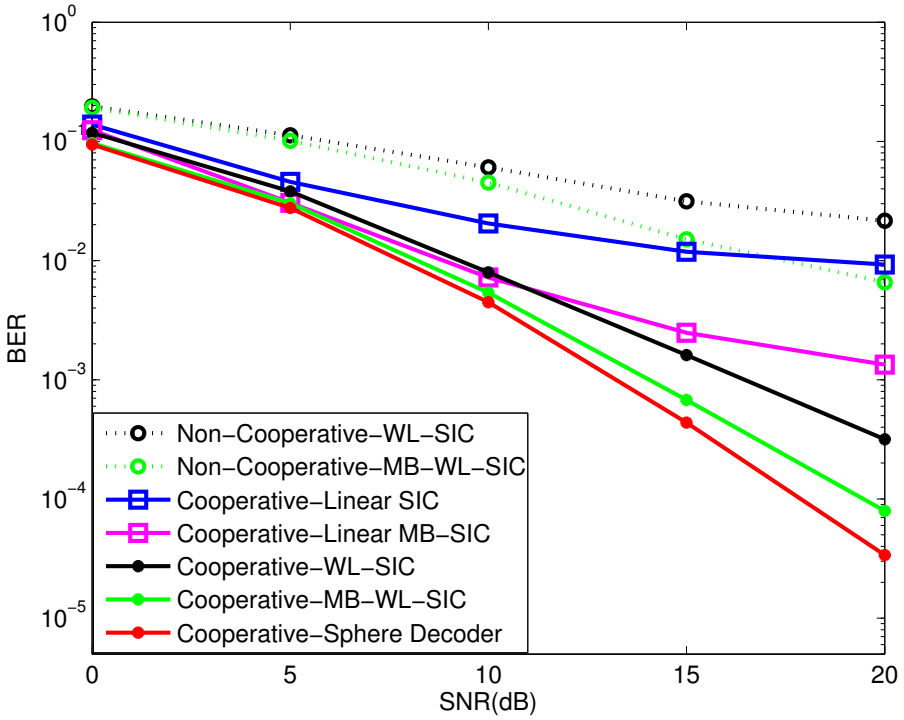

Figure 5.8: MIMO cooperative system with 2 AF relays, BPSK modulation, 8 single antenna users, 2 antennas at destination

BPSK is the symbol modulation scheme used for the system, and the destination is assumed to have 2 receive antennas. The channels are modelled with a LNS variance of 6dB and a path-loss exponent of 4. To ensure a fair comparison of the cooperative and non-cooperative cases, the Signal-to-Noise Ratio (SNR) used on the horizontal axis is defined as the ratio of each user's source transmission power to the destination's received noise power. The channels are also assumed to be quasi-static, and so are unchanging over a packet, but non-correlated between packets, with the destination having full knowledge of the system. Synchronous transmission by the relays in the second phase of transmission

is also assumed for simplicity although the system can be generalised to asynchronous transmission. The non-cooperative case (where the relays are not utilised) as well the cooperative case (where the relays are used) are considered in our results.

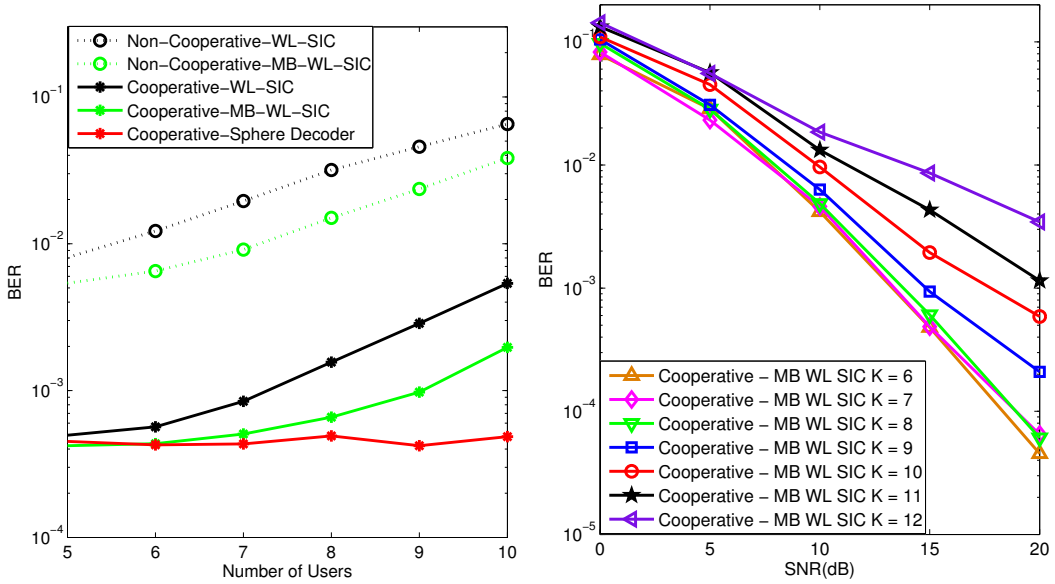

(a) 15dB SNR, BER vs K

(b) BER vs SNR

Figure 5.9: MIMO cooperative system with 2 AF relays and a variable number of single antenna users, BPSK modulation, 2 antennas at destination

Fig. 5.8 shows the results for the non-cooperative and the cooperative case, with 4 branches being processed in the MB-WL-SIC for 8 user sources, with the system also consisting of 2 AF relays. It can be seen that in the non-cooperative case, the WL-SIC quickly reaches a high error floor, and although the MB-WL-SIC performs over 7dB better at a BER level of $10^{-1.8}$, the MB-WL-SIC still reaches a relatively high error floor. For the cooperative case, the MB-WL-SIC is shown to be comparable to the ML solution (produced using the cooperative Sphere Decoder (SD) scheme in Chapter 3) up to a 15dB SNR, giving up to 4dB of gain over the WL-SIC at a BER level of $10^{-3.5}$, with the MB-WL-SIC cooperative case showing up to 10dB of gain over the equivalent non-cooperative case at a BER level of 10^{-2}. The WL SIC and WL MB SIC can be seen to have over 7dB of gain each over the equivalent linear detectors for the cooperative case at a BER level of 10^{-2} and $10^{-2.9}$ respectively, showing the advantage that WL filtering can give over linear filters for BPSK.

Fig. 5.9(a) shows the BER as compared to the number of source users, for a system

with 2 AF relays with an SNR of 15dB, with a 2 antenna destination. It can be seen that for up to 6-7 single antenna users, the cooperative MB-WL-SIC running 4 branches is equivalent to the SD. For the non-cooperative schemes, the error rate has consistently at least an order of magnitude worse performance than the cooperative case. The gap between the SD and MB-WL-SIC can be seen to widen as the number of users increases, but the MB-WL-SIC still maintains roughly half a magnitude performance gain over the WL-SIC. Fig. 5.9(b) shows the BER against the SNR for a varying number of users in the same system, showing that above 7-8 users, the performance degrades by 2-3dB for every extra user added.

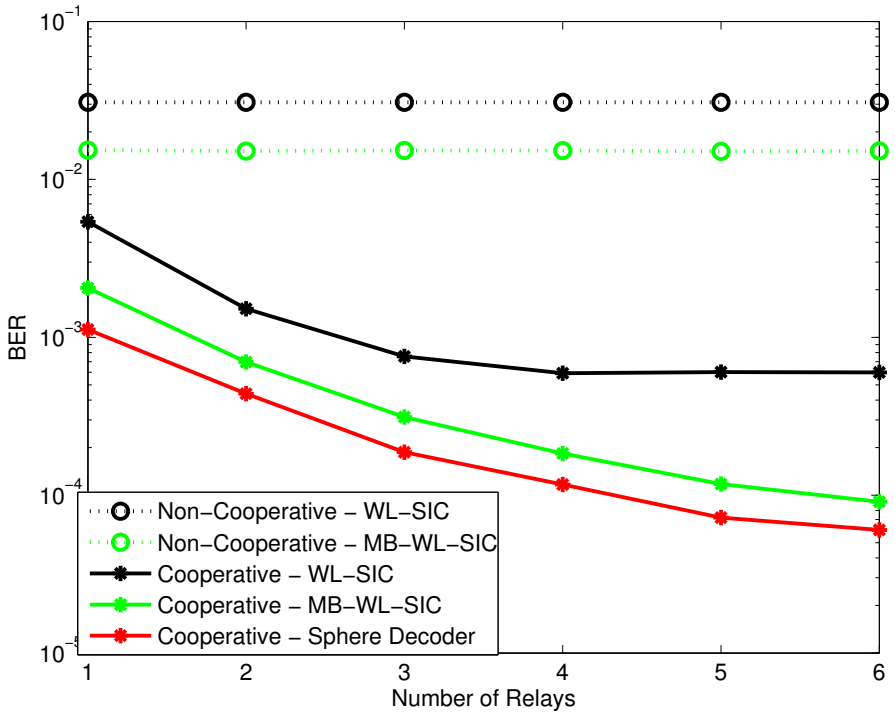

Figure 5.10: MIMO cooperative system with a variable number of AF relays, BPSK modulation, 8 single antenna users, 15dB SNR, 2 antennas at destination

Fig. 5.10 shows the BER as compared with the number of AF relays in the system for 8 users sources at 15dB SNR. As the number of relays increases, it can be seen that all the proposed cooperative schemes reach an error floor at around 5-6 relays. This could be due to the fact that the self interference between the relays becomes a major factor, and results in diminishing gain returns as the number of relays increases. The non-cooperative cases do not use the relays, and so remain at a constant performance level throughout.

Fig. 5.11 shows the BER performance against the SNR value for the dynamic branch

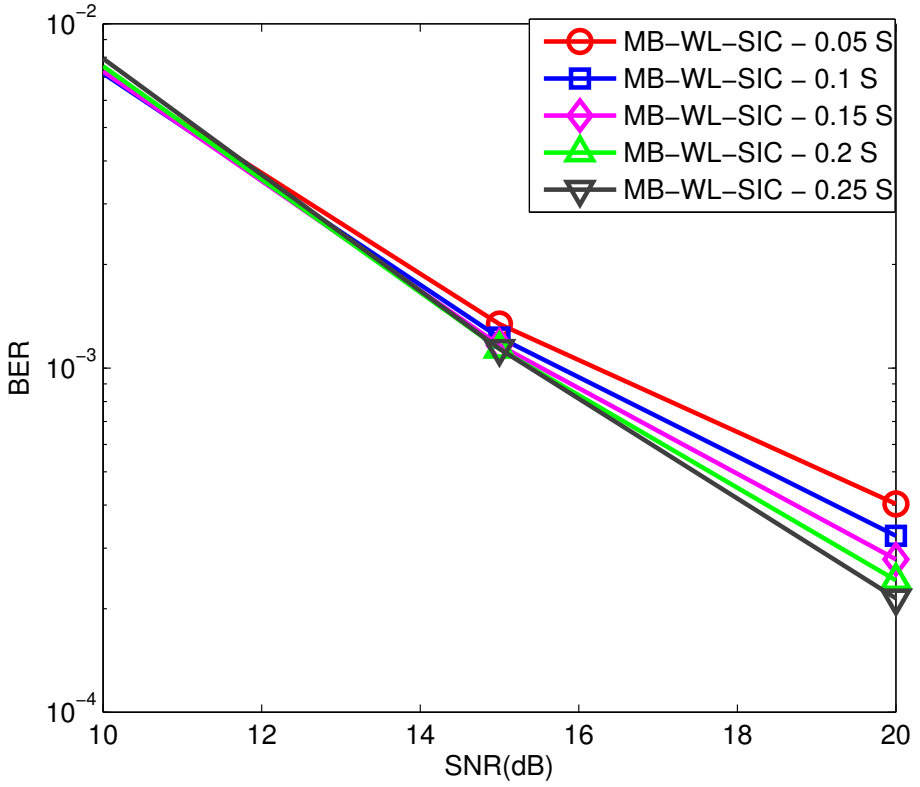

Figure 5.11: MIMO cooperative system with 2 AF relays, BPSK modulation, 8 single antenna users, 2 antennas at destination, dynamic branch selection with a variable shadowing criterion

choice selection scheme, demonstrating how the BER performance changes as the shadowing criterion value S used for the dynamic branching scheme is altered. It can be seen that for each 0.05 increment of S, the BER performance has between 0.5-1dB of gain at high SNR values, but this comes at the increased cost of computational complexity. It should also be noted, that if S is increased too high, that symbol estimates will begin to be described as unreliable erroneously, and start giving performance loss, similar to the effect observed in Chapter 4 for the MF-SIC and MF-RO-SIC.

Fig. 5.12 shows the coded BER performance against the SNR value for the list-based IDD system with an implementation of the WL, WL-SIC, and the proposed MB-WL-SIC with 4 branches as in Section 5.6. For a fair comparison, the maximum list size L_{max} is set to $B = 4$. A rate 1/2 [7, 5] convolutional code with a memory of 2 is used by the encoder and decoder in the IDD system, and it can be seen that for the first iteration, the MB-WL-SIC has a 1.5dB performance gain over the WL-SIC at a BER level of $10^{-3.5}$, and up to 4dB of gain over the WL filtering technique at a BER level of 10^{-3}. For the third

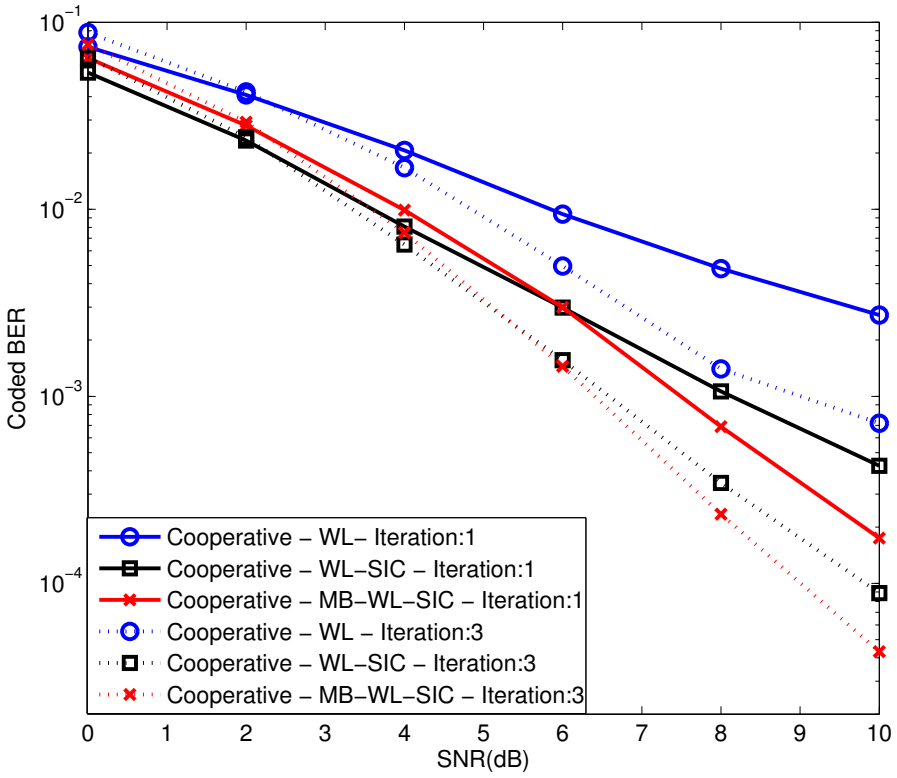

Figure 5.12: Coded MIMO cooperative system with 2 AF relays, BPSK modulation, 8 single antenna users, 2 antennas at destination

iteration, the MB-WL-SIC gains up to 2dB from the first iteration at a BER level of $10^{-3.5}$, and about 1dB over the third iteration of the WL-SIC at a BER level of 10^{-4}, with up to 3.5dB of gain over the third iteration of the WL filter at a BER level of 10^{-3}. It should be noted that at low SNR values, the MB-WL-SIC does not offer any gain over the WL-SIC, and can give a slight loss, suggesting that at very low SNR values, it is preferable to use the WL-SIC for IDD. However, both the WL-SIC and MB-WL-SIC both give gains over the WL filtering technique at low SNR values.

5.8 Summary

In this chapter, we have proposed a widely linear detection scheme for real-valued modulation schemes in an overloaded multi-user scenario with cooperative MIMO relaying, with a proposed list IDD system based on the MB-WL-SIC detector. A method of dy-

namically selecting the branches of the MB-WL-SIC has been proposed, and a complexity analysis of the proposed detector has been demonstrated. The proposed MB-WL-SIC detection scheme has shown up to 4dB gains over the conventional WL-SIC in the cooperative case, showing equivalent performance to the ML solution in some scenarios, with also the WL techniques being seen to have over 7dB of gain over the equivalent linear detectors for the cooperative case. The list-based IDD system has shown that the MB-WL-SIC can give some gains over the WL-SIC, with subsequent iterations giving up to 2dB of extra gains, also demonstrating how the list-based algorithm can be applied to the WL filtering and WL-SIC methods. It has been seen that the inclusion of a small number of single antenna AF relays can boost the performance of the system significantly, and give a low rate of errors in conjunction with the MB-WL-SIC, even in a very heavily overloaded system. The DMB-WL-SIC has shown that MB performance gains can be obtained, but with a lower average complexity cost, especially at high SNR values.

Chapter 6

Conclusions and Future Work

Contents

6.1 Summary and Conclusions

In this thesis, techniques of detection and link selection have been investigated and proposed for MIMO and cooperative relay systems, with analyses of computational complexity and implementations for IDD systems described. Results of simulation modelling for the proposed techniques have been presented and discussed, showing primarily the BER gains of the algorithms for a range of SNR values. Other metrics and parameters have also been highlighted appropriately to the algorithms being presented.

In Chapter 3, a cross-layer design for a cooperative MIMO relay system is proposed, deriving a cooperative ML detector for use with a SD from both phases of transmission in the system, and using a summed channel approximation to take advantage of the system information available at the destination device. The system model takes into account distance and shadowing effects in the channel, as well as relay positioning. The proposed cooperative ML detector is also formed such that the resulting channel that the SD operates on is the same matrix size as a non-cooperative, such that the SD will have a lower complexity for each time instant than the alternative of stacking the received signals. For this system, two new combinatorial link selection schemes were proposed, extending previously proposed link selection schemes to take into account sets of relays in the link selection metrics, rather than the individual relays. The proposed cooperative detector and link selection techniques were then integrated into an IDD system, which uses the LSD and MAP detection techniques with convolutional channel coding. Simulation results showed that the cooperative ML detector gives a good BER performance in the cooperative MIMO system with distance shadowing fading effects, and compared this with how the cooperative ML detector performs in system model from previous literature. The proposed combinatorial link selection techniques were shown to give good gains in BER performance over previous link selection strategies, but were also shown to have an increased computational complexity cost as a trade-off. The IDD scheme was demonstrated to work well with the proposed combinatorial link selection techniques for a rate 1/2 and rate 1/3 convolutional channel code, giving up to a decade and half of BER gain over the uncoded system.

In Chapter 4, a dynamically ordering, alternative cancellation candidate SIC detector is proposed for a MIMO system, using the methods of RO, which is derived from the LLR of the estimated data symbols, and the technique of MF, which tests for unreliable data symbol estimates during the cancellation process using a shadow criterion area based upon the Voronoi boundaries of the modulation scheme's constellation diagram. RO and MF techniques are combined into a single proposed detector, which is developed to reduce the extra complexity required to process per time instant as compared with either RO or MF, and a complexity analysis to compare the algorithms shows that the proposed MF-RO-SIC requires very little extra complexity as compared to the RO-SIC. A hard decision feedback IDD scheme is also developed, which uses the MAP detector, and re-encodes the detected bits into estimated symbols that can be used in the SIC process to increase the

accuracy of the cancelled symbols in the next iteration of detection. Simulation results showed that the proposed detector offers BER gains at high SNR values for both 4x4 and 8x8 systems, as well as for QPSK and 16-QAM modulation schemes. The effect on performance of varying the shadow criterion and the number of alternative candidates is shown, and the coded BER performance of the hard decision feedback IDD system with the proposed MF-RO-SIC is shown to have gains over the IDD system with the RO-SIC and MF-SIC.

In Chapter 5, a WL based detector is proposed using the method of MB for a heavily overloaded multiple user BPSK cooperative MIMO system. The WL-SIC is detailed for the non-circular signal case, and the MB technique is discussed, with the two techniques being combined, showing how the ordering of the branches involved is applied to the system. The choice of MB branches is then investigated, with a method of dynamically choosing branches during the cancellation process being developed, based upon the shadow criterion used in MF techniques. The algorithm for hopping between different branches is detailed, and a computational complexity analysis is performed, comparing the different cancellation algorithms. A list-based IDD scheme is then developed, adapting the proposed MB-WL-SIC to give a list output, and a list generation algorithm is detailed which is used to produce candidate lists from the single vector output of the WL filter and WL-SIC, and also to generate new lists per iteration using the *a priori* LLRVs. Simulation results show that the MB-WL-SIC can approach the cooperative ML detector BER performance for the heavily overloaded multiple user cooperative system with the use of a small number of AF relays. The BER performance of the proposed detector is also investigated as the number of users and relays in the system changes. The performance of the DMB-WL-SIC is also demonstrated for different values of the shadow criterion, and the list-based IDD scheme is shown to have BER gains when using the proposed detector with a list output.

6.2 Future Work

Many of the methods and algorithms detailed in this thesis have potential to be applied to scenarios, systems and techniques outside the scope of this thesis, and there is further

work and analysis that could be considered to extend the work that has been covered.

Cooperative MIMO systems in this thesis are limited to just two phases of transmission over a single set of relays, but this scenario could be extended to include multiple hops and phases of transmission within the system, and as such each technique designed for cooperative systems in this thesis could potentially be adapted for such a system. Of particular application might be the combinatorial link selection algorithms proposed in Chapter 3, and by extension the cross-layer cooperative ML detector design. Also, the overloaded multiple user cooperative system and the proposed methods in Chapter 5 could find use in mobile communications or wireless sensor networks (WSN), as typically a WSN consists of many small, single antenna devices transmitting at low data rates, that can relay data between each device to a single destination in a mesh network, and this fits well with the idea of using a few devices for simple relays, and the use of BPSK or similar non-circular modulation schemes. Thus, the MB and WL techniques in Chapter 5 could be used in order to improve the accuracy of data reception in such a network.

The techniques of MF and RO can also be applied to most SIC based algorithms, and it is possible to combine MF, RO, WL and MB methods together in many combinations, which could be altered and tuned to suit the application or scenario in which the hybrid detector would be used, with a great deal of flexibility due to the shadowing and candidate limit parameters of MF and the number and choice of branches in MB. The dynamic branching algorithm in Chapter 5 can also be used for linear filter MB-SIC for circular signal systems, and could potentially be adapted for other interference cancellation methods.

The three IDD schemes detailed during this thesis are generally portable to be used with other types and sizes of channel coding schemes, as well as being applicable to a variety of different detector algorithms. The LSD IDD scheme from Chapter 3 provides a platform for any ML based detectors, the hard decision feedback method in Chapter 4 could be adapted to other interference cancellation methods reliant on cancelling estimated symbols, and the list-based IDD method with the list generator in Chapter 5 can be used with any detector that outputs a list or a single vector estimate of the transmitted data, so there is a large scope of application.

Appendix

Derivation of Cooperative ML rule

Equating Eq. (3.15) and Eq. (3.16) gives:

$$\|\mathbf{y}_e - \tilde{\mathbf{H}}_e\mathbf{A}_e\mathbf{x}\|^2 = \|\mathbf{y}_{sd} - \tilde{\mathbf{H}}_{sd}\mathbf{A}_s\mathbf{x}\|^2 + \sum_{m\epsilon\Omega_s} \|\mathbf{y}_{rd_m} - \tilde{\mathbf{H}}_{rd_m}\mathbf{A}_{r_m}\mathbf{x}_m\|^2 \tag{A.1}$$

Using the matrix $\mathbf{S}$ defined in Eq. (3.19), we can find the approximation of the equated ML rules to be:

$$\|\mathbf{y}_e - \tilde{\mathbf{H}}_e\mathbf{A}_e\mathbf{x}\|^2 = \|\mathbf{y}_{sd} - \tilde{\mathbf{H}}_{sd}\mathbf{A}_s\mathbf{x}\|^2 + \|\mathbf{y}_{rd} - \mathbf{S}\mathbf{x}\|^2 \tag{A.2}$$

Expanding these equations gives:

$$\begin{aligned}\mathbf{y}_e^H\mathbf{y}_e + \mathbf{x}^H(\tilde{\mathbf{H}}_e\mathbf{A}_e)^H(\tilde{\mathbf{H}}_e\mathbf{A}_e)\mathbf{x} - \mathbf{y}_e^H(\tilde{\mathbf{H}}_e\mathbf{A}_e)\mathbf{x} - \mathbf{x}^H(\tilde{\mathbf{H}}_e\mathbf{A}_e)^H\mathbf{y}_e = \mathbf{y}_{sd}^H\mathbf{y}_{sd} + \mathbf{y}_{rd}^H\mathbf{y}_{rd} + \\ \mathbf{x}^H(\mathbf{A}_s^H\tilde{\mathbf{H}}_s^H\tilde{\mathbf{H}}_s\mathbf{A}_s + \mathbf{S}^H\mathbf{S})\mathbf{x} - (\mathbf{y}_{sd}^H\tilde{\mathbf{H}}_s\mathbf{A}_s + \mathbf{y}_{rd}^H\mathbf{S})\mathbf{x} - \mathbf{x}^H(\mathbf{A}_s^H\tilde{\mathbf{H}}_s^H\mathbf{y}_{sd} + \mathbf{S}^H\mathbf{y}_{rd})\end{aligned} \tag{A.3}$$

By equivalence, we can make the associations:

$$\mathbf{x}^H(\tilde{\mathbf{H}}_e\mathbf{A}_e)^H(\tilde{\mathbf{H}}_e\mathbf{A}_e)\mathbf{x} = \mathbf{x}^H(\mathbf{A}_s^H\tilde{\mathbf{H}}_s^H\tilde{\mathbf{H}}_s\mathbf{A}_s + \mathbf{S}^H\mathbf{S})\mathbf{x} \tag{A.4}$$

$$\mathbf{x}^H(\tilde{\mathbf{H}}_e\mathbf{A}_e)^H\mathbf{y}_e = \mathbf{x}^H(\mathbf{A}_s^H\tilde{\mathbf{H}}_s^H\mathbf{y}_{sd} + \mathbf{S}^H\mathbf{y}_{rd}) \tag{A.5}$$

Starting with Eq. (A.4) it is clear that:

$$(\tilde{\mathbf{H}}_e\mathbf{A}_e)^H(\tilde{\mathbf{H}}_e\mathbf{A}_e) = (\mathbf{A}_s^H\tilde{\mathbf{H}}_s^H\tilde{\mathbf{H}}_s\mathbf{A}_s + \mathbf{S}^H\mathbf{S}) \tag{A.6}$$

$$\tilde{\mathbf{H}}_e\mathbf{A}_e = (\mathbf{A}_s^H\tilde{\mathbf{H}}_s^H\tilde{\mathbf{H}}_s\mathbf{A}_s + \mathbf{S}^H\mathbf{S})^{1/2} \tag{A.7}$$

We can prove that the use of the matrix square root in this case is appropriate, as $\mathbf{A}_s^H\tilde{\mathbf{H}}_s^H\tilde{\mathbf{H}}_s\mathbf{A}_s$ and $\mathbf{S}^H\mathbf{S}$ are clearly square positive definite Hermitian (SPDH) matrices, and so their sum is also a SPDH.

Taking a SPDH matrix $\mathbf{K}$ of size n, we can diagonalise as such:

$$\mathbf{K} = \mathbf{P}^H diag(\lambda_1, \ldots, \lambda_n)\mathbf{P}, \tag{A.8}$$

where $\mathbf{P}$ is a unitary matrix, and λ is a positive eigenvalue. The matrix square root of $\mathbf{K}$ is therefore:

$$\sqrt{\mathbf{K}} = \mathbf{P}^H diag(\sqrt{\lambda_1}, \ldots, \sqrt{\lambda_n})\mathbf{P}, \tag{A.9}$$

which is clearly still a SPDH matrix. Therefore $\tilde{\mathbf{H}}_e\mathbf{A}_e$ is also a SPDH, which therefore means that $\tilde{\mathbf{H}}_e\mathbf{A}_e = (\tilde{\mathbf{H}}_e\mathbf{A}_e)^H$, so $(\tilde{\mathbf{H}}_e\mathbf{A}_e)^H(\tilde{\mathbf{H}}_e\mathbf{A}_e) = (\tilde{\mathbf{H}}_e\mathbf{A}_e)^2$ demonstrating that the matrix square root is an appropriate operation in this case.

Using the result of Eq. (A.7) in Eq. (A.5) and rearranging gives:

$$\mathbf{y}_e = (\tilde{\mathbf{H}}_e\mathbf{A}_e)^{-1}(\mathbf{A}_s^H\tilde{\mathbf{H}}_s^H\mathbf{y}_{sd} + \mathbf{S}^H\mathbf{y}_{rd}) \tag{A.10}$$

Glossary

16-QAM	**16** - **Q**uadrature **A**mplitude **M**odulation
AF	**A**mplify and **F**orward
ARQ	**A**utomatic **R**epeat Re**q**uest
ASK	**A**mplitude **S**hift **K**eying
AWGN	**A**dditive **W**hite **G**aussian **N**oise
BPSK	**B**inary **P**hase **S**hift **K**eying
BER	**B**it **E**rror **R**ate
CF	**C**ompress and **F**orward
CP	**C**hannel **P**ower
CSI	**C**hannel **S**tate **I**nformation
DF	**D**ecode and **F**orward
DMB	**D**ynamic **M**ultiple **B**ranch
ECC	**E**rror **C**orrection **C**ode
FEC	**F**orward **E**rror **C**orrection
IDD	**I**terative **D**etection and **D**ecoding
LDPC	**L**ow **D**ensity **P**arity **C**heck
LLR	**L**og **L**ikelihood **R**atio
LLRV	**L**og **L**ikelihood **R**atio **V**alue
LMS	**L**east **M**ean **S**quares
LNS	**L**og-**N**ormal **S**hadowing
LOS	**L**ine-**O**f-**S**ight
LS	**L**east **S**quares
LSD	**L**ist **S**phere **D**ecoder
MAP	**M**aximum **A** **P**osteriori

MB	**M**ultiple **B**ranch
MF	**M**ultiple **F**eedback
MH	**M**aximum **H**armonic
MHC	**M**aximum **H**armonic **C**ombinatorial
MIMO	**M**ultiple-**I**nput **M**ultiple-**O**utput
ML	**M**aximum **L**ikelihood
MM	**M**aximum **M**inimum
MMC	**M**aximum **M**inimum **C**ombinatorial
MMSE	**M**inimum **M**ean **S**quare **E**rror
MS	**M**aximum **S**um
MSE	**M**ean **S**quare **E**rror
OSIC	**O**rdered **S**uccessive **I**nterference **C**ancellation
QPSK	**Q**uadrature **P**hase **S**hift **K**eying
RO	**R**eliability **O**rdering
SD	**S**phere **D**ecoder
SG	**S**tochastic **G**radient
SIC	**S**uccessive **I**nterference **C**ancellation
SINR	**S**ignal to **I**nterference-plus-**N**oise **R**atio
SISO	**S**oft-**I**nput **S**oft-**O**utput
SNR	**S**ignal to **N**oise **R**atio
SPDH	**S**emi-**P**ositive **D**efinite **H**ermitian
VBLAST	**V**ertical **B**ell **LA**bs **S**pace-**T**ime
WL	**W**idely **L**inear
ZF	**Z**ero **F**orcing

Bibliography

[1] G. L. Turin, "Introduction to spread-spectrum antimultipath techniques and their application to urban digital radio," *Proceedings of the IEEE*, vol. 68, no. 3, p. 328–353, 1980.

[2] H. Suzuki, "A Statistical Model for Urban Radio Propogation," *IEEE Transactions on Communications*, vol. 25, no. 7, p. 673–680, 1977.

[3] A. J. Rustako, N. Amitay, G. J. Owens and R. S. Roman, "Radio propagation at microwave frequencies for line-of-sight microcellular mobile and personal communications," *IEEE Transactions on Vehicular Technology*, vol. 40, no. 1, p. 203–210, 1991.

[4] Y. Cho, J. Kim, W. Yang, and C. Kang, *MIMO-OFDM wireless communications with MATLAB*. Singapore ;;Hoboken NJ: IEEE Press ;J. Wiley & Sons (Asia), 2010.

[5] H. Bolcskei, "MIMO-OFDM wireless systems: basics, perspectives, and challenges," *Wireless Communications, IEEE*, vol. 13, no. 4, p. 31–37, 2006.

[6] G. Golden, C. Foschini, R. Valenzuela, and P. Wolniansky, "Detection algorithm and initial laboratory results using V-BLAST space-time communication architecture," *Electronics Letters*, vol. 35, no. 1, p. 14, 1999.

[7] N. Kim, Y. Lee, and H. Park, "Performance analysis of MIMO system with linear MMSE receiver," *IEEE Transactions on Wireless Communications*, vol. 7, no. 11, pp. 4474–4478, Nov. 2008.

[8] G. Foschini and M. Gans, "On limits of wireless communications in a fading environment when using multiple antennas," *Wireless personal communications*, vol. 6, no. 3, p. 311–335, 1998.

[9] E. Telatar, "Capacity of multi-antenna gaussian channels," *European Transactions on Telecommunications*, vol. 10, no. 6, pp. 585–595, Nov. 1999.

[10] S. Alamouti, "A simple transmit diversity technique for wireless communications," *IEEE Journal on Selected Areas in Communications*, vol. 16, no. 8, pp. 1451–1458, Oct. 1998.

[11] M. Dohler and Y. Li, *Cooperative communications : hardware, channel & PHY*. Chichester West Sussex U.K. Hoboken NJ: Wiley, 2010.

[12] D. Chen and J. N. Laneman, "Modulation and demodulation for cooperative diversity in wireless systems," *Wireless Communications, IEEE Transactions on*, vol. 5, no. 7, p. 1785–1794, 2006.

[13] A. Nosratinia, T. E. Hunter, and A. Hedayat, "Cooperative communication in wireless networks," *Communications Magazine, IEEE*, vol. 42, no. 10, p. 74–80, 2004.

[14] A. Sadek, W. Su, and K. Liu, "Multinode cooperative communications in wireless networks," *IEEE Transactions on Signal Processing*, vol. 55, no. 1, pp. 341–355, Jan. 2007.

[15] A. Sendonaris, E. Erkip, and B. Aazhang, "User cooperation diversity-part II: implementation aspects and performance analysis," *IEEE Transactions on Communications*, vol. 51, no. 11, pp. 1939–1948, Nov. 2003.

[16] J. Laneman, D. Tse, and G. Wornell, "Cooperative diversity in wireless networks: Efficient protocols and outage behavior," *IEEE Transactions on Information Theory*, vol. 50, no. 12, pp. 3062–3080, Dec. 2004.

[17] P. Clarke and R. C. de Lamare, "Transmit diversity and relay selection algorithms for multirelay cooperative MIMO systems," *IEEE Transactions on Vehicular Technology*, vol. 61, no. 3, pp. 1084–1098, Mar. 2012.

[18] S. Yang and J. Belfiore, "Optimal Space-Time codes for the MIMO Amplify-and-Forward cooperative channel," *IEEE Transactions on Information Theory*, vol. 53, no. 2, pp. 647–663, Feb. 2007.

[19] W. J. Huang, Y. W. Hong, and C. C. Kuo, "Decode-and-forward cooperative relay with multi-user detection in uplink CDMA networks," in *Proc. IEEE Global Telecommunications Conference*, 2007, p. 4397–4401.

[20] J. Luo, R. S. Blum, L. J. Cimini, L. J. Greenstein, and A. M. Haimovich, "Decode-and-forward cooperative diversity with power allocation in wireless networks," *Wireless Communications, IEEE Transactions on*, vol. 6, no. 3, p. 793–799, 2007.

[21] T. Rappaport, *Wireless communications : principles and practice*, 2nd ed. Upper Saddle River N.J.: Prentice Hall PTR, 2002.

[22] H. Zhang, J. Wang, T. Lu, and T. A. Gulliver, "Capacity of 60 GHz wireless communication systems over ricean fading channels." IEEE, Aug. 2011, pp. 437–440.

[23] G. Li and K. Yu, "Modelling and simulation of coherent weibull clutter," *IEE Proceedings, Part F: Radar and Signal Processing*, vol. 136, no. 1, pp. 2–12, Feb. 1989.

[24] N. S. Adawi, H. L. Bertoni, J. R. Child, W. A. Daniel, J. E. Dettra, and R. P. Eckert, "Coverage prediction for mobile radio systems operating in the 800/900 MHz frequency range," *IEEE Transactions on Vehicular Technology*, vol. 37, no. 1, pp. 3–72, Feb. 1988.

[25] H. Hashemi, "The indoor radio propagation channel," *Proceedings of the IEEE*, vol. 81, no. 7, pp. 943–968, Jul. 1993.

[26] Q. Zhu, X. Yu, J. Wang, D. Xu, and X. Chen, "A new generation method for Spatial-Temporal correlated MIMO nakagami fading channel," *International Journal of Antennas and Propagation*, vol. 2012, pp. 1–8, 2012.

[27] H. Hsu, *Schaum's outline of theory and problems of probability, random variables, and random processes*. New York: McGraw-Hill, 1997.

[28] V. Erceg, L. Greenstein, S. Tjandra, S. Parkoff, A. Gupta, B. Kulic, A. Julius, and R. Bianchi, "An empirically based path loss model for wireless channels in suburban environments," *IEEE Journal on Selected Areas in Communications*, vol. 17, no. 7, pp. 1205–1211, Jul. 1999.

[29] A. Paulraj and C. Papadias, "Space-time processing for wireless communications," *IEEE Signal Processing Magazine*, vol. 14, no. 6, pp. 49–83, Nov. 1997.

[30] J. Barnes and D. Allan, "A statistical model of flicker noise," *Proceedings of the IEEE*, vol. 54, no. 2, pp. 176–178, 1966.

[31] T. Sreenivas and P. Kirnapure, "Codebook constrained wiener filtering for speech enhancement," *IEEE Transactions on Speech and Audio Processing*, vol. 4, no. 5, pp. 383–389, Sep. 1996.

[32] L. Liu and T. Shimamura, "Pink noise whitening method for pitch synchronous LPC analysis," in *Signal & Information Processing Association Annual Summit and Conference (APSIPA ASC), 2012 Asia-Pacific*, Hollywood, CA, Dec. 2012, pp. 1–6.

[33] C. Studer, "Iterative MIMO decoding: Algorithms and VLSI implementation aspects," Ph.D. dissertation, ETH Zurich, Zurich, 2009.

[34] A. Stefanov and E. Erkip, "Cooperative Space-Time coding for wireless networks," *IEEE Transactions on Communications*, vol. 53, no. 11, pp. 1804–1809, Nov. 2005.

[35] N. Kim and H. Park, "Bit error performance of convolutional coded MIMO system with linear MMSE receiver," *IEEE Transactions on Wireless Communications*, vol. 8, no. 7, pp. 3420–3424, Jul. 2009.

[36] A. Berthet, B. Unal, and R. Visoz, "Iterative decoding of convolutionally encoded signals over multipath rayleigh fading channels," *IEEE Journal on Selected Areas in Communications*, vol. 19, no. 9, pp. 1729–1743, Sep. 2001.

[37] J. Heller and I. Jacobs, "Viterbi decoding for satellite and space communication," *IEEE Transactions on Communications*, vol. 19, no. 5, pp. 835–848, Oct. 1971.

[38] J. Omura, "On the viterbi decoding algorithm," *IEEE Transactions on Information Theory*, vol. 15, no. 1, pp. 177–179, Jan. 1969.

[39] R. McEliece, "On the BCJR trellis for linear block codes," *IEEE Transactions on Information Theory*, vol. 42, no. 4, pp. 1072–1092, Jul. 1996.

[40] C. Berrou and A. Glavieux, "Near optimum error correcting coding and decoding: turbo-codes," *IEEE Transactions on Communications*, vol. 44, no. 10, pp. 1261–1271, Oct. 1996.

[41] J. Hagenauer, E. Offer and L. Papke, "Iterative decoding of binary block and convolutional codes," *IEEE Transactions on Information Theory*, vol. 42, no. 2, pp. 429–445, Mar. 1996.

[42] T. J. Richardson, M. A. Shokrollahi and R. L. Urbanke, "Design of capacity-approaching irregular low-density parity-check codes," *IEEE Transactions on Information Theory*, vol. 47, no. 2, pp. 619–637, Feb. 2001.

[43] V. Oksman, and S. Galli, "G.hn: The new ITU-T home networking standard," *IEEE Communications Magazine*, vol. 47, no. 10, pp. 138–145, Oct. 2009.

[44] B. Classon, K. Blankenship, and V. Desai, "Channel coding for 4G systems with adaptive modulation and coding," *IEEE Wireless Communications*, vol. 9, no. 2, pp. 8–13, Apr. 2002.

[45] S. Haykin, *Adaptive filter theory.*, 4th ed. Upper Saddle River N.J.: Prentice Hall, 2002.

[46] T. Wang, R. C. de Lamare and P. Mitchell, "Low-Complexity Set-Membership Channel Estimation for Cooperative Wireless Sensor Networks," *IEEE Transactions on Vehicular Technology*, vol. 60, no. 6, pp. 2594–2607, Jul. 2011.

[47] T. Wang, R. C. de Lamare and P. Mitchell, "Low-Complexity Channel Estimation for Cooperative Wireless Sensor Networks Based on Data Selection," in *Vehicular Technology Conference (VTC 2010-Spring)*, Taipei, Taiwan, May. 2010, pp. 1–5.

[48] E. Karami, "Tracking performance of least squares MIMO channel estimation algorithm," *IEEE Transactions on Communications*, vol. 55, no. 11, pp. 2201–2209, Nov. 2007.

[49] Y. Eldar and A. Oppenheim, "Covariance shaping least-squares estimation," *IEEE Transactions on Signal Processing*, vol. 51, no. 3, pp. 686–697, Mar. 2003.

[50] L. E. Pooh, W. G. Lim, and H. Ali, "Adaptive channel estimation using least mean squares algorithm for cyclic prefix OFDM systems," in *2009 IEEE 9th Malaysia International Conference on Communications (MICC)*, Kuala Lumpur, Malaysia, Dec. 2009, pp. 789–793.

[51] S. Kinjo, "A new MMSE channel estimation algorithm for OFDM systems," *IEICE Electronics Express*, vol. 5, no. 18, pp. 738–743, 2008.

[52] M. Biguesh and A. Gershman, "Training-based MIMO channel estimation: a study of estimator tradeoffs and optimal training signals," *IEEE Transactions on Signal Processing*, vol. 54, no. 3, pp. 884–893, Mar. 2006.

[53] R. Trepkowski, "Channel estimation strategies for coded MIMO systems," Ph.D. dissertation, Virginia Polytechnic Institute and State University, 2004.

[54] R. C. de Lamare, "Joint iterative power allocation and linear interference suppression algorithms for cooperative DS-CDMA networks," *IET Communications*, vol. 6, no. 13, pp.1930–1942, Sep. 2012.

[55] T. Wang, R. C. de Lamare and A. Schmeink, "Joint Linear Receiver Design and Power Allocation Using Alternating Optimization Algorithms for Wireless Sensor Networks," *IEEE Transactions on Vehicular Technology*, vol. 61, no. 9, pp.4129–4141, Nov. 2012.

[56] Z. Yi, R. Adve, and J. L. Teng, "Improving amplify-and-forward relay networks: optimal power allocation versus selection," *IEEE Transactions on Wireless Communications*, vol. 6, no. 8, pp.3114–3123, Aug. 2007.

[57] P. Clarke and R. C. de Lamare, "Joint transmit diversity optimization and relay selection for Multi-Relay cooperative MIMO systems using discrete stochastic algorithms," *IEEE Communications Letters*, vol. 15, no. 10, pp. 1035–1037, 2011.

[58] A. Klein, G. Kaleh, and P. Baier, "Zero forcing and minimum mean-square-error equalization for multiuser detection in code-division multiple-access channels," *IEEE Transactions on Vehicular Technology*, vol. 45, no. 2, pp. 276–287, May 1996.

[59] R. H. Y. Louie, Y. Li, and B. Vucetic, "Zero forcing in general Two-Hop relay networks," *IEEE Transactions on Vehicular Technology*, vol. 59, no. 1, pp. 191–202, Jan. 2010.

[60] H. Poor and S. Verdu, "Probability of error in MMSE multiuser detection," *IEEE Transactions on Information Theory*, vol. 43, no. 3, pp. 858–871, May 1997.

[61] B. Picinbono and P. Chevalier, "Widely linear estimation with complex data," *IEEE Transactions on Signal Processing*, vol. 43, no. 8, pp. 2030–2033, Aug. 1995.

[62] F. Sterle, "Widely linear MMSE transceivers for MIMO channels," *IEEE Transactions on Signal Processing*, vol. 55, no. 8, pp. 4258–4270, Aug. 2007.

[63] G. Gelli, L. Paura, and A. Ragozini, "Blind widely linear multiuser detection," *IEEE Communications Letters*, vol. 4, no. 6, pp. 187–189, Jun. 2000.

[64] S. Buzzi, M. Lops, and S. Sardellitti, "Widely linear reception strategies for layered space-time wireless communications," *IEEE Transactions on Signal Processing*, vol. 54, no. 6, pp. 2252–2262, Jun. 2006.

[65] T. Liu, "Some results for the fast MMSE-SIC detection in spatially multiplexed MIMO systems," *IEEE Transactions on Wireless Communications*, vol. 8, no. 11, pp. 5443–5448, Nov. 2009.

[66] C. Ling, W. H. Mow, and L. Gan, "Dual-Lattice ordering and partial lattice reduction for SIC-Based MIMO detection," *IEEE Journal of Selected Topics in Signal Processing*, vol. 3, no. 6, pp. 975–985, Dec. 2009.

[67] M. Damen, H. E. Gamal, and G. Caire, "On maximum-likelihood detection and the search for the closest lattice point," *IEEE Transactions on Information Theory*, vol. 49, no. 10, pp. 2389–2402, Oct. 2003.

[68] S. Verdu, "Minimum probability of error for asynchronous gaussian multiple-access channels," *IEEE Transactions on Information Theory*, vol. 32, no. 1, pp. 85–96, Jan. 1986.

[69] R. C. de Lamare and R. Sampaio-Neto, "Minimum Mean-Squared error iterative successive parallel arbitrated decision feedback detectors for DS-CDMA systems," *IEEE Transactions on Communications*, vol. 56, no. 5, pp. 778–789, May 2008.

[70] L. Yang, "Receiver multiuser diversity aided Multi-Stage MMSE multiuser detection for DS-CDMA and SDMA systems employing I-Q modulation," in *Vehicular Technology Conference Fall (VTC 2010-Fall), 2010 IEEE 72nd*. IEEE, Sep. 2010, pp. 1–5.

[71] N. Song, R. C. de Lamare, M. Haardt, and M. Wolf, "Adaptive widely linear Reduced-Rank interference suppression based on the multistage wiener filter," *IEEE Transactions on Signal Processing*, vol. 60, no. 8, pp. 4003–4016, Aug. 2012.

[72] J. Olivier and W. Kleynhans, "Single antenna interference cancellation for synchronised GSM networks using a widely linear receiver," *IET Communications*, vol. 1, no. 1, p. 131, 2007.

[73] A. Aghaei, K. Plataniotis, and S. Pasupathy, "Widely linear MMSE receivers for linear dispersion space-time block-codes," *IEEE Transactions on Wireless Communications*, vol. 9, no. 1, pp. 8–13, Jan. 2010.

[74] J. G. Andrews, "Interference cancellation for cellular systems: A contemporary overview," *Wireless Communications, IEEE*, vol. 12, no. 2, p. 19–29, 2005.

[75] J. Benesty, Y. Huang, and J. Chen, "A fast recursive algorithm for optimum sequential signal detection in a BLAST system," *IEEE Transactions on Signal Processing*, vol. 51, no. 7, pp. 1722–1730, Jul. 2003.

[76] Y. Shang and X. gen Xia, "On fast recursive algorithms for V-BLAST with optimal ordered SIC detection," *IEEE Transactions on Wireless Communications*, vol. 8, no. 6, pp. 2860–2865, Jun. 2009.

[77] J. Choi, Heeju, and Y. Lee, "Adaptive MIMO decision feedback equalization for receivers with time-varying channels," *IEEE Transactions on Signal Processing*, vol. 53, no. 11, pp. 4295–4303, Nov. 2005.

[78] G. J. Foschini, "Layered space-time architecture for wireless communication in a fading environment when using multi-element antennas," *Bell Labs Technical Journal*, vol. 1, no. 2, pp. 41–59, 1996.

[79] C. Windpassinger, L. Lampe, R. Fischer, and T. Hehn, "A performance study of MIMO detectors," *IEEE Transactions on Wireless Communications*, vol. 5, no. 8, pp. 2004–2008, Aug. 2006.

[80] R. C. de Lamare, "Joint iterative power allocation and interference suppression algorithms for cooperative spread spectrum networks," in *Acoustics Speech and Signal Processing (ICASSP), 2010 IEEE International Conference on*. IEEE, 2010, pp. 3178–3181.

[81] G. Kramer, M. Gastpar, and P. Gupta, "Cooperative strategies and capacity theorems for relay networks," *IEEE Transactions on Information Theory*, vol. 51, no. 9, pp. 3037–3063, Sep. 2005.

[82] K. Amiri, M. Wu, J. R. Cavallaro, and J. Lilleberg, "Cooperative partial detection using MIMO relays," *IEEE Transactions on Signal Processing*, vol. 59, pp. 5039–5049, Oct. 2011.

[83] K. Amiri, M. Wu, M. Duarte, and J. R. Cavallaro, "Physical layer algorithm and hardware verification of MIMO relays using cooperative partial detection," in *2010 IEEE International Conference on Acoustics, Speech and Signal Processing*, Dallas, TX, USA, 2010, pp. 5614–5617.

[84] S. Han and C. Tellambura, "Complexity-efficient detection for MIMO relay networks," in *Information Theory (CWIT), 2011 12th Canadian Workshop on*. IEEE, May 2011, pp. 126–129.

[85] T. Hesketh, P. Clarke, R. C. de Lamare, and S. Wales, "Joint maximum likelihood detection and power allocation in cooperative MIMO relay systems," in *Smart Antennas (WSA), 2012 International ITG Workshop on*. IEEE, Mar. 2012, pp. 325–331.

[86] Y. Fan and J. Thompson, "MIMO configurations for relay channels: Theory and practice," *IEEE Transactions on Wireless Communications*, vol. 6, no. 5, pp. 1774–1786, May 2007.

[87] M. Zorzi, "Power control and diversity in mobile radio cellular systems in the presence of ricean fading and log-normal shadowing," *IEEE Transactions on Vehicular Technology*, vol. 45, no. 2, pp. 373–382, May 1996.

[88] A. Nasri and R. Schober, "Performance of cooperative diversity systems in Non-Gaussian environments," in *Communications (ICC), 2010 IEEE International Conference on*. Cape Town: IEEE, May 2010, pp. 1–6.

[89] I. Krikidis, J. Thompson, S. Mclaughlin, and N. Goertz, "Amplify-and-forward with partial relay selection," *IEEE Communications Letters*, vol. 12, no. 4, pp. 235–237, Apr. 2008.

[90] Y. Jing and H. Jafarkhani, "Single and multiple relay selection schemes and their achievable diversity orders," *IEEE Transactions on Wireless Communications*, vol. 8, no. 3, pp. 1414–1423, Mar. 2009.

[91] D. S. Michalopoulos, H. A. Suraweera, G. K. Karagiannidis, and R. Schober, "Amplify-and-Forward relay selection with outdated channel state information," in *Global Telecommunications Conference (GLOBECOM 2010), 2010 IEEE*. IEEE, Dec. 2010, pp. 1–6.

[92] A. Ikhlef, D. S. Michalopoulos, and R. Schober, "Buffers improve the performance of relay selection," in *Global Telecommunications Conference (GLOBECOM 2011), 2011 IEEE*. IEEE, Dec. 2011, pp. 1–6.

[93] J. Yang, Z. Zhang, and W. Meng, "A novel relay selection scheme in multi-antenna cooperative systems," in *Software Engineering and Service Sciences (ICSESS), 2010 IEEE International Conference on*. IEEE, Jul. 2010, pp. 427–430.

[94] A. Bletsas, A. Khisti, D. Reed, and A. Lippman, "A simple cooperative diversity method based on network path selection," *IEEE Journal on Selected Areas in Communications*, vol. 24, no. 3, pp. 659–672, Mar. 2006.

[95] H. Vikalo, B. Hassibi, and T. Kailath, "Iterative decoding for MIMO channels via modified sphere decoding," *IEEE Transactions on Wireless Communications*, vol. 3, no. 6, pp. 2299–2311, Nov. 2004.

[96] X. Wang and H. Poor, "Iterative (turbo) soft interference cancellation and decoding for coded CDMA," *IEEE Transactions on Communications*, vol. 47, no. 7, pp. 1046–1061, Jul. 1999.

[97] H. Le, B. Lee, and I. Lee, "Iterative detection and decoding with an improved V-BLAST for MIMO-OFDM systems," *IEEE Journal on Selected Areas in Communications*, vol. 24, no. 3, pp. 504–513, Mar. 2006.

[98] S. ten Brink and B. Hochwald, "Detection thresholds of iterative MIMO processing." IEEE, 2002, p. 22.

[99] B. Hochwald and S. ten Brink, "Achieving near-capacity on a multiple-antenna channel," *IEEE Transactions on Communications*, vol. 51, no. 3, pp. 389–399, Mar. 2003.

[100] P. W. Wolniansky, G. J. Foschini, G. D. Golden, and R. A. Valenzuela, "V-BLAST: an architecture for realizing very high data rates over the rich-scattering wireless

channel," in *Signals, Systems, and Electronics, 1998. ISSSE 98. 1998 URSI International Symposium on*, 2002, p. 295–300.

[101] D, Wubben, R. Bohnke, V. Kuhn, and K. D. Kammeyer, "MMSE extension of V-BLAST based on sorted QR decomposition," in *IEEE Vehicular Technology Conference Fall (VTC 2003-Fall)*. IEEE, Oct. 2003, pp. 508–512.

[102] R. C. de Lamare,"Adaptive and Iterative Multi-Branch MMSE Decision Feedback Detection Algorithms for Multi-Antenna Systems," *IEEE Transactions on Wireless Communications*, vol. 12, no. 10, pp.5294–5308, Oct. 2013.

[103] R. Fa and R. C. de Lamare, "Multi-branch successive interference cancellation for MIMO spatial multiplexing systems: design, analysis and adaptive implementation," *IET Communications*, vol. 5, no. 4, p. 484, 2011.

[104] P. Li, R. C. de Lamare, and R. Fa, "Multiple feedback successive interference cancellation detection for multiuser MIMO systems," *IEEE Transactions on Wireless Communications*, vol. 10, no. 8, pp. 2434–2439, Aug. 2011.

[105] Y. Cai and R. de Lamare, "Space-Time adaptive MMSE multiuser decision feedback detectors with Multiple-Feedback interference cancellation for CDMA systems," *IEEE Transactions on Vehicular Technology*, vol. 58, no. 8, pp. 4129–4140, Oct. 2009.

[106] P. Li and R. C. D. Lamare, "Adaptive Decision-Feedback detection with constellation constraints for MIMO systems," *IEEE Transactions on Vehicular Technology*, vol. 61, no. 2, pp. 853–859, Feb. 2012.

[107] L. Yang, "Using Multi-Stage MMSE detection to approach optimum error performance in multiantenna MIMO systems," in *Vehicular Technology Conference Fall (VTC 2009-Fall), 2009 IEEE 70th*. IEEE, Sep. 2009, pp. 1–5.

[108] G. Voronoï, "Nouvelles applications des paramètres continus à la théorie des formes quadratiques. Deuxième mémoire. Recherches sur les parallélloèdres primitifs," *Journal für die reine und angewandte Mathematik*, vol. 134, pp. 198–287, 1908.

[109] A. Okabe, B. Boots, K. Sugihara, S. N. Chiu, *Spatial tessellations: concepts and applications of Voronoi diagrams*. Chichester, West Sussex, U.K.: Wiley, 2009.

[110] F. Aurenhammer, "Voronoi diagrams - a survey of a fundamental geometric data structure," *ACM Computing Surveys (CSUR)*, vol. 23, no. 3, pp. 345–405, 1991.

[111] X. Li, and J. A. Ritcey, "Bit-interleaved coded modulation with iterative decoding," in *IEEE International Conference on Communications*. IEEE, 1999, pp. 858–863.

[112] W. Gerstacker, R. Schober, and A. Lampe, "Receivers with widely linear processing for frequency-selective channels," *IEEE Transactions on Communications*, vol. 51, no. 9, pp. 1512–1523, Sep. 2003.

[113] R. Schober, W. Gerstacker, and L. Lampe, "A widely linear DF-MMSE receiver for DS-CDMA with BPSK modulation," in *Global Telecommunications Conference, 2003. GLOBECOM '03*. IEEE, 2003, pp. 1548–1552.

[114] S. Abdallah and I. N. Psaromiligkos, "Widely linear versus conventional Subspace-Based estimation of SIMO Flat-Fading channels: Mean squared error analysis," *IEEE Transactions on Signal Processing*, vol. 60, no. 3, pp. 1307–1318, Mar. 2012.

[115] S. Verdu, *Multiuser detection*. Cambridge ; New York: Cambridge University Press, 1998.

[116] P. Chevalier and F. Dupuy, "Widely Linear Alamouti Receiver for the Reception of Real-Valued Constellations Corrupted by Interferences-The Alamouti-SAIC/MAIC Concept," *IEEE Transactions on Signal Processing*, vol. 59, no. 7, pp. 3339–3354, Jul. 2011.

[117] A. Cacciapuoti, G. Gelli, L. Paura, and F. Verde, "Widely linear versus linear blind multiuser detection with Subspace-Based channel estimation: Finite Sample-Size effects," *IEEE Transactions on Signal Processing*, vol. 57, no. 4, pp. 1426–1443, Apr. 2009.

[118] P. Li, R. C. de Lamare, and R. Fa, "Multi-Feedback successive interference cancellation with Multi-Branch processing for MIMO systems," in *VTC Spring 2011 - IEEE 73rd Vehicular Technology Conference*. IEEE, May 2011, pp. 1–5.

[119] R. C. de Lamare and D. L. Ruyet, "Multi-branch MMSE decision feedback detection algorithms with error propagation mitigation for MIMO systems," in *International Conference on Acoustics Speech and Signal Processing (ICASSP)*. IEEE, Mar. 2010, pp. 3450–3453.

[120] S. Nammi, “Threshold list subset detector for turbo MIMO systems” in *European Wireless Conference (EW)*. IEEE, Mar. 2009, pp. 276–281.

[121] S. Nammi, and D. K. Borah, “Iterative List Subset Detectors for Turbo Product Coded MIMO Wireless Systems.” in *VTC Spring 2007 - IEEE Vehicular Technology Conference*. IEEE, Apr. 2007, pp. 2023–2027.